
Application of the flow equation method to the out-of-equilibrium Anderson impurity model

Michael Johannes Möckel



München 2005

Application of the flow equation method to the out-of-equilibrium Anderson impurity model

Michael Johannes Möckel

Diplomarbeit
an der Fakultät für Physik
der Ludwig-Maximilians-Universität
München

vorgelegt von
Michael Johannes Möckel
aus Naila

München, den 27.9.2005

Erstgutachter: Prof. Dr. Jan von Delft
Zweitgutachter: Prof. Dr. Hermann Wolter

Contents

I Introduction and preparation of the Anderson impurity model	1
1 Introduction	3
1.1 Motivation	3
1.1.1 Philosophy of Hamiltonian diagonalization	3
1.1.2 Earlier works on the (out-of-equilibrium) Anderson impurity model	4
1.2 General aspects of impurity problems	6
1.2.1 Concept of impurity	6
1.2.2 Impurities in electronic systems	7
1.2.3 Established models for magnetic impurities	8
1.3 Anderson impurity model	9
1.3.1 Basic definition of the Anderson impurity model	9
1.3.2 AIM for quantum dots	11
1.4 Implementation of out-of-equilibrium conditions	13
1.4.1 Out-of-equilibrium description for the Anderson impurity model	14
1.4.2 Asymmetric coupling transformation	14
1.5 Outline of the project	15
1.5.1 Starting point: Anderson Hamiltonian	15
1.5.2 Energy scales and pre-diagonalization	15
1.5.3 Invariance of the ground state description	16
1.5.4 Application of the flow equation method to the pre-diagonalized Anderson impurity model	17
1.5.5 Formal development of the flow equations framework for Anderson-like Hamiltonians	18
2 Pre-diagonalization of the Hamiltonian	19
2.1 Multi-index notation	19
2.2 General approach to pre-diagonalization	21
2.2.1 Definition	21
2.2.2 General properties of the basis transformation \mathcal{B}	21
2.2.3 "Equation of motion" method	22
2.2.4 Assumptions on the model	22
2.3 Explicit transformation for one-level impurities	23
2.3.1 Implementation of assumptions	23
2.3.2 Matrix elements for discrete band energies	24
2.3.3 Renormalization of eigenenergies	26

2.3.4	Limit of continuous energy distribution	27
2.3.5	The hybridization function and its properties	29
2.4	Transformation of the Fermi functions	29
2.5	Summary	30
II Application of the flow equation method to a pre-diagonalized Anderson impurity model		33
3	Introduction to the flow equation method	35
3.1	History of the flow equations approach	35
3.1.1	Origins	35
3.1.2	Applications	35
3.2	Infinitesimal unitary transformations	36
3.2.1	Flow equation of an observable	36
3.2.2	Perturbation series in a small expansion parameter	37
3.2.3	Expansion in generalised coupling constants	38
3.2.4	Flow equations of the generalized coupling constants	39
3.2.5	Approximations to the flow equations	40
3.2.6	Transformation of the ground state	41
3.3	Continuous sequence of infinitesimal transformations	43
3.3.1	Parametrizations	43
3.3.2	Representation of the net transformation	43
3.3.3	Active and passive view on the transformation	44
3.3.4	Discussion of initial and final picture	45
3.3.5	Flow of generalized coupling constants	46
3.4	The flow equation method in the context of scaling and RG procedures	46
3.4.1	Pictorial understanding of flows in parameter space	46
3.4.2	Poor man scaling and similar approaches	47
3.4.3	Separation of energy scales	47
3.4.4	Comparison of scaling and the flow equation method	48
3.5	Definition of the generator	48
3.5.1	Canonical generator	49
3.5.2	Other choices of generators	49
4	Application of the flow equation method to Anderson-like Hamiltonians	51
4.1	Modifications to the Hamiltonian	51
4.1.1	Extension of the operator structure of the Hamiltonian	51
4.1.2	Assumptions to the Hamiltonian	52
4.1.3	Anderson-like Hamiltonian	52
4.1.4	Splitup of the Hamiltonian	53
4.2	Definition of the generator	53
4.2.1	Calculation of the canonical generator	53
4.2.2	Extension of the canonical generator	55
4.3	Flow equation for Anderson-like Hamiltonians	56

5	Diagonalization of the Anderson Hamiltonian	59
5.1	Reduction to the Anderson Hamiltonian	59
5.2	General flow equation for the Anderson Hamiltonian	60
5.3	Flow equation for the interaction U	62
5.3.1	Parametrizations of U	63
5.3.2	Flow equation for $U(B)$ to first order in U	63
5.3.3	Flow equation for $U(B)$ to second order in U	64
5.4	Flow of the interaction for the asymmetric model	66
5.4.1	Restrictions on energy contributions	66
5.4.2	Discussion of $U(B)$ for initial flow ($1/\sqrt{B} \gg \Delta$)	68
5.4.3	Re-arrangement of the flow equation of $U(B)$ at the Fermi energy	70
5.4.4	Discussion of Advanced Flow ($1/\sqrt{B} \ll \Delta$) at zero Temperature	73
5.4.5	Interaction as suitable perturbative parameter	77
5.5	Flow equation for the energies and scattering amplitudes	78
5.5.1	Flow equations for the renormalised energies and the potential scattering term	78
6	Transformation of the observables	81
6.1	Ansatz for the transformation of fundamental operators	81
6.1.1	Creation operator	81
6.1.2	Annihilation operator	82
6.1.3	Ansatz for the transformation of a composite object	83
6.2	Flow equations for the observable O^\dagger	83
6.2.1	Canonical part of the flow equation	84
6.2.2	Discussion of the flow equations	85
6.2.3	Amendments to the flow equations by the extended generator	86
6.3	Approximate analytical solutions to the flow equations of the observable	86
6.3.1	Parametrization of γ	86
6.3.2	First order solution for $M_{\uparrow\downarrow}$	87
6.3.3	Second order solution for γ	88
6.3.4	Discussion of γ in the limit of accomplished flow	89
7	Impurity spectral density	93
7.1	Greens function formalism	93
7.1.1	Definition and ansatz	93
7.1.2	Evaluation of time dependence	94
7.1.3	Evaluation of the Greens function	95
7.1.4	Contributions to the Greens function in $\mathcal{O}(U^2)$	96
7.1.5	Spectral density and Greens function of the impurity	97
7.2	Analytical solution for the spectral density	97
7.2.1	Second order correction to the spectral density	97
7.2.2	Discussion of the correction function	99
7.3	Conservation of spectral weight	100
7.3.1	Spectral integration and zero time retarded Greens function	100
7.3.2	Stability of Greens function at zero time	101
7.3.3	Conservation of spectral weight by the flow equations	102
7.3.4	Conservation of spectral weight by the approximate analytical solution	102

8	Numerical implementation	105
8.1	General approach	105
8.1.1	Separation of dependences	105
8.1.2	Processing of the correction function	106
8.2	Discretization	106
8.2.1	Transfer into discrete energy space	106
8.2.2	Discrete modelling	106
8.2.3	Discrete quantities	107
8.2.4	Principal value integration	107
8.3	Numerical complexity	108
8.4	Implementation in C^{++}	108
8.5	Calibration of numerical parameters	108
8.5.1	Choice of energy window size	108
8.5.2	Calibration of principal value evaluation	109
8.6	Numerical quality	109
8.6.1	Test of numerical stability	109
8.6.2	Estimation of numerical errors	109
9	Evaluation of the impurity spectral density	111
9.1	Equilibrium impurity spectral density	111
9.1.1	Expected observations	111
9.1.2	Artifacts and obvious limitations	111
9.2	Dependence of the correction function $\mathcal{C}(\omega)$ on the voltage bias	112
9.3	Impurity spectral function out of equilibrium	114
9.3.1	Evaluations for constant voltage	114
9.3.2	Spectral density for fixed correlation strength	116
10	Conclusions and outlook	121
	Acknowledgments	123
III	Appendix	125
A	Normal ordering and Fermi distribution functions	127
A.1	Technical aspects of normal ordering	127
A.2	Fermi distribution functions	128
B	Impurity with several spin levels	131
C	Some commutators and correlators	133
C.1	Decomposition of commutators into (anti-)commutators	133
C.2	Commutators and correlators of normal ordered operator products	134
	List of Figures	139
	Bibliography	141

Part I

Introduction and preparation of the Anderson impurity model

Chapter 1

Introduction

In this work we will present an application of the flow equation method to the out-of-equilibrium Anderson impurity model. Both method and model are well established approaches in condensed matter theory and have been independently studied in a huge variety of applications.

1.1 Motivation

As part of this introduction we will discuss an virtually omnipresent concept in theoretical physics in the context of condensed matter systems to make it evident to the reader why this and similar approaches are at the heart of any theoretical description. Afterwards we briefly review earlier works on this subject, lay out our approach and explain origin, meaning and modern applications of the Anderson impurity model. A detailed introduction to the flow equation approach can be found in chapter (3).

1.1.1 Philosophy of Hamiltonian diagonalization

It is well-known to any physicist that many challenges in theoretical physics arise from complications involved in the diagonalization of non-trivial (Hamilton) operators. We know that the theoretical frame of a quantum theory (e.g. quantum mechanics or quantum field theory) singles out a preferred basis for physical evaluations; it is the eigenbasis of the model Hamiltonian. In this basis important physical properties are either evident (eigenenergies) or can be calculated conveniently. In particular, all aspects tied to the time evolution of the system (e.g. the Greens functions formalism) can be easily described.

In condensed matter theory, another aspect is of crucial importance: The ground state of a multi-particle system is commonly described by a one-particle approximation for its energy levels and a distribution function which allocates particles to the various one-particle states of the system. For free fermionic particles, this distribution function is a simple result of Fermi-Dirac statistics. Yet for interacting particles, the one-particle approach is not well-founded any more and in many cases of practical importance it is all but easy to construct a correct interacting ground state. The crux of the matter lies in the fact that in equilibrium the occupation of one-particle energy levels can be trivially written down for diagonal Hamiltonians. It is a simple Fermi distribution of *quasiparticles* which are defined by the diagonal Hamiltonian itself (see chapter 3 for further details). As diagonalisation procedures are implemented

by (approximately) unitary transformations, all expectation values are (approximately) invariants of the transformation; hence all observable physical properties remain unchanged and the diagonalization approach reveals its true strength: It proves -at least in equilibrium- to be a method to avoid the construction of complex interacting ground states but to include all aspects of the interaction into the formal definition of more adequate operators.

This work is in particular motivated by this view on the diagonalisation process. Nonetheless, we introduce another complication by imposing out-of-equilibrium conditions onto the system. They are a new ingredient to the model and are independent of but not unrelated to the Hamiltonian. They do influence the occupation of energy states of a system which cannot be described by a simple Fermi-Dirac statistics any more. Similarly, it is no longer obvious that the ground state of a diagonal Hamiltonian can be described as a filled Fermi sea of quasiparticles. Despite of all the difficulties, we will follow this way to contribute to the discussion of the out-of-equilibrium Anderson impurity model.

Consequently, the predominant part of this work will deal with two different diagonalisation procedures for a quadratic and a non-quadratic Hamiltonian. While the first class of Hamiltonians can be diagonalised exactly by a linear transformation, this is not always possible for those Hamiltonians which include multi-particle interactions. Then approximative methods come into place, among which the flow equations technique should be counted.

1.1.2 Earlier works on the (out-of-equilibrium) Anderson impurity model

The Anderson impurity model has been introduced by Anderson in 1961 to describe the impact of localized magnetic moments in metals on observable magnetic and thermodynamic parameters [1]. Due to the definition of a non-trivial two-particle interaction it exhibits a rich physical structure. We will make the reader familiar with some of its details in section (1.3). Over the last decades a variety of approaches have been applied firstly to the equilibrium Anderson impurity model. Anderson himself relied on the Hartree-Fock-approximation, a major breakthrough was the exact solution by using a Bethe ansatz. It was obtained in 1980 by Andrei [2] for the closely related Kondo model [3] and brought forward to the Anderson impurity model by Wiegmann [4] in 1981.

Analytical approaches to the out-of equilibrium Anderson impurity model

With the development of new experimental techniques in the fabrication of heterostructures and the emergence of the field of quantum dots in the 1990ies the interest in out-of-equilibrium properties of the Anderson impurity model was stimulated. It received a further boost when in 1998 experiments on transport through quantum dots observed Kondo signatures [5][6].

Early analytical approaches by Hershfield, David and Wilkins [7] attempted non-equilibrium second order perturbation theory according to the Keldysh formalism in the -potentially large- interaction strength. They had found justification in the similarity with numerical Monte Carlo simulations performed by Silver et al. in 1990 [8]. Nonetheless this approach could not reproduce some features observed with other techniques, most importantly the out-of-equilibrium splitting of the Kondo resonance in the impurity density of states. Fujii and Ueda resumed this work in 2003 and studied a symmetric out-of-equilibrium Anderson impurity model in forth order perturbation theory based on the Keldysh formalism [9]. They have found the missing structure when the bias voltage exceeds the Kondo temperature.

Another way was taken by Wingreen and Meir in 1993 who used the non-crossing approximation for low temperature, out-of-equilibrium predictions on transport properties [10]. It requires infinite interaction strength and becomes exact in the limit of infinitely many spin channels. In the relevant case of two spin channels the authors expected an error of 15 percent in the linear conductance. The non-crossing approximation predicts a splitting of the Kondo resonance of the density of states but is –for principal reasons– unsuitable to discuss, for instance, the unitary conductance limit.

A different point of view can be taken when the focus is on the different parameter regimes of the Anderson impurity model.

Recently Anderson’s original unrestricted Hartree-Fock approach has been generalized to the nonequilibrium Anderson impurity model by Komnik and Gogolin [11]. They discussed the mean-field phase diagram for the Anderson impurity model, calculated an analytical expression for the critical curve between the magnetic and the non-magnetic phases in the symmetric case and showed that the magnetic phase exists for arbitrary voltages in the asymmetric model.

A few weeks ago a promising attempt to solve the problem of strongly correlated systems out of equilibrium for steady case situations exactly has been suggested by Metha and Andrei [12]. They describe a non-equilibrium steady-state by means of time-independent scattering theory and construct fully interacting multi-particle scattering eigenstates for integrable impurity models (e.g. the Kondo model).

Numerical methods

In many cases observable predictions for transport properties cannot be made without the help of numerical tools. Most of the numerical methods available to treat multi-particle systems have already been applied to the equilibrium Anderson impurity model, but their application to out-of-equilibrium situations is often not unproblematic.

For instance, the numerical renormalization group (NRG) according to Wilson has produced benchmarking results for an analysis of the resonance at the Fermi level. It is an excellent tool for predictions at low energies. Yet off the resonance, significant errors have to be expected. As it has been developed as a numerical tool to estimate the ground state of a Hamiltonian which is bounded from below it is not particularly suited to find the steady state of a system under out-of-equilibrium conditions.

Among other popular approaches to the equilibrium Anderson impurity model have been Quantum Monte Carlo simulations, the density matrix renormalization group (DMRG) and numerical exact diagonalisation techniques. These approaches allow for the calculation of the time evolution of a system which has been initialized in a specific state. This setup is –in principle– suitable for evaluations of non-equilibrium initial conditions. Nonetheless it requires large model systems to observe steady state behaviour which are often beyond the technical resources. Recently, some DMRG results have raised hope for further progress, but fully satisfying results have not yet been delivered.

Role of the flow equation technique

Therefore we conclude that despite of various analytical and numerical examinations of the Anderson impurity model, new approaches to the out-of-equilibrium case are still of interest. We will discuss why we think that the flow equation method has particularly useful

features which promise a successful application of this technique to out-of-equilibrium situations. Moreover, it provides a controlled way for approximations even for more complex models and interaction terms. Therefore it still might be a relevant approach if exact solutions for integrable models like the Anderson impurity model in non-equilibrium should be formulated in the future.

1.2 General aspects of impurity problems

Impurity problems in a very general sense of the word have been a point of interest in solid states physics throughout the times. Defects and contaminations define the properties of solids in various aspects. On the one hand, they are an unavoidable side effect in any technical application of materials, on the other they even developed into a controllable tool of engineering. For both reasons, they have become subject to extended and successful scientific research. Most strikingly, doping of semiconductures has opened the world of micro-electronics and provoked the last technical revolution of human civilization. Nonetheless we quickly leave this wide field of literally understood impurities and turn to the conceptual aspects of typical impurity models in theoretical physics.

1.2.1 Concept of impurity

The concept of a general circumstance ("as it should be") and impurities which disturb or complement this rule is virtually omnipresent in many disciplines of human reasoning and the empirical sciences. But in particular it suits the special approach of condensed matter theory. This physical subject studies the collective behaviour of condensed matter with regress to the individual nature of single atoms. For practical (e.g. numerical) and conceptual (e.g. unitarity) reasons the quantum mechanical descriptions of single atoms cannot be simply applied to a macroscopic object as a collection of -typically- 10^{23} (Avogadro's number) constituents.

Effective impurity models

A straightforward approach to overcome these limitations consists of formulating an effective theory. It is a multi-step approximation which includes a splitup of all particles involved:

- (a) The huge majority of particles are grouped into an arrangement which is described by its collective appearance. Such a model is not a quantum mechanical one in a strict meaning any more but may incorporate various features of quantum theories in an approximate way. A very common model, for instance, are electronic band structures which extend a one-electron quantum mechanical result (its level structure) to a multi-electron effective model. We will make use of this approach.
- (b) On the other hand, some particles are singled out and not included in this effective mean description. They carry particular individual properties and are embedded impurities in the effective background matrix. In their interaction with the collective background lies the true essence of the description; it should reproduce macroscopically observable properties which are beyond the features of the pure background matrix.

Separation in subsystems

First of all this concept represents a partitioning of the model in two subsystems which can be analysed separately. For both of them physical plausibilities are set up without respect to the other part to form a frame of the description. Usually an intuitive and imaginative approach to the subsystems is possible. Then general assumptions on the coupling between the systems are made. The main challenge of a theoretical description is always to derive the behaviour of the full system from its individual parts. Technically this shows up as a problem of Hamiltonian diagonalisation as from a full diagonal Hamiltonian important features like the energy spectrum are easily read off. But due to the coupling off-diagonal terms are present originally and need to be dissolved.

Local and delocalised aspects

Secondly, a typical trait of this partitioning in impurity models is the approximate separation between local and delocalised aspects. While the first ones are attributed to the impurities, the last ones are included in a uniform background. Hence impurity models in solid state physics often comment on the effects of localized features on a mean effective theory. We mention that this approximation may become problematic in a regime of strong coupling. Then we expect a mixing of impurity and background features which does not necessarily conserve localization. Nonetheless typical theoretical descriptions make use of it and implement quantum field theoretical or mean field approaches to the background as well as localized couplings of it to the impurity.

1.2.2 Impurities in electronic systems

In condensed matter theory impurity problems have been studied primarily in electronic systems¹.

Adiabatic approximation and Bloch states

Such treatments start with an approximate division of a condensed matter system into an electronic part, called the quasi-free electron gas, and a remaining lattice of positive ions (nuclei and bound electrons) which solely enters the theory via an effective periodic potential. It includes all interactions between the electrons and the ions. [13] [14]

For an ideal, strictly periodic potential of the lattice the electronic eigenstates are given by *Bloch states* which show the same periodicity as the lattice and hence are delocalized. These one-electron eigenstates are the defining ones for all further treatment of the electronic system. They are used to determine the band structure and are the basis for second quantization. We stress that an electronic creation or annihilation operator generates or destroys an electron already in a Bloch eigenstate. Nonetheless we will call these particles electrons².

Typical features of impurity models

Inserting a local impurity singles out one site in position space and shows the separation of delocalized band electrons described by Bloch states and local properties on the impurity. The

¹The author is not aware of impurity treatments for the nuclei.

²N.B. in a lattice sense

concept of an impurity added to the system establishes a new link between the free electron gas and the lattice structure. By this it provides a tool to study the effects of small violations of the crystal lattice, e.g. due to foreign atoms, on the electronic system.

Note that an impurity approach does not primarily focus on just a perturbative deformation of the lattice at a particular site. Its point of view is the addition of further aspects to the system: Fundamentally new properties which are not common to all the other ions in the lattice can be defined on the impurity. A typical example is the definition of an on-site two-particle interaction on the impurity which only becomes effective when both electrons are jointly present on the impurity. It is this feature which makes impurity models attractive for solid state problems.

Magnetic impurities

If, furthermore, the spin of the electrons is considered, *magnetic impurities* can be described. Their interaction with band electrons can be dominated by the emergence of a single spin on the impurity if a strong Coulomb repulsion prevents spin pairing. This feature has made impurity setups to model systems for studies of magnetism and strongly correlated systems. A major example is the discovery and explanation of the *Kondo effect*.

1.2.3 Established models for magnetic impurities

A wide range of models has been developed to discuss features of magnetic impurities. A good overview over commonly used models is given for instance by A.C. Hewson which can be highly recommended. [15] We only mention some basic aspects of the most important models here. All of them are simple effective models which restrict to the most relevant effects of impurities in the limit of low energy excitations off a ground state.

Potential scattering model

A basic approach is known as the potential scattering model which describes the effects of an impurity on band electrons by an additional effective scattering potential. This potential both includes the Coulomb potential of an excess charge of the impurity and its screening by band electrons. An examination of the bound states in such potentials with respect to electronic bands leads to the concept of *virtual bound states*. A resonance in the conduction band density of states is observed whenever such a bound state is energetically located inside the conduction band. Thus the impurity induces a redistribution of the density of states within the band: This can be expressed as an impurity density of states which is peaked at the impurity bound state and approximately of Lorentzian shape. We will observe the same resonance in the (interaction free) Anderson model using a different approach later on. Note that in the potential scattering model only a scattering potential is added to the description of free band electrons. Thus the integrated impurity density of states must vanish as no new impurity states are introduced. Hence we expect negative contributions to the impurity density of states far off the resonance (where the Lorentzian approximation does not hold any more). The Anderson model explicitly differs in this point as a separate impurity level is defined. Finally we remark on the fact that the potential scattering model does not describe magnetic impurities in an adequate way. For this reason, more elaborate models need to be discussed.

Kondo model

The Kondo model³ highlights on the specific spin-induced effects of magnetic impurities. It stands in the tradition of Heisenberg exchange models which describe an effective interaction between two coupled spins. In the Kondo model, one of these spins is given by the local moment of a magnetic impurity, the other one is represented by a collective band effect. This allows for a more detailed study of spin-spin interactions in the presence of an electronic conduction band. The model is (formally) form invariant under an additional inclusion of a potential scattering term and a simultaneous change into an eigenbasis of the scattering model, such that these effects can be implicitly included.

The most spectacular observation made in this model is the *Kondo effect*, which is characterized by an enhanced scattering off an impurity at low temperature. It requires the existence of two energetically degenerate spin levels of opposite orientation on the impurity which is occupied by a single electron only. Then second order perturbation theory shows that spin-flip processes on the impurity are responsible for the Kondo behaviour. They mediate a strong correlation between the band and the impurity spin. The observable signatures of this effect are dramatically dissimilar in different physical setups but can be explained easily (see 1.3.2).

1.3 Anderson impurity model

In this work we study a third well-established impurity model which we therefore present in more detail. It was set up by Anderson in 1961 to describe the effects of transition metal or rare earth ions with a magnetic moment embedded in a metallic phase. Typical model systems, for instance *Fe* in *Cu*, showed anomalous contributions to metallic properties. Nowadays it is a very popular and common approach to describe quantum dot systems which we will explain in the following sections.

1.3.1 Basic definition of the Anderson impurity model

The principal idea of the Anderson impurity model as proposed by Anderson is to depict an impurity as an individual ion embedded in a metallic background. The model combines atomic properties of the ion with the nature of electrons in a conduction band by defining a coupling of these subsystems.

Free Anderson Hamiltonian

The ion is usually simply represented by a one-level system but respects different spin orientations of an electron in this level. For the band one usually assumes flatness, i.e. a constant density of states in energy. Although the Anderson impurity model is often discussed for finite bandwidth we will work with unlimited bands. Thus we avoid the emergence of features which are typical effects of band edges to have a clearer view on those properties which are induced by the occupation of the bands. All energy levels are spin degenerate. In second quantized form the free Anderson Hamiltonian can be written as a simple sum of the two

³The Kondo model was used but not developed by Kondo. Sometimes it is referred to as the 's-d exchange model' and attributed to Zener (1951), e.g. in [15]

subsystems:

$$H_{free} = \sum_{\sigma} \epsilon_d d_{\sigma}^{\dagger} d_{\sigma} + \sum_{k,\sigma} \epsilon_k c_{k\sigma}^{\dagger} c_{k\sigma} \quad (1.1)$$

While d_{σ}^{\dagger} represents an atomic creation operator which generates an electron with spin orientation σ in the one-level system, $c_{k\sigma}^{\dagger}$ does the same for a band electron of momentum k . We note that the label d originally denoted the d-level of a transition metal which dominates the interaction of such an ion with the conduction band. In later applications of the Anderson impurity model to quantum dot systems it should be read as the 'dot level'.

Hybridization

The coupling of the Anderson Hamiltonian has originally been defined by the overlap of the outer electronic wavefunction of the ion with the Wannier wavefunctions of the conduction band electrons at the impurity site. In a quantum dot context this only serves as a motivation; the matrix element V_k of the coupling is then imposed by physical plausibilities. We refer to this coupling as the *hybridization* of one-level system with the conduction band to distinguish it from a further interaction introduced later on. The hybridization term of the Anderson Hamiltonian is formed in a straightforward way.

$$H_{Hyb} = \sum_{k\sigma} \left(V_k d_{\sigma}^{\dagger} c_{k\sigma} + V_k^* c_{k\sigma}^{\dagger} d_{\sigma} \right) \quad (1.2)$$

The sharp localization of the impurity is mirrored by a delta-shape of the hybridization matrix element in position space. In momentum space this corresponds to a constant run and we can assume $V_k = V_k^* = V$. For quantum dots this is a rough but commonly used and acceptable approximation.

This form of the Anderson impurity model does not significantly differ from a potential scattering approach. But important new properties are added by a modification of the one-level system, the definition of a two-particle on-site interaction.

On-site interelectron interaction

According to the Pauli exclusion principle there are no restrictions on the occupation of an energy level with several electrons of pairwise different spin orientations. A standard way for describing the occupation of various atomic energy levels with electrons roots in a simple one-electron approximation for the atomic level structure which is filled up with interaction free electrons. In particular, such approaches usually neglect the mutual Coulomb repulsion of the outer electrons.

The Anderson impurity model instead explicitly includes this interaction. This is motivated by the concept that electrons on the impurity are restricted to a very small region in position space. Hence the Coulomb repulsion becomes a dominating factor. It is essential for the existence of magnetic moments on impurities.

Therefore a two-particle interaction is defined. For two spin-distinct electrons in the formerly degenerate one-level structure the interaction strength (i.e. the matrix element) is given by an average Coulomb interaction calculated with respect to the wavefunctions of both electrons. For a one-level system these wavefunctions are equal, for a multi-level structure an inter-level

Coulomb repulsion could as well be imposed [16].

$$U = \int \Phi_d^*(r)\Phi_d^*(r')\frac{e^2}{|r-r'|}\Phi_d(r)\Phi_d(r')drdr' \quad (1.3)$$

The on-site interaction term of the one-level Anderson impurity model is then given by

$$H_{int} = Ud_{\uparrow}^{\dagger}d_{\uparrow}d_{\downarrow}^{\dagger}d_{\downarrow} \quad (1.4)$$

Thus the full Anderson Hamiltonian consists of the free part (1.1), the hybridization (1.2) and the on-site interaction term (1.4) and is written down in complete form in (1.6). Furtheron we refer to the on-site interelectron interaction U simply as the *interaction*.

Mapping onto the Kondo model: The Schrieffer-Wolff transformation

For large on-site interaction and weak hybridization the full Anderson Hamiltonian expresses the behaviour of a local spin in a background of band electrons. Due to the large cost of inserting another electron into the impurity level we expect it to be -on average- singly occupied. This exposes a net magnetic moment at the impurity which interacts with band electrons due to the hybridization. Consequently, this regime is called the local moment regime of the Anderson impurity model. It can be mapped onto the Kondo model by a single unitary transformation as was shown by Schrieffer and Wolff in 1966 [3]. This transformation already shows some similarities with the flow equation transformation which we will discuss in great detail later in this work.

Moreover, the Schrieffer-Wolff transformation has been used to check the suitability of the flow equation method for constructing effective Hamiltonians in a systematic way. Summing up one can say that a characteristic feature of the flow equation method, namely its intrinsic energy scale separation, enables a satisfactory mapping of the Anderson model onto an effective Kondo Hamiltonian, including the production of the correct parameters[17]. This is a strong motivation for applying the flow equation method to other aspects of the Anderson model.

1.3.2 Extensions of the Anderson impurity model for quantum dot systems

For a physical setup given by quantum dot experiments some modifications need to be introduced. The rapid progress in experimental examinations of quantum dots stimulates our interest in a further analysis of the Anderson impurity model. To explain the following extensions of the original Anderson impurity model we briefly sketch the basic features of such systems.

Quantum dots

For about ten years physicists possess the technological means to create semiconducting heterostructures which show structures below the limit of 100 nm. Such extensions approach the de Broglie wavelength of quasi-free electrons in a condensed matter system. Hence geometrical constraints can impose quantum-mechanically relevant restrictions on the electron gas.

Quantum dots are most commonly implemented as such structures which confine a limited number of electrons to a well-defined and controllable environment of similar size. Effectively, a zero-dimensional quantum gas of electrons is formed and treated, to first order, as an

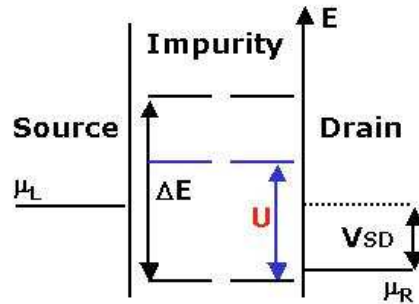


Figure 1.1: Energy level scheme of an impurity model for a quantum dot.

artificial atom. It is coupled to metallic leads by tunnel barriers which impose a hybridisation of the quantum dot energy levels with the conduction bands.

The one-electron energy levels of a quantum dot are described by a straightforward box model. It predicts an equidistant level spacing ΔE which can be observed in experiments. Each level can be occupied by two electrons of different spin. Nonetheless the tight localization of the electrons inside the dot demands for a treatment of the Coulomb repulsion of electrons. Although the Coulomb force acts between all electrons of the model and should be considered by a shift of all multi-particle energy levels with respect to the one-particle model, it becomes particularly relevant for those electronic states which have originally been degenerate. In the box model these are the two spin states of each level. Due to the Coulomb repulsion the addition of a second electron into an already singly occupied level is suppressed by the Coulomb (or charging) energy. Typical estimations of this energy refer to the classical electrostatic capacitance of an electron constrained in the box. An implementation of a quantum dot and its energy level diagram are depicted in figure (1.3.2).

In quantum dot setups the impurity energy levels can be shifted with respect to the Fermi energy of the leads by an outer voltage, called gate voltage. It is applied through a third metallic lead and allows for a change of the average number of electrons on the dot. The addition and the removal of a single electron can be easily observed.

This exposition of the physical setup shows that the Anderson impurity model is a most suitable approach to integrate these aspects into a theoretically treatable model system. Only minor changes need to be included.

One-dimensional implementation and transport mechanism

First of all, the embedding of the impurity is thought of in a one-dimensional context. Now the impurity separates the metallic environment into two distinct parts, the left and the right lead. All band indices and their summations acquire an extension, referring to the left (L) or the right (R) lead, respectively.

A new aspect of quantum dots is the spatial separation between three subsystems. We note that the theoretical description of the Anderson impurity model does not account for that. Both labels L and R represent electronic structures which are completely delocalised, the geometric scales of the impurity enter the model at most indirectly by the size of the box

model and are neglected totally in one-level approaches.

Nonetheless both leads act differently as source and drain and allow for studies of transport through a single impurity if a voltage bias is applied. In a quantum dot setup transport from the left into the right lead always implies a scattering at the impurity. The role scattering plays for transport properties is now completely reversed: In the case of impurities which are embedded in a metallic host electron transport is primarily conducted by band electrons without any involvement of the impurity. Instead, scattering of transport electrons at the impurity redefines their state (we could roughly describe scattering as flips of the momentum direction for states close to the Ewald sphere[13]). On average, it only accounts for an increased resistance.

In the other case of a quantum dot, scattering off the impurity is the only process which enables an interchange of electrons between both leads. Thus enhanced scattering reduces the resistance and contributes positively to transport properties. This different behaviour can be, for instance, observed in the transport signatures of the Kondo effect for both physical setups.

Dot level structure

Following the above description of a quantum dot an inclusion of more than a single dot level would be appropriate. We will do so in principle. But as we expect that the most interesting physics occurs at the Fermi edge we only consider that dot level which is closest to the Fermi energy. This is a notable simplification for the pre-diagonalizing transformation of the Anderson Hamiltonian (cf chapter 2) and its application in the flow equation framework (cf chapter 5). Nonetheless the cornerstones of the flow equation formalism for the Anderson impurity model would not change. We will derive them for a more general setup than the simple Anderson Hamiltonian.

1.4 Implementation of out-of-equilibrium conditions

We already introduced the concept of transport through an impurity which is a typical out-of-equilibrium situation, as the system is driven by an external voltage. For weakly coupled systems, quantum statistical mechanics provides an established description of this situation. Next to the Hamiltonian boundary conditions are defined which set up the statistical properties of the out-of-equilibrium situation. Usually different chemical potentials are attributed to distinct subsystems within the model.

A proper formulation of such boundary conditions for strongly correlated systems is a long standing problem and still under discussion (see, for instance, [12]). We will restrict to a straightforward approach which extends the description for weak coupling to the case of stronger correlations. We defer any questions on its legitimacy as we evaluate the results of our calculation for modest interaction strength only. Furthermore, we limit our considerations to systems which are in steady state, i.e. which are fully characterized by a time-independent model.

1.4.1 Standard implementation of out-of-equilibrium conditions for the Anderson impurity model

Quantum dot experiments provide an excellent tool to study transport properties of impurities. We therefore discuss the introduction of out-of-equilibrium conditions particularly for this experimental implementation.

When a voltage bias is applied between the source and the drain a quantum dot is brought into an out-of-equilibrium regime. Then a common way of describing the leads is to model them as two independent electronic reservoirs which are equilibrated at different chemical potentials μ_L and μ_R . The difference of the chemical potentials equals the applied voltage bias. Moreover we assume that both reservoirs represent continuous band structures. Then each of them can be considered as a Fermi sea filled according to a Fermi distribution function. Hence for each of them a pseudo-equilibrium description is applied. At zero temperature both distributions are constant in two sections but show a sharp Fermi edge which is situated at the respective chemical potential. Interchange of electrons between both reservoirs is only possible by scattering at the impurity.

This composite description of out-of-equilibrium allows for an emergence of time independent stationary states. In particular we expect that a constant voltage drop over the impurity should lead to a time independent average net current between the leads.

1.4.2 Asymmetric coupling transformation

The emergence of two different leads constitutes an avoidable complication of the model which we simply consider as a two-channel system in the following section. Under certain assumptions a linear unitary transformation of both channels can be found such that one of them decouples from the impurity.

Such a transformation has been regularly used to treat an impurity in equilibrium which is coupled to both leads by an asymmetric hybridization. For instance, in real quantum dots such asymmetries are common due to limited precession of fabrication techniques.

Fortunately, for one-level impurities a simple basis transformation decomposes the index sector of the leads into a symmetric and an asymmetric channel even for asymmetric tunnel couplings. The asymmetric channel decouples from the impurity and can be neglected; it just contributes a new energy offset of the Hamiltonian. Finally, a (channel-) symmetric version of the Anderson impurity model remains with a new hybridization matrix element given by $\tilde{V} = \sqrt{V_L^2 + V_R^2}$ and new band operators $\tilde{c}_{k\sigma} = V_R/\tilde{V} c_{k\sigma R} + V_L/\tilde{V} c_{k\sigma L}$. Some further aspects and illustrations of the transformation can be found in [16].

We apply this transformation to change to a single electronic reservoir. This implies a linear superposition of the Fermi functions of both leads according to

$$\begin{aligned} \tilde{n}^+(\epsilon) &\stackrel{\text{def}}{=} \langle \tilde{c}_{k\sigma}^\dagger \tilde{c}_{k\sigma} \rangle \stackrel{T}{=} \left(\frac{V_R}{V} \right)^2 \langle c_{k\sigma R}^\dagger c_{k\sigma R} \rangle + \left(\frac{V_L}{V} \right)^2 \langle c_{k\sigma L}^\dagger c_{k\sigma L} \rangle \\ &= \left(\frac{V_R}{V} \right)^2 n_R^+(\epsilon) + \left(\frac{V_L}{V} \right)^2 n_L^+(\epsilon) \end{aligned} \quad (1.5)$$

For the symmetrically coupled case ($V_R = V_L$) the new distribution can be described by the mean of the Fermi functions of both leads. It should be understood as an out-of-equilibrium distribution of a single quasiparticle reservoir. Between the two chemical potentials it takes the value 0.5.

For a more extended introduction to simple Fermi functions in and out of equilibrium we refer to the appendix (A.2). Here we only ask the reader to memorize the following, virtually omnipresent combination of Fermi functions

$$Q_{12'2} = n^+(\epsilon_1) n^+(\epsilon_2) - n^+(\epsilon_1) n^+(\epsilon_{2'}) + n^+(\epsilon_{2'}) (1 - n^+(\epsilon_2)) \quad (\rightarrow \text{A.15})$$

We will heavily make use of this notation.

1.5 Outline of the project

1.5.1 Starting point: Anderson Hamiltonian

Finally we have come to a starting point for our examinations of the Anderson model. The Hamiltonian describes a one-level impurity coupled to unlimited flat conduction bands by a symmetric and localized hybridization. On the impurity level we include a two-particle Coulomb interaction which is –due to the Pauli principle– only effective between electrons of different spins.

$$H_{Anderson} = \sum_{k,\sigma} \epsilon_k c_{k\sigma}^\dagger c_{k\sigma} + \sum_{\sigma} \epsilon_d d_{\sigma}^\dagger d_{\sigma} + V \sum_{k\sigma} \left(d_{\sigma}^\dagger c_{k\sigma} + c_{k\sigma}^\dagger d_{\sigma} \right) + U d_{\uparrow}^\dagger d_{\uparrow} d_{\downarrow}^\dagger d_{\downarrow} \quad (1.6)$$

All momentum summations are performed with respect to a one-dimensional system.

1.5.2 Energy scales and pre-diagonalization

Obviously, the Anderson Hamiltonian contains two independent interactions which have to be treated separately. A further energy scale is introduced by outer conditions, namely the voltage bias, which brings the system into out-of-equilibrium. We consider a system at zero temperature only.

Energy scales and dependencies

Our first intention is to study the system in a regime where all energy scales are of similar order of magnitude. Nonetheless we focus on the on-site interaction strength U as we aim at a study of correlation effects under the influence of out-of-equilibrium conditions. The interaction U and the voltage bias are considered to be tunable parameters and the behaviour of the system under their change is analyzed. On the other hand, we keep the hybridization coupling fixed at an arbitrary value. In quantum dot experiments, this coupling is usually a rather weak one and it is justified to think of it as the –in general– smallest energy of the problem. Hence we will define the energy scale of the hybridization (cf. 2.3.2) as the energy unit and express all other energies in multiples of it.

We point out here again that the intention of this work is not the study of strongly correlated systems. Instead, our interest is in the regime of medium correlation strength U which we study for out-of-equilibrium situations. This allows for the overall assumption that it can be subject to a perturbative treatment.

Order of the treatment of different energy scales

The appearance of two independent couplings raises the question in which order they should be treated in a diagonalization approach. In general, large energy scales should be dealt with before lower energy scales are considered. But for this out-of-equilibrium examination, other aspects become important.

Firstly, we observe that an exact diagonalisation is possible for vanishing on-site interaction. Then the Anderson Hamiltonian is equivalent to the two-channel resonant level model. Since this Hamiltonian is of quadratic structure we expect that it can be diagonalised in an exact way.

Secondly, we note that the diagonalisation is independent of the external voltage bias. It only includes the hybridization scale. This suggests to start with a pre-diagonalization of the Anderson Hamiltonian in the case of vanishing interaction. In a second step, perturbation theory in the interaction strength could be applied.

Moreover, it has been shown in other works (e.g.[18]) that a perturbative expansion in terms of the hybridization is not advisable. This can be seen if the non-equilibrium impurity occupation is studied for the resonant level model. It depends on out-of-equilibrium properties even in zeroth order of the perturbation expansion in the hybridization and does not reflect the exact results.

Pre-diagonalization with respect to the hybridization

For the pre-diagonalization of an interaction-free Anderson Hamiltonian we refer to the *equation of motion* technique. In chapter (2) we show that this transformation does not significantly renormalize the band energies of the Hamiltonian and leaves the density of states unaffected. We calculate the matrix elements of this transformation, observe that it dissolves the impurity into a collective band phenomenon and note that the impurity spectral density is turned into a Lorentian distribution; its width reflects the energy scale of the hybridization.

1.5.3 Invariance of the ground state description

In *equilibrium*, the (interacting) ground state of the diagonalized resonant level model can be easily described as a Fermi sea of quasi-particles. For the full Hamiltonian, the same argument can be applied after the diagonalization process has been completed. Thus we find the same description of a non-interacting ground state of (quasi-) particles at three steps of the calculation: For the electronic bands in the original definition of the problem, for the diagonalized resonant level model and, finally, for the completely diagonalized Anderson Hamiltonian. Hence we assume that on all steps of our calculation the (interacting) ground state of the system can be approximated by a Fermi sea of those particles which are described by the current form of the free Hamilton operator. The transformation of the ground state is not explicitly discussed. This implicitly induces a perturbative notion, as both couplings, the hybridization and the on-site interaction, are assumed to have just a small and negligible effect on the re-definition of the ground state of the (interacting) system. We consider both as small perturbations from the non-interacting ground state. But as the assumption of an invariant ground state corresponds to perturbation theory in zeroth order of any expansion parameter, the order of the treatment of both couplings is irrelevant.

For *out-of-equilibrium* situations we simply refer to the same assumptions but implement an out-of-equilibrium Fermi distribution function by (1.5). Again, we should consider this as a

result in zeroth order of perturbation theory; it does not include potentially emerging changes to the boundary conditions of an out-of-equilibrium description under increased interaction strength. In part II of this work we will observe that the invariance of the ground state correlator, i.e. the Fermi function, is a crucial prerequisite of the flow equation approach. Moreover, these assumptions will limit the applicability of this approach to rather small values of the on-site interaction. A correct description of a strongly correlated impurity cannot be expected a priori. Further research in the applicability of these assumptions is needed and strongly encouraged. Unfortunately, it is beyond the scope of this work.

1.5.4 Application of the flow equation method to the pre-diagonalized Anderson impurity model

In a second step, we re-formulate the Anderson Hamiltonian in the diagonal basis of the resonant level model, which we simply call the *pre-diagonalized basis* of the Anderson Hamiltonian. Now a diagonalization with respect to the on-site interaction has to be performed. For this purpose we make use of the flow equation technique. A general introduction to this method is given in chapter 3. It presents the method as an approximate diagonalization procedure and points out why it is a promising technique for out-of-equilibrium examinations. In chapter 4 we develop the framework of the flow equation formalism for a more general class of Anderson-like Hamiltonians which include the one-level Anderson impurity model. The diagonalization of the Anderson Hamiltonian (chapter 3) and the corresponding transformation of the observables (chapter 6) are discussed. Both evaluations rely on the identification of a perturbative parameter. We will show in chapter 5 that the interaction strength U is a suitable one and allows for a controlled perturbation expansion.

Perturbative approximations and non-perturbative elements

Approximations to the differential flow equations are in both cases perturbatively defined by the choice of a certain truncation scheme (for further explanations see chapter 3). They are applied at an infinitesimal level of the transformation. If the set of differential flow equations is solved exactly, i.e. if it is fully integrated, a re-arrangement of the perturbative expansion is performed and higher orders are implicitly included by the backaction of different variables onto each other. This would exceed a simple perturbative treatment and induce non-perturbative features. Yet such an approach cannot be performed in an analytic way, a numeric evaluation of the differential equations would be necessary. In this work we will not touch the –potentially– non-perturbative character of the flow equation method.

Approximate analytical solution of the flow equations

Instead, we focus on an *approximate analytical solution* of the set of differential flow equations. For a second time, perturbative arguments are applied. The backaction of variables is restricted by the limitation on second order results in U . This brings about major simplifications of all differential equations, including an important decoupling of equations. Therefore an approximate analytic solution is possible for all but the very last step of the evaluations (chapters 5 - 7).

The limitations of this approach become obvious in characteristic second order artifacts of the solution. They fix a definite boundary around and beyond of which no reliable results can be expected.

Evaluation of the impurity Green's function

Finally, we express the impurity Greens function in terms of the flow equation formalism (chapter 7) and evaluate it for the approximate analytical solution. Then the impurity spectral density can be easily obtained. For a final evaluation and a diagrammatic plot of the spectral density we rely on simple numerics. Chapter 8 explains the numerical implementation, in chapter 9 the results for the impurity spectral density are presented for various regimes of the interaction strength and outer bias voltage.

1.5.5 Formal development of the flow equations framework for Anderson-like Hamiltonians

We add a final remark on the presentation of the flow equations formalism. One of the aims of this project is to establish the flow equation approach to the Anderson impurity model. Nonetheless we note that many aspects of the derivation primarily depend on the operator structure⁴ of the considered model. This comes from the fact that the framework of the flow equation approach heavily makes use of (anti-) commutators and correlators of operator products. The evaluation of such structures is done by forming contractions which solely depend on the canonical (anti-) commutation rules of the operators. The common definition of a fundamental fermionic anticommutator or bosonic commutator [19]

$$[a_i, a_{i'}^\dagger]_{\pm} = \delta_i^{i'}, \text{ all unrelated vanish,} \quad (1.7)$$

does not demand a detailed specification of the indices of the creation and annihilation operator. The only aspect needed is an equivalence relation on the set of all possible indices. Thus we are free not to fix all of those characteristic features of the model which can be expressed by a choice of indices. Instead we work with general and –temporarily– unspecified multi-indices. They may account for properties like spin, a number of an impurity in a lattice or of a metallic lead (e.g. source or drain in a quantum dot), etc.

We calculate the main operational structures of the flow equation method for such a more general class of Anderson-like Hamiltonians in chapter 4. In particular, non-trivial commutators are calculated which can be used for further reference. Nonetheless the final evaluation of these structures, i.e. the setup and solution of the flow equations, is done for the actual Anderson impurity model.

⁴With this expression we regularly refer to the character of operator products, in particular their size (length) and the arrangement of creation and annihilation operators.

Chapter 2

Pre-diagonalization of an interaction free Anderson Hamiltonian

(Diagonalization of the resonant level model)

In this section we deal with the hybridization of an Anderson-like Hamiltonian before flow equation methods will be developed in a later part of this work. Our aim is to diagonalize the Hamiltonian in the case of vanishing Coulomb interaction and calculate the eigenenergies of the diagonal Hamiltonian and the matrix elements of this transformation explicitly. The latter will be used to express the two-particle on-site interaction in the pre-diagonalized basis. We will formulate an ansatz for a more general Anderson-like Hamiltonian but perform the diagonalization procedure for a one-level Anderson impurity model with vanishing interaction only. Such a simplified Anderson impurity model is commonly known as the resonant level model. In this case an analytical result can be obtained.

2.1 Multi-index notation

For convenience and to maintain the possibility of an easy extension of the formalism to further dependencies we introduce a multi-index notation. Furthermore we will systematically identify operators in different basis representations by their indices. This enables us to do without auxiliary notation like tildes, hats, etc. which are often used for this purpose but may easily complicate notation. Thus we make the following definitions:

Physical basis

In the original basis (we call it the *physical* basis) in which we have defined the impurity and conduction band operators and written down the Anderson Hamiltonian multi-index labels are introduced for both kinds of operators separately. All labels of conduction band operators referring to momentum, spin, etc. are summed up in the index $t = (k, \sigma_C, \dots)$. For the multi-index of the impurity we choose -under slight abuse of notation- the letter $d = (d_{level}, \sigma_I, \dots)$. Note that d_{level} already labels the different levels of a multi-level impurity. As we will restrict to one-level impurities in most places confusion will be unlikely and it will show up to be

	Conduction band	Impurity
Physical basis	$t = (k, \sigma_{CB}, \dots)$	$d = (d_{level}, \sigma_I, \dots)$
	jointly: j	
Pre-diagonalized basis	s	

Table 2.1: Summary of multi-index definitions

the more intuitive notation. σ_{CB} and σ_I refer to the conduction band electron spin and the impurity spin, respectively, k is a conduction band momentum label.

Generalized operators

Moreover, we introduce generalized operators b and b' . In the physical basis they can be identified with the band or impurity operators if they carry corresponding indices (e.g. $b_d^\dagger = d^\dagger$ (impurity), $b_t = c_t$ (band), etc.). If no particular reference to either band or impurity is intended they are labelled in the physical basis by j .

In this representation, we write a quadratic Anderson-like Hamiltonian with respect to a general matrix element of the Hamiltonian

$$H_{j'j} = \begin{cases} \epsilon_t & \text{if } j' = j = t \\ \epsilon_d & \text{if } j' = j = d \\ V_{td} & \text{if } j' = t \text{ and } j = d \quad \text{or if } j' = d \text{ and } j = t \end{cases} \quad (2.1)$$

$$H = \sum_t \epsilon_t c_t^\dagger c_t + \sum_d \epsilon_d d_d^\dagger d_d + \sum_{td} V_{td} (d_d^\dagger c_t + c_t^\dagger d_d) = \sum_{j'j} H_{j'j} b_{j'}^\dagger b_j \quad (2.2)$$

Pre-diagonalized basis

After the pre-diagonalizing transformation has been performed we expect a mixing of band and impurity operators by linear superposition. Hence only the use of generalised operators makes sense. In this basis, they are labelled by the multi-index s .

A summary of all multi-index definitions for further reference is given in table (2.1).

If more than one index is needed

If more than one index is needed in a particular basis they are distinguished by numeral subindices. To allow for easy consistency checks in later steps of this work we introduce two independent numberings for indices, one is primed, the other unprimed. As a general guiding rule (which does not come without reasonable exceptions) we use primed indices for creation operators and unprimed ones for annihilation operators. This notation is commonly used in the literature on flow equation applications.

2.2 General approach to pre-diagonalization

2.2.1 Definition

We now define the basis transformation \mathcal{B} as the one¹ which describes the change from the physical basis into the eigenbasis of the Anderson Hamiltonian for vanishing on-site interaction. We denote it by its matrix elements B_{sj} .

$$b_s = \sum_j B_{sj} b_j \quad (2.3)$$

2.2.2 General properties of the basis transformation \mathcal{B}

We will make use of the following properties of the transformation:

Unitarity and conservation of the (anti-)commutator

We expect that a diagonalizing transformation preserves the canonical (anti-) commutation relations which are imposed on basis operators. The following lines show that this demand is equivalent to unitarity of a basis transformation.

In the pre-diagonalised basis we set up the anticommutator for the fermionic basis operators b_s and $b_{s'}^\dagger$ and insert the transformation (2.3).

$$\{b_{s'}^\dagger, b_s\} = \sum_{j'j} B_{s'j'}^* B_{sj} \underbrace{\{b_{j'}^\dagger, b_j\}}_{\delta_{j'j}} = \sum_j B_{s'j}^* B_{sj} \stackrel{!}{=} \delta_s^{s'} \quad (2.4)$$

In matrix notation, this reads $B^\dagger B = \mathbb{1}$ and mirrors unitarity of the transformation. We will make use of this property and prove unitarity by checking the invariance of the anticommutator in chapter 7.

Inverse transformation

The inverse of a unitary transformation is easily given by $B^{-1} = B^\dagger$ and its matrix elements by $(B^{-1})_{js} = B_{sj}^*$. For all cases considered here we can choose the transformation to be orthogonal and the inverse is easily given by index permutation: $(B^{-1})_{js} = B_{sj}$.

Relation between transformation matrix elements and the (free) impurity density of states

The free spectral function at zero temperature in equilibrium is closely related to the pre-diagonalising transformation. In chapter 7 we will see that

$$\rho_d^{free}(\omega) = \sum_s |B_{sd}(\epsilon_s)|^2 \delta(\omega - \epsilon_s) \rightarrow |B_d(\omega)|^2 \quad (2.5)$$

The last step holds in the continuous limit, where the dependences on s and ω coincide. Therefore, the squared transformation matrix elements $|B_{sd}|^2$ represent directly the impurity density of states.

¹We assume existence and do not care about uniqueness

2.2.3 "Equation of motion" method

One established way of diagonalizing a quadratic Hamiltonian is to compare the commutators of the transformed operator b_s with the Hamiltonian in both the original and the diagonal basis. From this comparison defining relations for an explicit calculation of the transformation matrix elements can be derived. This method is known under the name of "equation of motion" method which alludes at its obvious similarity with the Heisenberg equation of motion for operators. Both sides of the comparing equation are evaluated separately:

$$[b_s, H_{original}] = [b_s, H_{diagonal}] \quad (2.6)$$

$$\left[\sum_{j_0} B_{sj_0} b_{j_0}, \sum_{j_1', j_1} H_{j_1', j_1} b_{j_1'}^\dagger b_{j_1} \right] = [b_s, \sum_{s_1} \epsilon_{s_1} b_{s_1}^\dagger b_{s_1}] \quad (2.7)$$

$$\sum_{j_0} B_{sj_0} \sum_{j_1', j_1} H_{j_1', j_1} [b_{j_0}, b_{j_1'}^\dagger b_{j_1}] = \sum_{s_1} \epsilon_{s_1} [b_s, b_{s_1}^\dagger b_{s_1}] \quad (2.8)$$

$$\sum_{j_0} B_{sj_0} \sum_{j_1', j_1} H_{j_1', j_1} \delta_{j_0}^{j_1'} b_{j_1} = \epsilon_s b_s \quad (2.9)$$

$$\sum_{j_0} B_{sj_0} \sum_{j_1} H_{j_0 j_1} b_{j_1} = \epsilon_s \sum_{j_1} B_{sj_1} b_{j_1} \quad (2.10)$$

In equation (2.8) we made use of the unitarity of the transformation which conserves the commutator (cf 2.2.2), in the last step on the right hand side we changed back from the pre-diagonal into the physical basis.

Now we employ the linear independence of all operators

$$\sum_{j_0} B_{sj_0} H_{j_0 j_1} b_{j_1} = \epsilon_s B_{sj_1} b_{j_1} \quad \forall j_1 \quad (2.11)$$

and make this relation explicit for the coupling to the band ($j_1 = t$) and to the impurity ($j_1 = d$) operators. Thus we can write

$$\epsilon_t B_{st} + \sum_d B_{sd} V_{td} = \epsilon_s B_{st} \quad (2.12)$$

$$\epsilon_d B_{sd} + \sum_t B_{st} V_{td} = \epsilon_s B_{sd} \quad (2.13)$$

These equations can be used to calculate the transformation B for different models, particularly for different assumptions to the hybridization V .

2.2.4 Assumptions on the model

In order to allow for an easy analytical solution of the equations (2.12) and (2.13) we make use of the following assumptions. They are sufficient to apply the pre-diagonalizing transformation to the Anderson impurity Hamiltonian.

Localized hybridization

First of all we assume a localized hybridization, i.e. $V(x) \sim \delta(x)$, which implies $V(k) = \text{const}$ is flat in momentum space. Any other conceivable dependency of the hybridization is neglected.

One-level-impurity

Moreover we only consider a single impurity with a unique energy level. This assumption simplifies equation (2.12) tremendously as the sum over d reduces to a sum over degenerate spin states of the impurity.

Single spin channel

Finally we even restrict our attention to a single spin channel of the model. In the appendix (B) we show that the inclusion of several degenerate spin levels (i.e. of more than one spin channel) can be absorbed by a re-definition of the hybridization whenever the number of spin states on the impurity and in the bands is equal. This is a trivial fact if we assume electrons with two possible different spin orientations to occupy both the conduction band and the impurity. Therefore we only consider a single spin channel and replace the multi-index t by the momentum label k of the conduction band electrons.

This assumption again simplifies equation (2.12) tremendously as the sum over d vanishes.

2.3 Explicit transformation for one-level impurities

In this section, we aim at an explicit solution for the pre-diagonalizing matrix elements which we will use to reexpress the Anderson Hamiltonian. We follow the spirit of von Delft and Schoeller [20] (Appendix I).

2.3.1 Implementation of assumptions

As a first step we implement the assumptions made above in the equations (2.13) and (2.12) and arrive at a simple set of coupled linear equations for the matrix elements.

$$\epsilon_s B_{sk} = \epsilon_k B_{sk} + V B_{sd} \quad (2.14)$$

$$\epsilon_s B_{sd} = \epsilon_d B_{sd} + V \sum_k B_{sk} \quad (2.15)$$

Self-consistency equation for energies

By eliminating the matrix elements of the transformation we receive a self-consistency equation for the transformed energies ϵ_s

$$1 = \frac{V^2}{\epsilon_s - \epsilon_d} \sum_k \frac{1}{\epsilon_s - \epsilon_k} =: \frac{V^2}{\epsilon_s - \epsilon_d} S^{(1)}(\epsilon_s) \quad (2.16)$$

Transformation matrix elements

Directly one recognizes the following relation between the matrix elements:

$$B_{sk} = \frac{VB_{sd}}{\epsilon_s - \epsilon_k} \quad (2.17)$$

Using the normalisation condition for the (unitary) transformation

$$\sum_k |B_{sk}|^2 + |B_{sd}|^2 = 1 \quad (2.18)$$

we obtain for the matrix elements of the transformation

$$|B_{sd}|^2 = \frac{1}{V^2 S^{(2)} + 1} \quad (2.19)$$

We can choose \mathcal{B} to be orthogonal and do not need to care about a potential phase factor.

Energy sums as main structures

Consequently, the transformation \mathcal{B} is known as soon as the following sums have been calculated

$$S^{(1)}(\epsilon_s) = \sum_k \frac{1}{(\epsilon_s - \epsilon_k)} \quad (2.20)$$

$$S^{(2)}(\epsilon_s) = \sum_k \frac{1}{(\epsilon_s - \epsilon_k)^2} \quad (2.21)$$

2.3.2 Evaluation of the transformation matrix elements for a discrete set of band energies

In the following section we calculate the energy sums $S^{(1)}$ and $S^{(2)}$ for a discrete distribution of band energies. This corresponds to a restriction of the system to a limited volume only ("box model") and introduces dependencies on its scale into wave functions and matrix elements. Noting that both the hybridization V and the band energies ϵ_k are defined as matrix elements according to the formalism of second quantisation, and considering the localization of the impurity they acquire the following scaling behavior:

$$V \rightarrow \sqrt{\Delta_L} V_0 \quad \epsilon_k \rightarrow \Delta_L \epsilon_k^0 \quad (2.22)$$

Furthermore, we assume a constant energy level spacing Δ_L for the conduction band, unlimited bandwidth and a linear dispersion relation

$$\epsilon_k = \Delta_L \nu \left(k + \frac{1}{2} \right) \quad (2.23)$$

The constant offset in the dispersion relation was defined for convenience; it will not have any impact on the final result.

Details of the calculation*

All summations extend to infinity as we assume unlimited bandwidth. Using the properties of the Ψ_γ -function [21]

$$\begin{aligned}\Psi(1 - \alpha) &= \sum_{k=1}^{\infty} \frac{1}{\alpha + k} \\ \Psi(1 + \alpha) &= \Psi(\alpha) + \frac{1}{\alpha} \\ \Psi(1 - \alpha) &= \Psi(\alpha) + \pi \cot(\pi\alpha)\end{aligned}$$

sums extending to infinity on both sides are easily written as

$$\sum_{k=-\infty}^{\infty} \frac{1}{\alpha + k} = \pi \cot(\pi\alpha) \quad (2.24)$$

Evaluating the sum $S^{(1)}(\epsilon_s)$ results in

$$\begin{aligned}S^{(1)}(\epsilon_s) &= \sum_k \frac{1}{(\epsilon_s - \epsilon_k)} = \sum_{k=-\infty}^{\infty} \frac{1}{\epsilon_s - \Delta_L \nu (k + \frac{1}{2})} \\ &= \frac{-1}{\Delta_L \nu} \sum_{k=-\infty}^{\infty} \frac{1}{k + 1/2 - \frac{\epsilon_s}{\Delta_L \nu}} = \frac{-\pi}{\Delta_L \nu} \cot\left(\frac{\pi}{2} - \frac{\pi}{\Delta_L \nu} \epsilon_s\right) \\ &= \frac{-\pi}{\Delta_L \nu} \tan\left(\frac{\pi}{\Delta_L \nu} \epsilon_s\right)\end{aligned}$$

The sum $S^{(2)}$ can be regarded as a derivative of $S^{(1)}$.

$$\begin{aligned}S^{(2)}(\epsilon_s) &= \sum_k \frac{1}{(\epsilon_s - \epsilon_k)^2} = -\frac{\partial}{\partial \epsilon_s} \sum_k \frac{1}{\epsilon_s - \epsilon_k} \\ &= \frac{\partial}{\partial \epsilon_s} \frac{\pi}{\Delta_L \nu} \tan\left(\frac{\pi}{\Delta_L \nu} \epsilon_s\right) = \frac{\pi^2}{\Delta_L^2 \nu^2} \frac{1}{\cos^2\left(\frac{\pi}{\Delta_L \nu} \epsilon_s\right)} \\ &= \frac{\pi^2}{\Delta_L^2 \nu^2} + \left[S^{(1)}(\epsilon_s)\right]^2 = \frac{\pi^2}{\Delta_L^2 \nu^2} + \left[\frac{\epsilon_s - \epsilon_d}{V_0^2 \Delta_L}\right]^2\end{aligned}$$

In the last step we used the self-consistency equation (2.16) and the scaling behavior of V . We insert this result into equation (2.19) and separate off the system size according to (2.22).

Functional form of matrix elements

Finally we obtain the following squared matrix elements of the transformation $|B_{sd}|^2$, which couple the transformed band operators b_s to the impurity operator d :

$$|B_{sd}|^2 = |B_{sd}(\epsilon_s - \epsilon_d)|^2 = \frac{\Delta_L}{\frac{V_0^2 \pi^2}{\nu^2} + \Delta_L + \frac{(\epsilon_s - \epsilon_d)^2}{V_0^2}} \quad (2.25)$$

We observe that the hybridization causes a coupling of the impurity to band electrons of a -practically- limited section of the energy spectrum. The matrix elements show the relative weight of the coupling which is Lorentz-distributed with respect to the energy difference $\epsilon_s - \epsilon_d$ and peaked at the impurity energy. This coupling effectively promotes the localized impurity to a collective band phenomenon.

Energy scale of the hybridization

A typical energy scale is set up by the width (half width at half height) of the Lorentzian curve $\Delta \stackrel{\text{Def}}{=} V_0 \sqrt{\frac{V_0^2 \pi^2}{\nu^2} + \Delta_L}$; we will refer to it as a natural unit of energy in the Hamiltonian. Note that Δ has a well-defined value in the limit $\Delta_L \rightarrow 0$ which is for small energy level spacing the dominating part.

Physical interpretation of the hybridization coupling

We choose $s = d$ and study the appearance of the original impurity level after the pre-diagonalization has been applied. In the case of significant contributions to the denominator by the constant $\frac{V^2 \pi^2}{\nu^2} + \Delta_L$ and the availability of band energies around the impurity energy the transformed $b_{s=d}$ - operator loses its formerly exceptional character and is constructed primarily as a linear superposition of band operators. Hence we cannot speak of a strict localization of an electron situated at the impurity any more. We see that due to barrier tunneling induced by the hybridization, the impurity eigenstates acquire a non-vanishing amplitude outside of the impurity region.

Summary of discrete results

We briefly summarize the results for discrete band energies for later reference.

$$|B_{sd}|^2 = \frac{\Delta_L}{\frac{V_0^2 \pi^2}{\nu^2} + \Delta_L + \frac{(\epsilon_s - \epsilon_d)^2}{V_0^2}} \quad (2.26)$$

$$|B_{sk}| = \frac{V}{\epsilon_s - \epsilon_k} B_{sd} \quad (2.27)$$

$$\epsilon_s - \epsilon_d = -\sqrt{\Delta^2 + V_0^2 \Delta_L} \tan\left(\frac{\pi}{\Delta_L} \epsilon_s\right) \quad (2.28)$$

In the last line we have rewritten the self-consistency equation (2.16) in terms of the energy scale of the system.

2.3.3 Renormalization of eigenenergies

Under the pre-diagonalization we expect the diagonal elements of the Hamiltonian, which are the eigenenergies in the case of the accomplished transformation, to change. In this section we will show that this change is a irrelevant effect.

In a discrete model, energy changes could be -in principle- calculated from the self-consistency equation (2.28) which we approximate for the case $\Delta^2 \gg V_0^2 \Delta_L$:

$$\frac{\epsilon_s - \epsilon_d}{\Delta} = -\tan\left(\frac{\pi}{\Delta_L \nu} \epsilon_s\right) \quad (\rightarrow 2.28)$$

Graphical or numerical approaches are possible to solve this equation. To get a rough idea of the renormalisation changes we apply the linear dispersion relation (2.23) for the renormalised energy and discuss the equation in momentum space.

$$\frac{\Delta_L \nu}{\Delta} \left(k + \frac{1}{2}\right) - \frac{\epsilon_d}{\Delta} = -\tan\left(\pi \left(k + \frac{1}{2}\right)\right) \quad (2.29)$$

For a graphical solution we treat the left hand side and the right hand side of the self-consistency equation (2.29) as independent functions which depend on a continuous parameter k and study the intersection of their graphs. The projection of the point of intersection onto the energy axis defines (via the dispersion relation) the renormalised energies.

For an uncoupled impurity, i.e. for $\Delta \rightarrow 0$, the eigenenergies clearly coincide with the poles of the tangens function. Equation (2.29) shows that a nonvanishing hybridization strength simply enters through the denominator on the left hand side and thus only determines the gradient of the straight line. Figure (2.1) explains how the shift of band energies depends on the hybridization and the impurity energy level and illustrates that only a limited number of band energies close to the impurity level experience a nonvanishing energy shift. Moreover the clear dependence on the hybridization makes it easy to relate the solutions of the self-consistency equation with the unrenormalised energy values. This shows that the energy shifts are always smaller than the level spacing. Therefore we do not expect a significant change in the density of states around the impurity. Finally, the sharp descent of the tangens function close to its pole guarantees that all other energies are practically unaffected.

Renormalisation of continuous band energies

In the case of a continuous energy band with unlimited bandwidth such renormalisation changes only become important if they redistribute the density of states in energy space. Figure 2.1 shows that we can neglect such effects. Hence we continue to work with a constant density of states.

2.3.4 Limit of continuous energy distribution

We proceed to an infinite size box model by taking the limit $L \rightarrow \infty$. It corresponds to the limit of a continuous band energy distribution, i.e. $\Delta_L \rightarrow 0$. We emphasize the fact that the matrix elements of equation (2.25) represent a discrete distribution of the weight of a unitary transformation and think of it as a step function in (continuous) energy space; it changes at integer values which are separated by energy intervals of length Δ_L . Thus the limiting procedure must be defined in a way which preserves normalisation. We set

$$\Delta_L \rightarrow 0 \tag{2.30}$$

under the condition that

$$\Delta_L \sum_k \longrightarrow \int d\epsilon_k \rho \tag{2.31}$$

remains invariant. $\rho = \frac{\partial k}{\partial \epsilon}$ is the density of states which is for a linear dispersion relation equal to the inverse of $\nu \Delta_L$ (cf 2.23). It diverges in the limit of $\Delta_L \rightarrow 0$ such that it could be reasonable not to perform this limit completely but to stop at a small value of Δ_L which corresponds to the correct physical density of states. Then an almost continuous electronic band is produced.

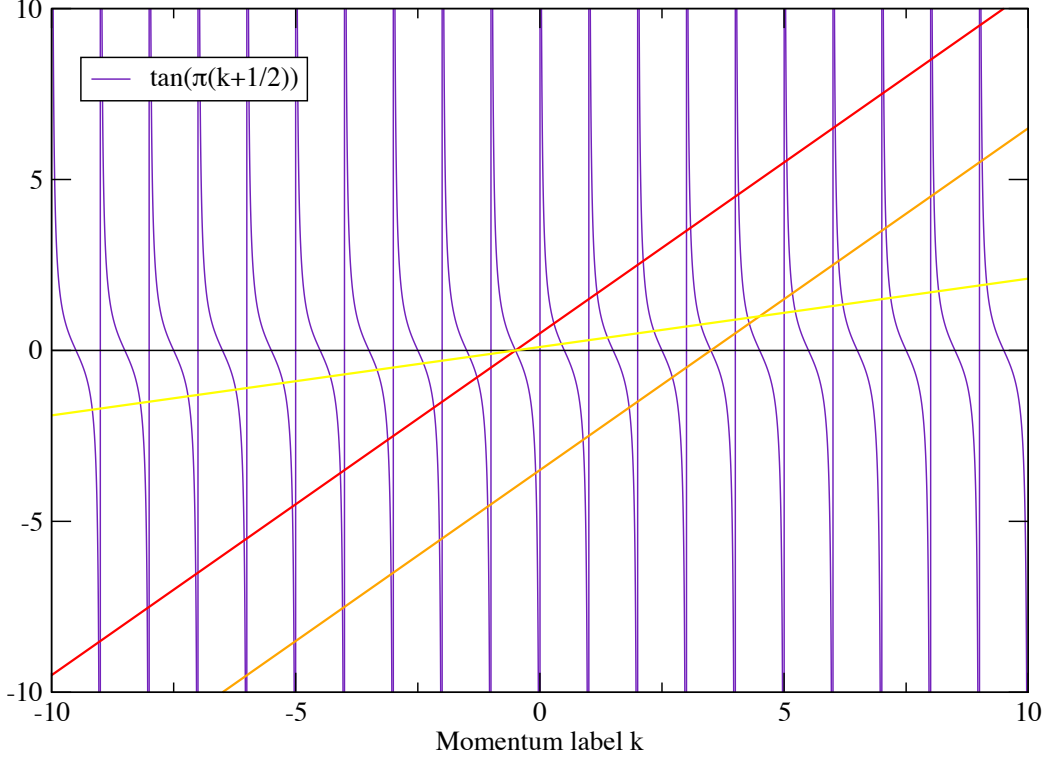


Figure 2.1: Renormalization of discrete band energies under the pre-diagonalising transformation. The self-consistency equation (2.29) is evaluated graphically in momentum space. At the poles of the tangens function the free band energies are located. The projection of the intersections with one of the straight lines defines approximately the renormalised energies. The straight lines represent the left hand side of (2.29) for different configurations. The red and the orange line show the case of unit hybridization for a symmetric ($\epsilon_d = 0$) and an asymmetric ($\epsilon_d = 4\Delta$) impurity. One observes that the greatest energy shifts occur for few eigenenergies close to the impurity level. All energy shifts are smaller than the level spacing. Far off energies are practically not affected.

The influence of the hybridization strength in the case of $\epsilon_d = 0$ can be studied by comparing the red ($\Delta = 1\Delta_0$) and the yellow ($\Delta = 5\Delta_0$) line. With increasing hybridization the energy shifts grow and are relevant in an extended region which size is proportional to the hybridization strength. The plot is for $\frac{\Delta_L \nu}{\Delta_0} = 1$.

In the limit of $\Delta_L \rightarrow 0$ the left hand side of (2.29) is a constant. Then we observe an irrelevant constant shift of all energies but no changes of their relative distances. This means that the density of states does not experience any inhomogeneities at all. See, for instance, the intersection points of the tangens curve with the zero line (momentum axis).

2.3.5 The hybridization function and its properties

In this limit the transformation matrix elements (2.25) for a one-level impurity model can be expressed as a continuous weight function of Lorentzian shape:

$$W^2(\epsilon_s) = \frac{1}{\Delta\pi\rho} \frac{1}{1 + \frac{(\epsilon_s - \epsilon_d)^2}{\Delta^2}} \quad (2.32)$$

with the hybridization energy scale $\Delta = V_0^2 \rho \pi$ given by the width of the Lorentzian curve. We call W^2 the *hybridization function* and refer to its energy dependence either explicitly or by labelling it with the index of its argument ($W(\epsilon_i) \equiv W_i$). As this function will appear in many cases we introduce a shorthand notation for products:

$$W_{ijkl\dots} \equiv W(\epsilon_i) W(\epsilon_j) W(\epsilon_k) W(\epsilon_l) \dots$$

and similarly for higher powers

$$W_{ijkl\dots}^2 \equiv W^2(\epsilon_i) W^2(\epsilon_j) W^2(\epsilon_k) W^2(\epsilon_l) \dots$$

Normalisation

It can be easily seen that the hybridization function is normalised in energy space. We use the substitution $x = \frac{\epsilon - \epsilon_d}{\Delta}$.

$$\int_{-\infty}^{\infty} d\epsilon \rho W^2(\epsilon) = \frac{1}{\pi} \int_{-\infty}^{\infty} dx \frac{1}{1 + x^2} = 1 \quad (2.33)$$

Kramers-Kronig transform of the hybridization

For later evaluations we calculate the Kramers-Kronig transform $K(\omega)$ of the hybridization. We denote its definition in momentum space and energy space by

$$K(\omega) = \sum_k W^2(\epsilon_k) \frac{1}{\omega - \epsilon_k} = \rho \int d\epsilon W^2(\epsilon_k) \frac{1}{\omega - \epsilon_k} \quad (2.34)$$

We refer to [22] (p. 80, 2.18) for an analytic solution of the integral and use the normalisation of W^2 in energy space.

$$K(\omega) = \pi\rho \frac{\omega - \epsilon_d}{\Delta} W^2(\omega) \underbrace{\int d\epsilon_k W^2(\epsilon_k)}_1 = \pi\rho \frac{\omega - \epsilon_d}{\Delta} W^2(\omega) \quad (2.35)$$

2.4 Transformation of the Fermi functions

Fermi functions are defined as correlators, i.e. as expectation values with respect to a ground state. Thus we can study the behaviour of Fermi functions under the transformation by analyzing the correlator. We assume that the multi-particle ground state which can be described

as a Fermi sea is not significantly changed; all variations are considered to arise from the transformation of the operators.

$$\begin{aligned}
\tilde{n}^+(\epsilon_s) &= \langle \tilde{G}S | b_s^\dagger b_s | \tilde{G}S \rangle \approx \sum_{j',j} B_{sj'}^\dagger B_{sj} \langle b_{j'}^\dagger b_j \rangle \\
&= \sum_{k'k} B_{sk'}^\dagger B_{sk} \underbrace{\langle c_{k'}^\dagger c_k \rangle}_{n^+(\epsilon_k)} + B_{sd}^\dagger B_{sd} \underbrace{\langle d^\dagger d \rangle}_{n_d} \\
&= \sum_k |B_{sk}|^2 n^+(\epsilon_k) + |B_{sd}|^2 n_d \\
&\stackrel{(2.17)}{=} |B_{sd}|^2 \left[V^2 \sum_k \frac{n^+(\epsilon_k)}{|\epsilon_s - \epsilon_k|^2} + n_d \right] \tag{2.36}
\end{aligned}$$

We discuss this relation at zero temperature. Then the Fermi function is given by

$$n^+(\epsilon) = \begin{cases} 1 & \text{for } \epsilon < 0 \\ 0 & \text{for } \epsilon > 0 \end{cases} \tag{2.37}$$

and imposes effectively a restriction on the domain of the summation in (2.36) which terminates at the Fermi energy $\epsilon_F = 0$:

$$\sum_k n^+(\epsilon_k) \rightarrow \sum_{k=-\infty}^0$$

For $\epsilon_s \ll 0$ this restriction does not change the value of the summation dramatically as the main contributions come from the region around the pole at ϵ_s which remains unaffected. With (2.19) we find $n^+(\epsilon_s \ll 0) = 1$.

For $\epsilon_s \gg 0$ we face a contrary situation: The relevant contributions to the sum all vanish and so does the squared matrix element $|B_{sd}|^2 = W^2(\epsilon_s)$ itself. This results in $n^+(\epsilon_s \gg 0) = 0$.

Thus we only expect changes to the Fermi distribution function for a small energy interval of size $\sim \frac{\Delta}{N}$ around the Fermi energy. In this regime the original sharp Fermi edge is smoothed under the hybridization. A detailed analysis of the sums involved or a numerical treatment could show the dependence on the inverse of the number of discrete band energies N , i.e. on the system size. Thus we expect that these corrections vanish in the continuous limit $N \rightarrow \infty$ and continue to work with an unchanged Fermi function (2.37) in the pre-diagonalized basis.

2.5 Summary

In this chapter we have applied a basis transformation to treat the hybridization coupling in a resonant level model, i.e. for zero on-site interaction. We have calculated the matrix elements B_{sj} of the transformation and proved the approximate invariance of the band energies and the Fermi distribution function. If more complex multi-level systems have to be considered, such a pre-diagonalization may be done differently, for example by numerical methods.

Re-expressed Anderson Hamiltonian

For our purpose it is sufficient to write down the full (one-level) Anderson Hamiltonian (1.6) in the pre-diagonalised basis. It will be the starting point for an application of the flow equation

technique. Again we use multi-index notation and recapitulate that the hybridization function $W_s = W(\epsilon_s)$ is independent of the spin part of the multi-index s .

$$H_{\text{Anderson}} = \sum_s \epsilon_s :b_s^\dagger b_s: + U \sum_{s_1' s_2' s_1 s_2} W_{s_1' s_1 s_2' s_2} :b_{s_1'}^\dagger b_{s_1} b_{s_2'}^\dagger b_{s_2}: \quad (2.38)$$

From a physical point of view this transfers the Anderson Hamiltonian into a quasiparticle - multiparticle basis which already includes the effects caused by the hybridization. Consequently, the free part of the Hamiltonian already represents electronic bands, the impurity part and their interaction.

Re-definition of the coupling constant

In this basis it is more reasonable to talk about a two-quasiparticle interaction as the impurity has changed into a collective band phenomenon. We introduce a set of coupling constants by

$$U_{s_1' s_1 s_2' s_2} = U W_{s_1' s_1 s_2' s_2} \quad (2.39)$$

This will simplify necessary generalizations in the flow equations approach. There we will allow for a flow of the coupling U under which it will acquire a more distinguished energy dependence.

Part II

Application of the flow equation method to a pre-diagonalized Anderson impurity model

Chapter 3

Introduction to the flow equation method

In the last chapter we have obtained a diagonal representation of a quadratic Hamiltonian. We continue the examination of the Anderson impurity model in this particular basis but include the quartic interaction term. In general an exact diagonalization of this kind of Hamiltonians is not possible. We therefore develop the flow equation method as an approximate diagonalization procedure.

3.1 History of the flow equations approach

3.1.1 Origins

The flow equation method is a rather new development proposed independently by Wilson and Glazek in the field of high energy physics under the name *Similarity renormalization scheme* in 1993 and by Wegner in a context of condensed matter theory in 1994 [23][24][25]. The flow equation method is characterised by the merger of two fruitful ideas of theoretical physics: On the one hand, it reverts to perturbation theory to define an infinitesimal unitary transformation in a controlled sequence of contributions, on the other hand it incorporates scaling and renormalization group ideas to extend the infinitesimal structure to finite transformations. From this crossover the method acquires highly desirable features, first of all a well-defined way to separate and to conserve different energy scales.

3.1.2 Applications

The flow equation method has already been applied to a variety of different model systems. For instance, quantum dissipation has been studied, e.g. in the spin-boson model [26] by means of flow equations. Moreover, they have proved to be a reliable tool to treat strongly correlated systems like the Sine-Gordon model and the Kondo model [27].

In the recent past the flow equation method has been identified as a promising technique to approach out-of-equilibrium situations even in strong coupling regimes. For instance, in 2004 Kehrein discussed scaling and decoherence properties of the out-of-equilibrium Kondo model [28]. This and many other works will be presented in great detail in his book on flow equations [29].

3.2 Infinitesimal unitary transformations

In contrast to the straightforward approach of finding a single transformation which fully diagonalizes the Hamiltonian we study infinitesimal unitary transformations which make the Hamiltonian in a well-defined sense more energy diagonal by re-distributing weight of the off-diagonal matrix elements onto the diagonal ones. In a second step they will be arranged in a continuous order to generate an effective transformation.

3.2.1 Flow equation of an observable

The cornerstone of the flow equation method is a detailed analysis of such infinitesimal unitary transformations. In this section we develop a particular formalism to treat interactive systems which transfers unitary transformations on operator space into sets of coupled differential equations for generalized coupling constants. This analysis holds for arbitrary elements of the operator space, which we simply refer to as *observables*. Although the driving motivation for our approach is the diagonalisation of the Hamiltonian, we proceed with a more general treatment to highlight the particular role that unitary transformations play in this method.

Definitions

We start with defining an observable $A \in \mathbb{S}$ on the conventional operator space \mathbb{S} of quantum mechanics and introduce a unitary transformation U . It can be represented as an exponential of an element living on the corresponding Lie algebra, called its *generator* and denoted by η . To ensure unitarity η has to be an antihermitian operator. We label the observable before and after the transformation by values of a continuous parameter, furtheron called the *flow parameter* B .

$$A(B) = U(B, B_0)A(B_0)U^{-1}(B, B_0) = e^{\eta(B_0)(B-B_0)}A(B_0)e^{-\eta(B_0)(B-B_0)} \quad (3.1)$$

Formal derivation

For an infinitesimal transformation promoting $A(B_0)$ to $A(B)$ we compute the change of the observable:

$$\frac{\partial A(B)}{\partial B} = (\partial_B U(B, B_0))U^{-1}UA(B_0)U^{-1} + UA(B_0)U^{-1}(U\partial_B U^{-1}(B, B_0)) \quad (3.2)$$

Since $\partial_B(UU^{-1}) = 0$ we can define the anti-hermitian generator

$$\eta(B, B_0) \stackrel{\text{def}}{=} (\partial_B U(B, B_0))U^{-1}(B, B_0) = -U\partial_B U^{-1} = -\eta^\dagger(B, B_0) \quad (3.3)$$

Referring to (3.1) we can express the right hand side of equation (3.2) as a commutator. In the infinitesimal limit the values of B_0 and B coincide and we obtain the *flow equation of an observable*.

$$\frac{\partial A(B)}{\partial B} = [\eta(B), A(B)] \quad (3.4)$$

First order result for an explicit representation

For the exponential representation of the unitary transformation, one can explicitly derive the flow equation as a first order result using the Baker-Hausdorff identity.

$$\begin{aligned}
 A(B) &= e^{\eta(B_0)(B-B_0)} A(B_0) e^{-\eta(B_0)(B-B_0)} = \\
 &A(B_0) + dB [\eta(B), A(B_0)] + (dB)^2 \frac{1}{2} [\eta(B), [\eta(B), A(B_0)]] + \dots = \\
 &\sum_{n=0}^{\infty} \frac{1}{n!} (dB)^n [\eta(B), [\eta(B), [\eta(B), \dots A(B_0)]]] \quad (3.5)
 \end{aligned}$$

Now we take the limit $dB \rightarrow 0$ and obtain the same flow equation of A :

$$\lim_{dB \rightarrow 0} \frac{A(B) - A(B_0)}{dB} = \frac{\partial A(B)}{\partial B} = [\eta(B), A(B)] \quad (3.6)$$

3.2.2 Perturbation series in a small expansion parameter

In this form we can easily apply perturbative approximations to the flow equation. Our aim is to split up the observable into a power series in an expansion parameter λ , defining various terms $A^{(n)}$. If A represents the Hamiltonian, they should be considered as interaction terms.

$$A = A_0 + \lambda A^{(1)} + \lambda^2 A^{(2)} + \dots = A_0 + \sum_{n=1}^{\infty} \lambda^n A^{(n)} \quad (3.7)$$

Choice of expansion parameter

To do so we need to identify a suitable expansion parameter of the model. In many cases it is possible to treat the prefactor of the dominating interaction term in the Hamiltonian as such an expansion parameter. In some models, a more subtle choice of the parameter leads to an improved convergence behaviour of the expansion (see, for instance, [28]).

It is important to notice that the perturbative approximations are imposed on the infinitesimal structure of the flow equations. Thus it is crucial to ensure that the expansion retains its convergence properties even under a continuous sequence of transformations. Therefore the analysis of the expansion parameter under a continuous sequence of infinitesimal transformations will be an important part of the work (see chapter 5).

We will find out that for the Anderson impurity model a straightforward choice is possible and restrict to this case.

Expansion of the generator

The same expansion as in 3.7) is done for the generator η . Keeping in mind that for $\lambda = 0$ the Hamiltonian would already be diagonal we note that η must be at least first order in the expansion parameter.

$$\eta = \lambda \eta^{(1)} + \lambda^2 \eta^{(2)} + \dots = \sum_{n=1}^{\infty} \lambda^n \eta^{(n)} \quad (3.8)$$

Expanded flow equation

Inserting these expansions into (3.6) we obtain the following series:

$$\frac{\partial A(B)}{\partial B} = \lambda [\eta^{(1)}, A_0] + \lambda^2 \left([\eta^{(1)}, A^{(1)}] + [\eta^{(2)}, A_0] \right) + O(\lambda^3) \quad (3.9)$$

While this expansion in λ primarily aims at providing perturbatively consistent approximations and largely depends on the identification of a suitable expansion parameter, the expansion of an observable in terms of generalized coupling constants is of immense practical importance. Both expansions do not need to coincide.

3.2.3 Expansion in generalised coupling constants

Choice of a multiparticle basis

The expansion of an observable A in terms of generalized coupling constants can be explained as a representation of A in a canonical multiparticle basis of the operator space \mathbb{S} . Such a multiparticle basis may be defined as a union of all subsets containing single creation or annihilation operators, then operator products of length two, three and so on.

$$S_{(1,0)} = \{b_{s'_1}^\dagger\} \quad S_{(0,1)} = \{b_{s_1}\} \quad (3.10)$$

$$S_{(1,1)} = \{ :b_{s'_1}^\dagger b_{s_1} : \} \quad S_{(0,2)} = \{ :b_{s_1} b_{s_2} : \} \quad \dots \quad (3.11)$$

The subsets shall contain all operator products in the parameter range of their multi-indices. For physical reasons explained in detail in section (3.2.5) we choose a basis of normal ordered products. Therefore the subsets $S_{(m,n)}$ can be characterized by the number of creation (m) and annihilation (n) operators of their elements.

Multiparticle basis representation of an observable

We now represent an observable in this basis:

$$A = \sum_{m,n} \sum_{s'_1 s'_2 \dots s'_m, s_1 s_2 \dots s_n} g_{s'_1 s'_2 \dots s'_m, s_1 s_2 \dots s_n} :b_{s'_1}^\dagger b_{s'_2}^\dagger \dots b_{s'_m}^\dagger b_{s_1} b_{s_2} \dots b_{s_n}: \quad (3.12)$$

where the coefficients $g_{s'_1 s'_2 \dots s'_m, s_1 s_2 \dots s_n}$ may be called generalized coupling constants. For any observable defined to describe a physical system usually only a very limited number of subsets contribute. If we, for instance, consider the Hamiltonian, this representation corresponds to its decomposition into a free part and various interaction terms:

$$H = H_0 + H_{int}^{(1)} + H_{int}^{(2)} + \dots \quad (3.13)$$

Putting aspects of normal ordering on hold, we rediscover the language of second quantization. The coefficients g coincide with the one-particle energies, the coupling constants of scattering processes and those of higher order excitations.

Similarly we expand the generator in this basis, denoting the generalised coupling constants by $\eta_{t'_1 t'_2 \dots t'_k, t_1 t_2 \dots t_l}$.

3.2.4 Flow equations of the generalized coupling constants

We proceed with developing the conventional framework for the flow equation formalism. We now explicitly focus on the change of the coefficients of the basis expansion, i.e. on the behaviour of the generalized coupling constants under infinitesimal unitary transformations. We insert the basis expansion (3.12) of the generator and the observable into the flow equation (3.6)

$$\begin{aligned} \frac{\partial A(B)}{\partial B} &= [\eta(B), A(B)] \\ &= \sum_{k,l} \sum_{m,n} \sum_{t'_1 \dots t'_k, t_1 \dots t_l} \sum_{s'_1 \dots s'_m, s_1 \dots s_n} \eta_{t'_1 \dots t'_k, t_1 \dots t_l}(B) g_{s'_1 \dots s'_m, s_1 \dots s_n}(B) \\ &\quad [:b_{t'_1}^\dagger \dots b_{t'_k}^\dagger b_{t_1} \dots b_{t_l} : , :b_{s'_1}^\dagger \dots b_{s'_m}^\dagger b_{s_1} \dots b_{s_n} :] \end{aligned} \quad (3.14)$$

Obviously, lengthy commutator structures appear; evaluating them is a major effort when applying the flow equation method to physical systems. The experienced reader might already guess that for most practical purposes approximations are necessary to handle the expressions involved. An important observation shows that these have to be introduced with due diligence: we notice that due to the presence of higher commutators a nonzero change of a generalized coupling constants might arise even if this constant did not contribute to the original basis expansion of the observable. This means that after the transformation the observable may contain newly generated contributions ('interactions'), potentially even of higher order¹.

The reader might be already reminded of renormalization group ideas. Therefore we stress that until this point no 'thinning out' of any degrees of freedom occurred; we still analyze a unitary transformation. The emergence of higher order terms is not a consequence of any kind of thinning procedure.

We will postpone the issue of approximations to formulate the flow equations for the generalized coupling constants first. We re-arrange the various constants involved in the right hand side of equation (3.14) and write it in terms of a basis expansion with new generalized coupling constants $f_{(m,n)}(\eta_{(k,l)}(B), g_{(m,n)})$. These are functions of the coefficients of the observable ($g_{(m,n)}$) and the generator ($\eta_{(k,l)}$) as well as of correlators introduced by the normal ordering procedure. They contain the full information of the infinitesimal unitary transformation.

$$\frac{\partial A(B)}{\partial B} = \sum_{m,n} \sum_{s'_1 \dots s'_m, s_1 \dots s_n} f_{s'_1 \dots s'_m, s_1 \dots s_n}(\eta_{(k,l)}(B), g_{(m,n)}) :b_{s'_1}^\dagger \dots b_{s'_m}^\dagger b_{s_1} \dots b_{s_n} : \quad (3.15)$$

Inserting the basis representation of the observable (3.12) into the left hand side of this equation allows for a comparison of the coefficients. Note that such a comparison is always possible if the generalized coupling constants are considered as generic variables. It produces a set of coupled differential equations for these generalized coupling constants, commonly referred to as the *flow equations*:

$$\frac{\partial g_{s'_1 s'_2 \dots s'_m, s_1 s_2 \dots s_n}(B)}{\partial B} = f_{s'_1 s'_2 \dots s'_m, s_1 s_2 \dots s_n}(\eta_{(k,l)}(B), g_{(m,n)}) \quad (3.16)$$

¹ A commutator of operator products of length l and m might contain products up to length $l + m - 2$.

3.2.5 Approximations to the flow equations

We already mentioned the need for approximations in the formalism developed above. The first and obvious way to reduce the number and the complexity of the differential flow equations is to truncate the basis expansion of the observable considered. To prevent misunderstandings we emphasize that we do not intend to approximate the observable by cutting of contributions of its basis expansion present before the unitary transformation was applied. We only limit the number of newly generated contributions, i.e. of generalized coupling constants which vanished originally but not so their flow equation (their derivative). The main challenge of this approach is to identify those terms which dominate and which induce the most interesting physical aspects into the formalism.

Role of normal ordering

A crucial role for a controlled approximation is played by a carefully observed normal ordering of all operator products; therefore we restricted all basis elements to such products. Truly this is only a special choice of the basis used as any operator product can be expressed by a linear superposition of normal ordered products of the same or shorter length.²

Normal ordering is defined with respect to a (ground) state and implements a full deduction of lower order³ expectation values in this particular state from arbitrary operator products. This leads to a desirable separation of physical properties: The coefficients of one-particle operators of the form $b_{s_1}^\dagger, b_{s_1}$ describe in the Hamiltonian the eigenenergies ($s_{1'} = s_1$) and scattering amplitudes ($s_{1'} \neq s_1$). Normal ordering this term deducts its correlator, i.e. its (ground) state expectation value and resets the (ground) state energy. This separates the physical aspect of a free definition of a total energy in the Hamiltonian from one-particle properties. Similarly, two particle operators denoted by $b_{s_1}^\dagger, b_{s_1}, b_{s_2}^\dagger, b_{s_2}$ include for certain parameter values ($s_{1'} = s_1$, etc.) one particle properties. Introducing normal ordering explicitly extracts these contributions by forming mixed terms of a contraction multiplied with a one particle operator. Resumming the coefficients of identical operator products leads to a simple decomposition in terms of a normal ordered basis and physically meaningful generalized coupling constants. This shows that a decomposition of any observable in a normal ordered basis creates an expansion in terms of one-, two- and arbitrary multiparticle properties. Moreover, normal ordering guarantees that neglecting higher order normal ordered terms during a calculation does not implicitly affect lower orders.

To avoid confusion we should underline that normal ordering by itself cannot define a perturbative argument to restrict higher order processes. The commutator of the generator and the observable present in the flow equation might induce a coupling (backaction) of m - and n -particle contributions. Normal ordering this commutator may highlight this effect and allows for safely dropping high particle excitations beyond those originally considered. It does not answer the question how detailed the initial basis representation of an observable should be. This has to be done by studying the dependence of the generalized coupling constants on a universal expansion parameter.

²See appendix (A.1) for technical details.

³'Order' in the context of normal ordering refers to the length of operator products, i.e. to one, two, multiparticle aspects.

Practical generation of a truncation scheme

When a truncation scheme for any observable has to be chosen, a generator is fixed and the observable is represented in the physically most obvious way. Then the flow equation for this observable (3.6) is deduced and in particular the newly generated couplings are studied. Their set of differential flow equations is derived, then searched for a universal expansion parameter and finally analysed to decide in which order of this parameter the various new generalized coupling constants are generated. Depending on the intended accuracy of the calculation, the most dominant new coupling constants are singled out. They are included in the original representation of the observable and the procedure has to be repeated. If the generator was chosen suitably, only a limited number of newly generated structures need to be taken into account in any order of the perturbative parameter.

3.2.6 Transformation of the ground state

In the last section we discussed the effect of an infinitesimal unitary transformation on the operator space of quantum mechanics. Observable physical properties are, instead, defined by expectation values of operators with respect to the considered state of the system; mostly the ground state is of particular interest. As these quantities should be unaffected by any formal transformation applied, the class of unitary transformations is distinguished.

$$\begin{aligned}\langle GS|O|GS\rangle &= \langle GS|U^{-1}UOU^{-1}U|GS\rangle = \\ &= \langle GS|U^\dagger[UOU^\dagger]U|GS\rangle = \langle \tilde{G}S|\tilde{O}|\tilde{G}S\rangle\end{aligned}$$

In many cases, the transformation has to be implemented on the state space and a transformed ground state has to be found. Then meaningful physical properties can be calculated in a straightforward manner.

Perturbative study of the relevance of a ground state transformation

Yet for some specific statements it is sufficient to convince oneself of the irrelevance of the ground state transformation. To do so, we discuss the perturbation series for both the transformed ground state of the system and an arbitrary observable.

$$|\tilde{\Psi}\rangle = U|\Psi\rangle = \frac{1}{N(\lambda)}|\Psi^0\rangle + \lambda|\Psi^1\rangle + \lambda^2|\Psi^2\rangle + \dots \quad (3.17)$$

$$\tilde{O} = UOU^\dagger = O^0 + \lambda O^1 + \lambda^2 O^2 + \dots \quad (3.18)$$

We can choose all states $|\Psi^i\rangle$ for $i > 0$ to be orthogonal to the non-interacting ground state $|\Psi^0\rangle$. This introduces a normalization constant $N(\lambda) = 1 + \alpha_2\lambda^2 + \dots$ which includes no first order term in λ . Now we perform an expansion of expectation values in terms of the perturbative parameter λ .

$$\begin{aligned}\langle \tilde{\Psi}|O|\tilde{\Psi}\rangle &= \lambda^0 \langle \Psi^0|O^0|\Psi^0\rangle + \\ &\lambda^1 [\langle \Psi^0|O^0|\Psi^1\rangle + \langle \Psi^1|O^0|\Psi^0\rangle + \langle \Psi^0|O^1|\Psi^0\rangle] + \\ &\lambda^2 [\langle \Psi^0|O^0|\Psi^2\rangle + \langle \Psi^0|O^2|\Psi^0\rangle + \langle \Psi^2|O^0|\Psi^0\rangle + \\ &\quad \langle \Psi^0|O^1|\Psi^1\rangle + \langle \Psi^1|O^1|\Psi^0\rangle + \langle \Psi^1|O^0|\Psi^1\rangle + \\ &\quad 2\alpha_2 \langle \Psi^0|O^0|\Psi^0\rangle] + \dots\end{aligned} \quad (3.19)$$

In general, all these matrix elements have to be evaluated to obtain consistent results in a fixed order of an expansion parameter.

Application to special operators

We already note in this place that the transformation of the ground state is not a relevant aspect of this work. We will identify the on-site interaction U as a suitable expansion parameter. For all observables which are used to calculate properties of the Anderson impurity model in this work we can show that ground state transformation only introduces corrections which are of higher than second order in the expansion parameter. Therefore we neglect them. A mix of arguments which refer to the orthogonality of the corrections to the ground state (3.17) and to the special properties of the particular operators makes clear that up second order of the expansion only those matrix elements remain which are formed with respect to the non-interacting ground state.

- (1) In order to calculate the retarded impurity Greens function the *anti-commutator* $\{b^\dagger, b\}$ is evaluated. We will find that it has the following expansion:

$$O^0 \sim 1, \quad O^1 = 0, \quad O^2 \sim P$$

P is a non-trivial operator product of creation and annihilation operators. We now apply a special trick: As the zeroth order part $O^0 \sim c$ is a number we do *not* apply a perturbative expansion of the transformed state state but note that a number commutes with any unitary operation.

$$\langle \tilde{\Psi} | c | \tilde{\Psi} \rangle = c \langle \Psi | \underbrace{U^\dagger U}_1 | \Psi \rangle = \langle \Psi | c | \Psi \rangle = \langle \Psi | O^0 | \Psi \rangle \quad (3.20)$$

For the higher order terms we return to the expansion and observe that all first order and all but one second order contributions vanish. Note that the term $2\alpha_2\lambda^2 \langle \Psi^0 | O^0 | \Psi^0 \rangle$ is not present in the expansion now as the O^0 -contributions have been treated in an exact way.

In total, the remaining matrix elements can be re-arranged and understood –in a second order sense– as an evaluation of the operator \tilde{O} with respect to the non-interacting ground state.

$$\langle \tilde{\Psi} | \tilde{O} | \tilde{\Psi} \rangle \stackrel{\mathcal{O}(\lambda^2)}{=} \langle \Psi | \tilde{O} | \Psi \rangle \quad (3.21)$$

- (2) Implicitly, we will assume the same property for the *number operator* as well. In the flow equation approach it is a common assumption that the Fermi function (i.e. the correlator) does not change under the transformation. Otherwise the infinitesimal transformation of the observable could not easily be promoted to a continuous transformation as we will do in the following section. The expansion of the number operator is of the following form:

$$O^0 \sim b^\dagger b, \quad O^1 = 0, \quad O^2 \sim P'$$

While the first order contributions vanish again significant second order corrections remain, foremost the term $\langle \Psi^1 | O^0 | \Psi^1 \rangle$. Fortunately, these corrections finally appear to be not of second but of higher order in the perturbative parameter as pre-factors introduce further powers of it.

We conclude that for the purpose of this work we do not need to refer to the ground state transformation but can constantly assume to work with an unchanged non-interacting ground state. Nonetheless we add the remark that this is different if other operators should be considered, e.g. for the current operator.

3.3 Continuous sequence of infinitesimal transformations

At the heart of the flow equation method lies the idea of applying an ordered, continuous sequence of infinitesimal transformations to the operator space to obtain a significant transformation of an observable. This sequence is chosen under the specific constraint that finally the full net transformation diagonalizes the Hamiltonian. This splitting up of an effective (net) transformation into an infinite sequence of steps introduces an order parameter comparable with time and gives way to separate the treatment of different aspects of the transformation process at different values of this order parameter (at different 'times'). The flow equation method makes use of this opportunity in particular by dealing with different energy scales in a controlled and ordered manner.

3.3.1 Parametrizations

Creating such a sequence of transformations is naturally accompanied by an introduction of parametrization. A one-dimensional flow parameter, denoted by B , is introduced and fixed by the following boundary conditions: $B = 0$ shall refer to the initial step before the transformation is applied, $B \rightarrow \infty$ characterizes the final outcome of the full net transformation. Both the observables (directly or via the generalized coupling constants) and the generator become dependent on this parameter. Studying these quantities or the procedure itself for various values of B is commonly referred to as studying them 'under the flow of B '.

As we restrict to unitary transformations, all infinitesimal transformations appearing in this sequence show the same differential structure explained above, but differ from each other by the precise form of their generators. This freedom to change the generator under the flow is a decisive strength of the method and is the source of energy scale separation. In particular, this makes it different from more conventional approaches which restrict to single unitary transformations. A good example may be the re-examination of the Schrieffer- Wolff-transformation with flow equations [17].

Consequently, the first step is to define a continuous parametrization of the generator with respect to a flow parameter B . This will be presented in the next section. We just briefly mention that various possibilities to choose the generators exist.

3.3.2 Representation of the net transformation

After a parametrization has been introduced, the net transformation performed at a certain value of B can be evaluated by integrating up the infinitesimal transformations. This is done by solving a differential equation for $U(B)$ which directly follows from the definition of the generator in equation (3.3).

$$\eta(B) = (\partial_B U(B)) U^{-1}$$

It can be re-written as a Schroedinger-like equation for a time evolution operator $U(B)$ with the flow parameter replacing time.

$$\partial_B U(B) = \eta(B)U(B) \quad (3.22)$$

The calculation can be found in many textbooks on quantum mechanics and leads to a B -ordered product (denoted by the ordering operator T_B) of the form

$$U(B) = T_B e^{\int_0^B dB' \eta(B')} \quad (3.23)$$

Although this is an exact result, the complicated B -ordering involved renders this result unpractical for non-trivial generators. Therefore it is usually avoided to refer to the full net transformation $U(B)$.

3.3.3 Active and passive view on the transformation

Unitary transformations are linear maps which implement a change between basis representations. They can be equivalently approached from two different points of view.

Sometimes, the features of a basis change are highlighted which means that, in particular, the basis elements are changed themselves. This is commonly known under the name of a 'passive' transformation (figuratively, this is the rotation of the coordinate system under an fixed object). On the other hand, it is sometimes advantageous to think of the transformation as a plain linear map between different objects which are all represented in a fixed operator basis. Then we call it an 'active' transformation (which corresponds to an rotation of the object in a fixed frame). Both views are equivalent but should not be confused.

For the purpose of diagonalizing the Hamiltonian it is commonly referred to the 'passive' view. Yet the transformation of any observable in the flow equation framework is most easily understood if continuous unitary transformations in the constantly fixed original operator basis are considered.

Continuous change of basis representation

In many theories the diagonalization of an Hamiltonian is commonly discussed in terms of the 'passive' view. This could be done in the flow equation framework as well. Then it implies that the basis elements acquire a dependence on the flow parameter. In order to keep the flow equation formalism valid throughout the flow, we have to impose the same canonic (fermionic) anticommutation relations on the fundamental operators at any value of B . This resembles 'equal time anticommutation relations' in conventional quantum field theory.

$$\begin{aligned} \left\{ b_{s'}^\dagger(B), b_s(B) \right\} &= \delta_s^{s'} \\ \left\{ b_{s'_1}^\dagger(B), b_{s'_2}^\dagger(B) \right\} &= \left\{ b_{s_1}(B), b_{s_2}(B) \right\} = 0 \end{aligned}$$

Such conditions define the character of the fundamental operators and, in consequence, of all basis elements of a canonical normal ordered multiparticle operator basis at arbitrary B . Comparing operators at different values of the flow parameter is only possible if both are expressed in a common basis representation, i.e. if they are considered at 'equal time'. Therefore a general procedure is needed to change between different basis representations; it is given by the transformation of the basis elements (observables).

Fixed operator basis

For obvious reasons, such a transformation is best studied in the active picture. Exemplified for a creation operator we see that in the permanently changing frame the operator maintains a simple formal representation $\mathcal{F}_B [b^\dagger(B=0)] = b^\dagger(B)$. Here we denoted the effective unitary transformation by \mathcal{F}_B .

If we, instead, express the transformed operator in terms of the original basis, the action of the unitary transformation is made more explicit:

$$\mathcal{F}_B [b^\dagger(B=0)] = \sum_{m,n} \sum_{s'_1 \dots s'_m, s_1 \dots s_n} g_{s'_1 \dots s'_m, s_1 \dots s_n}(B) :b_{s'_1}^\dagger(0) \dots b_{s'_m}^\dagger(0) b_{s_1}(0) \dots b_{s_n}(0): \quad (3.24)$$

Under the flow, new contributions to the basis expansion emerge. The behaviour of the generalized coupling constants of such observables can be again studied using the flow equation formalism.

In the following part of this work we will only refer to the active view. It has the major advantage that all B -dependence is attributed to the generalized coupling constants and can be easily evaluated by means of real-valued differential equations.

3.3.4 Discussion of initial and final picture

As the flow equation method is a diagonalization procedure it singles out two particular choices of a basis: An initial one is used to define the Hamiltonian; it corresponds to $B=0$. The final basis is defined as the (approximate) eigenbasis of the Hamiltonian. It is reached at the end of the flow procedure ($B \rightarrow \infty$). We briefly review the physical aspects of both descriptions.

Initial basis representation

In the initial representation the diagonal part of the Hamiltonian describes a conduction band of particles. Due to the pre-diagonalization applied to the Anderson impurity model these particles are no physical band electrons of the metallic leads any more. Yet they are quasi-particles which already incorporate the hybridization with a local impurity. To keep notation easy we call them particles nonetheless. The nature of the free Hamiltonian (H_0) defines the character of the creation and annihilation operators which create and destroy one such particle in a specified state. This can be easily expressed by the commutator

$$[H_0(B=0), b_s^\dagger(B=0)] = \epsilon_s(B=0) b_s^\dagger(B=0) \quad (3.25)$$

In this physically accessible basis the two-particle interaction on the impurity is defined in a straightforward manner, similarly the (approximate) non-interacting ground state of the system (the Fermi sea) and, consequently, the one-point correlator are known.

Yet we study a (strongly) interacting system which has to be described by an unknown and potentially complex interacting ground state. This is why we perform a change into the final basis representation.

Final basis representation

When the flow parameter approaches infinity the diagonal basis of the Hamiltonian is reached. Now the full Hamiltonian defines the physical character of the fundamental operators.

$$[H(B = \infty), b_s^\dagger(B = \infty)] = \epsilon_s(B = \infty) b_s^\dagger(B = \infty) \quad (3.26)$$

It describes the creation and annihilation of quasiparticles which additionally include the two-particle interaction on the impurity. They are the proper excitations of the fully interacting system. In this eigenbasis of the system we study its density of states to gain insight into the effects caused by the interactions in and out of equilibrium. A more detailed understanding of the nature of the quasiparticles is provided by the (inverse) transformation of the observable: It shows that expressing the 'quasiparticle' (i.e. $B \rightarrow \infty$) creation and annihilation operators in terms of the 'particle' ($B = 0$) basis makes a sequence of multiparticle contributions explicit. Their quantitative weight increases with the progression of the flow parameter.

3.3.5 Flow of generalized coupling constants

Such and similar quantitative studies of the behaviour of observables under the flow are an interesting aspect of the flow equation method. Again we refer to the expansion of the observable in terms of generalized coupling constants. The opportunity to focus on the individual behaviour of flowing coupling constants is a major strength of the method.

After parametrization of the generalized coupling constants and of the generator by a flow parameter, the flow equations derived in (3.16) hold for all values of B , i.e. they describe the behaviour of the generalized coupling constants under the change of B throughout the flow. Solving this system of differential equations for all values of B makes the continuous change of the observables, in particular the stepwise diagonalization of the Hamiltonian, accessible in a quantitative way. This reminds of scaling and renormalization group ideas which we will briefly discuss in the following section.

3.4 The flow equation method in the context of scaling and RG procedures

We already mentioned that the flow equation method is closely linked to RG and scaling ideas. We will study some of the aspects which relate both approaches with each other.

3.4.1 Pictorial understanding of flows in parameter space

Diagonalization of the Hamiltonian in this framework can be understood as a flow of its coupling constants in parameter space. We follow this very intuitive description which was originally presented in the context of high energy physics by Wilson. Each point of the parameter space corresponds to a certain 'degree' of diagonalization in the sense that the off-diagonal elements in the Hamiltonian have a certain relative weight. In this picture, the flow parameter takes the role of the parametrization of a trajectory which represents the progression of the diagonalization transformation.

If a generator can be found such that a full diagonalization of the Hamiltonian is possible, the original coupling constants of the off-diagonal parts of the Hamiltonian should die away; approximations might change the real behaviour of the coupling constant. Note that this

does not simply imply an equivalent growth of the coupling constant of the diagonal terms in the Hamiltonian, e.g. of the 'renormalized' energies. The flow equation method re-distributes relative weight not just within the original coupling constants of the Hamiltonian, but on a wider range throughout the operator space by means of multi-particle basis transformations. Other off-diagonal elements may emerge and represent an increasing flow. Thus they might require further treatment. In our analysis of the Anderson Hamiltonian we will, for instance, observe the generation of an (off-diagonal) potential scattering term.

3.4.2 Poor man scaling and similar approaches

A straightforward scaling approach known as *Poor man's scaling* has been introduced by Anderson for the study of the Kondo model in 1970 [30] and later on applied to the equilibrium Anderson impurity model by Haldane [31]. Reprints of these early works and slightly fusty but valuable introductions can be found in [32]. Scaling is implemented as a reduction of a cut-off parameter at the band edge which eliminates states around it. The effects of these removed states are absorbed into renormalized parameters of an effective, form-invariant Hamiltonian. Similar ideas have been used to study the out-of-equilibrium Anderson model. Scaling has been straightforwardly and independently applied around the two different Fermi edges of the left and the right electronic reservoir. Such a setup is -in principle- inherently independent of an important energy scale of the system, namely the voltage bias. In the low energy regime the energy difference between both Fermi edges is effectively neglected and intermediate states between both Fermi edges are lost. As transport properties should depend heavily on those it is not obvious that this approach suits the special character of out-of-equilibrium situations. The flow equation method, instead, is rooted in a unitary transformation and retains all energy scales of the system. Therefore we assume that it is particularly well-designed for an examination of models in non-equilibrium and could be understood as a generalization of Anderson's poor man scaling approach. Still, a scaling picture of flowing couplings can be drawn and, moreover, a certain order in the treatment of energy contributions can be achieved.

3.4.3 Separation of energy scales

Many problems in condensed matter theory are characterized by the emergence of different energy scales: For instance, impurity problems show the coexistence of Coulomb repulsion energies of magnitude eV, electronic excitations around the Fermi surface comparable to temperature (typically meV), potentially large electronic bandwidths and possibly applied outer voltages. A careless use of ordinary perturbation theory might simply disregard energies which have a fundamental impact on the description of the physical system and produce meaningless results.

In such situations, scaling and RG arguments are commonly used to extend a perturbative treatment of high energies successively to the low energy sector which one is usually interested in. This is accompanied by a thinning procedure which takes out explicit high energy contributions and absorbs them implicitly in the low energy properties of the model. This procedure is iteratively applied until an effective theory for the low energy limit has been constructed.

The flow equation method incorporates the same spirit for diagonalizing the Hamiltonian, but replaces the thinning out of high energies by suppressing far energy correlations; instead

of absolute energy values energy differences are continuously removed. This implies the conservation of energy scales in the following sense: Throughout the process all energy scales contribute but subsequently correlations between distant energy regimes are suppressed. A special choice of the generator ensures that, firstly, correlations between far off energy regimes vanish, but within the individual regimes the procedure remains uneffective. With growing flow parameter even lower correlations are dealt with such that the couplings of even closer lying energy scales disappear. Transitions between far-off energy regimes are now described by multi-step processes including intermediate energies. They are usually suppressed by higher orders of a perturbative parameter and therefore effectively dropped. Finally, with the flow parameter approaching infinity, the Hamiltonian assumes diagonal shape.

3.4.4 Comparison of scaling and the flow equation method

Summing up the last ideas leads to an imaginative comparison of the scaling and the flow equation procedure. We choose a matrix representation of the Hamiltonian and study the successive effects of both methods on its appearance.

While the scaling procedure is characterized by reducing the dimension of the Hilbert space by eliminating high energy degrees of freedom, the flow equation method retains the full Hilbert space. Flow equations diagonalize the Hamiltonian by transferring weight from off-diagonal elements onto the diagonal line. The scale Λ_{feq} measures the degree of diagonalisation and corresponds to the cut-off Λ_{RG} of the RG technique. If these values coincide we expect a similar description of the low energy limit $E \ll \Lambda$ by both methods: The main difference between both approaches, the remaining energy scales beyond the size of Λ in the flow equation Hamiltonian, does not affect the low energy properties as it could contribute only in terms of rare multi-particle processes. This highlights again the special notion of energy scale separation in the context of the flow equation method: The pure conservation of all the scales is a remnant of unitarity, the decoupling of these scales induces RG-like behaviour and the main advantage of the flow equation approach shows up as soon as different energy scales are still present in the transformed model. Then every region around a chosen energy $E_0 \gg \Lambda_{feq}$ with $|E - E_0| < \Lambda_{feq}$ is treated like a low energy regime in conventional scaling techniques. We use this particular feature to study low energy properties of a system under out-of-equilibrium conditions which are characterized by the presence of another energy scale, the voltage bias applied to the system.

3.5 Definition of the generator

All characteristic features of a specific unitary transformation are pre-defined by the choice of its generator⁴. Therefore the generator plays a decisive role when studying the properties of the flow equation method. As already mentioned, the strength of this approach lies in the controlled change of the generator under the flow. Therefore our first goal is a parametrization of $\eta(B)$ in terms of B . Although the choice of the generator and its parametrization is under the general constriction that it should create a diagonal Hamiltonian in the limit $B \rightarrow \infty$ and a continuous transformation starting at $U(B = 0) = \mathbb{1}$ various choices are possible. This allows for raising further demands.

⁴We use the term 'generator' both for single unitary transformations and for continuous flow equation method.

We already noted that the conservation of all energy scales is an important aspect of unitarity; by a certain choice of the generator the even more desirable feature of energy scale separation can be implemented. We will now present the most popular generator which achieves this goal.

3.5.1 Canonical generator

Motivated by the Jacobi method for numerical diagonalization of matrices Wegner suggested the use of the *canonical generator* for Hamiltonians which can be split up into an diagonal (free) and an interaction part. In most physical systems such a splitting is unproblematic and quite obvious.

$$\eta(B) = [H_0(B), H_{int}(B)] \quad (3.27)$$

This generator is trivially antihermitian as H_0 and H_{int} are hermitian operators and it has dimension energy squared. To ensure a dimensionless exponential in (3.5) the flow parameter has to be of inverse dimension, i.e. $B \sim (\text{energy})^{-2}$. Moreover the generator is of first order in any common perturbative parameter which is present in the interaction part of the Hamiltonian. This implies that in the flow equation formalism terms which are newly generated under the influence of an interaction come up in higher orders of a perturbative constant; by this it is ensured that -for considerations up to a certain perturbative order-truncation schemes can be formulated consistently.

Yet the main advantage of this choice is a generic appearance of differences between one-particle energies when the commutator is explicitly evaluated. It shows that the structure of the canonical generator itself can be understood as a kind of scattering operator multiplied by the energy transfer of the (formal) scattering process. This energy transfer represents an energy correlation and re-appears in the actual flow equations of the coupling constants of the Hamiltonian in quadratic order with an overall negative sign. By this the feature of energy scale separation enters the set of differential equations.

It must be noticed that these energy differences enter the formalism in a way which inherently includes an effective regularization of energy divergences. This is an obvious reason for the popularity of Wegner's suggestion.

3.5.2 Other choices of generators

The choice of a generator is in many ways accompanied by a certain degree of arbitrariness. This allows for pragmatic steps to simplify calculations by a re-definition of the generator which show special properties beyond those of the canonical one.

Pragmatic additions to the generator

In some cases it might be practical, for instance, to define additions to the canonical generator which compensate for the emergence of certain off-diagonal terms under the flow. If calculations are performed up to a fixed order in the perturbative parameter only it may be possible to restrict the effects of the additional generator to the intended compensation effect. This may sound like a miracle but simply represents a different way of arranging the perturbation expansion. Typically, the new part of the generator induces new structures into the transformation of the observables such that no physically relevant information is lost.

Nonetheless it is most advisable to consider any side effects which may result from a redefinition of the generator carefully. Most importantly, questions referring to the regularization of potentially divergent structures or convergence properties should be raised. Moreover, limiting procedures, e.g. the study of properties in the final basis representation ($B \rightarrow \infty$) may be critical steps. They are not necessarily invariant under a change of the generator, i.e. under the switch to a different unitary transformation.

Chapter 4

Application of the flow equation method to Anderson-like Hamiltonians

In the last chapter we have presented the central ideas of the flow equation method in an abstract way to provide the reader with an overall view on important aspects and a coherent background. Now we aim at applying this method to the Anderson impurity model. Again, we try to keep the formalism as general as justifiable with respect to the complexity of the arithmetic operations. Therefore we discuss an Anderson-like Hamiltonian which could be used to study a variety of different physical situations. All of them share a common operator structure of the free part and the interaction part of the Hamiltonian. Therefore they form a class of models which are described by formally similar flow equations for their (generalized) coupling constants. Their particularities are contained in a specific choice of multi-indices which becomes a selective feature whenever contractions of operator products are formed.

Whenever technical difficulties or unreasonable tedious calculations come up we restrict the class of models. The original Anderson impurity model always remains among the models considered.

4.1 Modifications to the Hamiltonian

4.1.1 Extension of the operator structure of the Hamiltonian

As a starting point we take the pre-diagonalized Anderson-like Hamiltonian (2.38) and the re-defined couplings (2.39). We introduce a dependence on the flow parameter B to all energies and couplings to allow for their change under the flow equation procedure.

In chapter (3) we have seen that under the flow new interaction terms can be generated. We will find out that this is true for the generation of a potential scattering term which cannot be neglected in a second order calculation. To avoid further repetitions we already include it into the Hamiltonian. Moreover, we think of the on-site interaction in a slightly more general way. Thus we can write the operator structure of an Anderson-like Hamiltonian in the following

form.

$$\begin{aligned}
 H(B) = & \sum_{s_1' s_1 \beta_1' \beta_1} \epsilon_{s_1' \beta_1' s_1 \beta_1}(B) :b_{s_1' \beta_1'}^\dagger b_{s_1 \beta_1}: + \\
 & \sum_{s_1' s_2' s_1 s_2 \beta_1' \beta_1 \beta_2' \beta_2} U_{s_1' s_1 s_2' s_2 \beta_1' \beta_1 \beta_2' \beta_2}(B) :b_{s_1' \beta_1'}^\dagger b_{s_1 \beta_1} b_{s_2' \beta_2'}^\dagger b_{s_2 \beta_2}:
 \end{aligned}$$

We use multi-index notation but separate between an energy-like part (Latin indices, usually denoted by s) and a spin-like part (Greek letters) to allow for an easy implementations of model assumptions.

4.1.2 Assumptions to the Hamiltonian

For the practical purpose of simplifying calculations we make assumptions to the spin structure of the Hamiltonian. Firstly we assume spin degeneracy in the energy levels of the system and spin conservation in one-particle scattering processes. Consequently the energies become spin independent and one-particle scattering amplitudes ϵ spin diagonal. We neglect any possibly remaining spin dependence of the scattering amplitudes.

Moreover, we impose constraining properties on the two-particle interaction U . We demand that it should

- (1) conserve the number of particles in the subsystem of the impurity(ies). Therefore it is represented by two creation and two destruction operators.
- (2) be spin conserving, i.e. it should be pairwise diagonal in the spin indices of (β_1', β_1) and (β_2', β_2) or of (β_1', β_2) and (β_2', β_1) . Without loss of generality we restrict to the first case.
- (3) respect the Pauli principle. This is a more delicate demand which we implement in a very approximative way: Thinking of the interaction as a kind of Coulomb interaction between two electrons motivates the idea that particles of the same spin orientation should occupy very distinct states in position space; on average they are fairly separated such that Coulomb forces are suppressed. We therefore assume that the interaction should not act between particles of the same spin, i.e. we demand $\beta_1 \neq \beta_2$.

This demand has some important technical advantages and reduces paperwork as it takes out quite a few contractions of normal ordered operator products.

We note that this type of interaction still includes joint spin-flip processes of two particles which are characteristic for the physics of strongly correlated systems, notably the Kondo effect.

4.1.3 Anderson-like Hamiltonian

We implement all assumptions and arrive at the following Hamiltonian:

$$\begin{aligned}
 H(B) = & \sum_{s\alpha} \epsilon_s(B) :b_{s\alpha}^\dagger b_{s\alpha}: + \sum_{s_1' \neq s_1} \sum_{\alpha} P_{s_1' s_1}(B) :b_{s_1' \alpha}^\dagger b_{s_1 \alpha}: + \\
 & \sum_{s_1' s_2' s_1 s_2 \beta_1 \beta_2} U_{s_1' s_1 s_2' s_2 \beta_1 \beta_2}(B) :b_{s_1' \beta_1'}^\dagger b_{s_1 \beta_1} b_{s_2' \beta_2'}^\dagger b_{s_2 \beta_2}:
 \end{aligned} \tag{4.1}$$

For this Hamiltonian we will derive its flow equation.

4.1.4 Splitup of the Hamiltonian

To proceed with the flow equation formalism we need to define a free part and an interacting part of the Hamiltonian. We can read off this splitting in (5.3) where an obvious way to rearrange the quadratic contributions has already been made explicit. The first term is diagonal and represents the eigenenergies of the particles created and annihilated by the operators b' , b . We therefore choose it as the free Hamiltonian.

$$H_0(B) = \sum_{s\alpha} \epsilon_s(B) \quad :b_{s\alpha}^\dagger b_{s\alpha}: \quad (4.2)$$

Yet the off-diagonal quadratic elements of the Hamiltonian describe one-particle scattering processes, their coefficients $P_{s_1', s_1}(B)$ represent scattering amplitudes whenever the multi-index pairs labelled by s_1' and s_1 do not coincide.

When we discuss the flow equations of the Anderson impurity model, we start with a Hamiltonian which does not contain a potential scattering term. We note that nonetheless we have to consider its structure in the interaction Hamiltonian to account for the generation of this term under the flow. This can be expressed in terms of the initial condition $P_{s_1', s_1}(B=0) = 0$ whenever $s_1' \neq s_1$. We will see that in the case of the Anderson impurity model this leads to a consistent truncation scheme for the Hamiltonian.

The interacting part of the Hamiltonian is given by the second and the third term in (5.3), namely

$$H_{int}^{(1)} = \sum_{s_1' s_2' s_1 s_2} \sum_{\beta_1 \beta_2} U_{s_1' s_1 s_2' s_2 \beta_1 \beta_2}(B) \quad :b_{s_1' \beta_1}^\dagger b_{s_1 \beta_1} b_{s_2' \beta_2}^\dagger b_{s_2 \beta_2}: \quad (4.3)$$

$$H_{int}^{(2)} = \sum_{s_1' \neq s_1} \sum_{\alpha} P_{s_1' s_1}(B) \quad :b_{s_1' \alpha}^\dagger b_{s_1 \alpha}: \quad (4.4)$$

4.2 Definition of the generator

4.2.1 Calculation of the canonical generator

We follow the route shown in the introduction to the flow equation method (chapter 3) and calculate the canonical generator. It is defined as the commutator of the free and the interaction part of the Hamiltonian and therefore consists of two contributions.

$$\eta^{(1)} = [H_0, H_{int}^{(1)}] = -[H_{int}^{(1)}, H_0] \quad (4.5)$$

$$\eta^{(2)} = [H_0, H_{int}^{(2)}] \quad (4.6)$$

Evaluation of $\eta^{(1)}$

For the Anderson impurity model the most important part of the canonical generator is given by $\eta^{(1)}$. This results from the fact that the corresponding interaction term in the Hamiltonian is the only one with non-vanishing initial conditions, i.e. it dominates the behavior of the flowing coupling constants for small values of the flow parameter.

The decisive step in the calculation of $\eta^{(1)}$ is the algebraic treatment of a structure which we simply and for obvious reasons refer to as the $[:4:, 2]$ -commutator¹. In order to make the reader familiar with typical aspects of evaluating commutators of fermionic normal ordered operator products we present this calculation in detail.

Detailed calculation of the $[:4:, 2]$ -commutator*: First of all we note that within commutators normal ordered operator products of length two are equivalent to the operator product itself as their difference, namely number-valued correlators, commute. Normal ordering therefore becomes relevant in higher operator products only. It is treated by resolving the normal ordered expression into ordinary operator products or, for convenience, to normal ordered products of length two by making use of the Wegner formula outlined in the appendix (A.1).

$$\begin{aligned} [:\mathbf{b}_{s'_1\beta_1}^\dagger \mathbf{b}_{s_1\beta_1} \mathbf{b}_{s'_2\beta_2}^\dagger \mathbf{b}_{s_2\beta_2} \mathbf{:}, : \mathbf{b}_{s\alpha}^\dagger \mathbf{b}_{s\alpha} \mathbf{:}] &= [:\mathbf{b}_{s'_1\beta_1}^\dagger \mathbf{b}_{s_1\beta_1} \mathbf{:} : \mathbf{b}_{s'_2\beta_2}^\dagger \mathbf{b}_{s_2\beta_2} \mathbf{:}, \mathbf{b}_{s\alpha}^\dagger \mathbf{b}_{s\alpha}] \\ &+ n^+(s_{1'}) \delta_{s_1'}^{s_2} \delta_{\beta_1}^{\beta_2} [\mathbf{b}_{s'_2\beta_2}^\dagger \mathbf{b}_{s_1\beta_1}, \mathbf{b}_{s\alpha}^\dagger \mathbf{b}_{s\alpha}] \\ &- n^-(s_1) \delta_{s_1}^{s'_2} \delta_{\beta_1}^{\beta_2} [\mathbf{b}_{s'_1\beta_1}^\dagger \mathbf{b}_{s_2\beta_2}, \mathbf{b}_{s\alpha}^\dagger \mathbf{b}_{s\alpha}] \end{aligned}$$

Afterwards, we make use of the fundamental relations given in the appendix (C.1) and evaluate the remaining commutators. A bunch of various contractions arises. At any step of the calculation we instantly drop contractions which vanish due to the constraints we have put on the multi-indices. We equally drop constants inside of commutators.

$$\begin{aligned} [:\mathbf{b}_{s'_1\beta_1}^\dagger \mathbf{b}_{s_1\beta_1} \mathbf{b}_{s'_2\beta_2}^\dagger \mathbf{b}_{s_2\beta_2} \mathbf{:}, : \mathbf{b}_{s\alpha}^\dagger \mathbf{b}_{s\alpha} \mathbf{:}] &= :\mathbf{b}_{s'_1\beta_1}^\dagger \mathbf{b}_{s_1\beta_1} \mathbf{:} (\delta_s^{s_2} \delta_\alpha^{\beta_2} \mathbf{b}_{s'_2\beta_2}^\dagger \mathbf{b}_{s\alpha} - \delta_s^{s'_2} \delta_\alpha^{\beta_2} \mathbf{b}_{s\alpha}^\dagger \mathbf{b}_{s_2\beta_2}) \\ &+ (\delta_s^{s_1} \delta_\alpha^{\beta_1} \mathbf{b}_{s'_1\beta_1}^\dagger \mathbf{b}_{s\alpha} - \delta_s^{s'_1} \delta_\alpha^{\beta_1} \mathbf{b}_{s\alpha}^\dagger \mathbf{b}_{s_1\beta_1}) : \mathbf{b}_{s'_2\beta_2}^\dagger \mathbf{b}_{s_2\beta_2} \mathbf{:} \end{aligned}$$

Normal ordering is re-introduced and all vanishing terms are skipped. We obtain a result which shows characteristic symmetries in the indices and signs involved:

$$\begin{aligned} [:\mathbf{b}_{s'_1\beta_1}^\dagger \mathbf{b}_{s_1\beta_1} \mathbf{b}_{s'_2\beta_2}^\dagger \mathbf{b}_{s_2\beta_2} \mathbf{:}, : \mathbf{b}_{s\alpha}^\dagger \mathbf{b}_{s\alpha} \mathbf{:}] &= \mathbf{b}_{s'_1\beta_1}^\dagger \mathbf{b}_{s_1\beta_1} \mathbf{b}_{s'_2\beta_2}^\dagger \mathbf{b}_{s\alpha} : \delta_s^{s_2} \delta_\alpha^{\beta_2} \\ &- \mathbf{b}_{s'_1\beta_1}^\dagger \mathbf{b}_{s_1\beta_1} \mathbf{b}_{s\alpha}^\dagger \mathbf{b}_{s_2\beta_2} : \delta_s^{s'_2} \delta_\alpha^{\beta_2} \\ &+ \mathbf{b}_{s'_1\beta_1}^\dagger \mathbf{b}_{s\alpha} \mathbf{b}_{s'_2\beta_2}^\dagger \mathbf{b}_{s_2\beta_2} : \delta_s^{s_1} \delta_\alpha^{\beta_1} \\ &- \mathbf{b}_{s\alpha}^\dagger \mathbf{b}_{s_1\beta_1} \mathbf{b}_{s'_2\beta_2}^\dagger \mathbf{b}_{s_2\beta_2} : \delta_s^{s'_1} \delta_\alpha^{\beta_1} \\ &+ \mathbf{b}_{s'_1\beta_1}^\dagger \mathbf{b}_{s_1\beta_1} : (n^+(s_2') - n^+(s_2)) \delta_s^{s_2'} \delta_s^{s_2} \delta_\alpha^{\beta_2} \\ &+ \mathbf{b}_{s'_2\beta_2}^\dagger \mathbf{b}_{s_2\beta_2} : (n^+(s_1') - n^+(s_1)) \delta_s^{s_1'} \delta_s^{s_1} \delta_\alpha^{\beta_1} \end{aligned}$$

¹We simply denote commutator structures by this suggestive notation of the product lengths involved. We always imply that the operator product consists of an equal number of creation and annihilation operators in alternating order.

As the algebraic evaluation of the comutator is now complete we can easily write down the quartic generator by

$$\begin{aligned}
\eta^{(1)} &= -[H_{int}^{(1)}, H_0] \\
&= - \sum_{s_1' s_2' s_1 s_2} \sum_{\beta_1 \beta_2} U_{s_1' s_1 s_2' s_2 \beta_1 \beta_2}(B) \sum_{s\alpha} \epsilon_{s\alpha} [:b_{s_1' \beta_1}^\dagger b_{s_1 \beta_1} b_{s_2' \beta_2}^\dagger b_{s_2 \beta_2} : , b_{s\alpha}^\dagger b_{s\alpha}] \\
&= \sum_{s_1' s_2' s_1 s_2} \sum_{\beta_1 \beta_2} U_{s_1' s_1 s_2' s_2 \beta_1 \beta_2}(B) (\epsilon_{s_2' \beta_2} - \epsilon_{s_2 \beta_2} + \epsilon_{s_1' \beta_1} - \epsilon_{s_1 \beta_1}) \\
&\quad :b_{s_1' \beta_1}^\dagger b_{s_1 \beta_1} b_{s_2' \beta_2}^\dagger b_{s_2 \beta_2} :
\end{aligned} \tag{4.7}$$

We note that $\eta^{(1)}$ is first order in the on-site interaction U .

Evaluation of $\eta^{(2)}$

The canonical generator as introduced by Wegner is defined as the commutator of the free part and the interaction part of the Hamiltonian which both depend on the flow parameter. Consequently, higher order interaction terms should be taken into account with increasing flow. A straightforward way would be to calculate the higher order part $\eta^{(2)}$ of the generator.

$$\eta^{(2)} = \sum_{s_1' \neq s_1} \sum_{\beta_1} P_{s_1' s_1}(B) (\epsilon_{s_1'} - \epsilon_{s_1}) :b_{s_1' \beta_1}^\dagger b_{s_1 \beta_1} : \tag{4.8}$$

We find again the characteristic emergence of an energy difference between creation and annihilation operator and see that this higher order term assists energy scale separation. The later analysis of the flow equations for the Anderson impurity model will show that this part of the generator produces terms in higher orders of a perturbative parameter only. Therefore we neglect it.

4.2.2 Extension of the canonical generator

We have already spoken of the remarkable freedom to choose the precise form of the generator in the flow equation approach. It allows for finding generators which are particularly suitable to achieve a (nearly) complete diagonalization of the Hamiltonian. Now we make use of this opportunity and define an addition to the canonical generator. Similar approaches have been chosen occasionally, among others by Kehrein and Mielke in [17].

Our goal is to prevent the generation of a potential scattering term in the Hamiltonian under the flow. Therefore we design the generator in such a way that its contribution to the flow equation of the Hamiltonian compensates for expressions which are responsible for the creation of such a term. Thus we ensure that the diagonalization procedure is not spoiled by this newly generated off-diagonal term. It is helpful to think of this extension as an approximate 'correction' to the canonical generator as this may illustrate the discussion of relevant and less important contributions which are additionally produced in the flow equations. Last but not least we mention that this additional part of the generator plays an important role in the transformation of the observables. We start the calculation of the extension $\eta^{(2a)}$ with the general ansatz

$$\eta^{(2a)} = \sum_{s_1' s_1 \beta_1} G_{s_1' s_1}(B) :b_{s_1' \beta_1}^\dagger b_{s_1 \beta_1} : \tag{4.9}$$

and specify its matrix elements $G_{s_1', s_1}(B)$ by defining its lowest order contribution to the flow equations. It is induced by the free Hamiltonian and shall compensate for the arising scattering term.

$$\begin{aligned}
 [\eta^{(2a)}, H_0] &= \sum_{s\alpha} \epsilon_{s\alpha} \sum_{s_1', s_1, \beta_1} G_{s_1', s_1}(B) \quad [:b_{s_1', \beta_1}^\dagger b_{s_1, \beta_1} : , :b_{s\alpha}^\dagger b_{s\alpha} :] \\
 &= \sum_{s_1', s_1, \beta_1} G_{s_1', s_1}(B) \quad (\epsilon_{s_1} - \epsilon_{s_1'}) \left(:b_{s_1', \beta_1}^\dagger b_{s_1, \beta_1} : + \delta_{s_1}^{s_1'} n^+(s_1) \right) \\
 &\stackrel{!}{=} \sum_{s_1', s_1, \beta_1} (-1) \frac{\partial P_{s_1', s_1}(B)}{\partial B} :b_{s_1', \beta_1}^\dagger b_{s_1, \beta_1} : \quad (4.10)
 \end{aligned}$$

Again we simply drop the ground state expectation value introduced by the regress to the normal ordered product as it is irrelevant for an object that only appears inside commutators. Of course, the differential flow equation for the scattering amplitudes $P_{s_1', s_1}(B)$ has to be calculated with respect to the canonical generator to make this trick work. Similarly one has to check that there is no relevant backaction of the commutator $[\eta^{(2a)}, H_{int}^{(1)}]$ onto the flow equation of the scattering amplitudes. This is most easily done by a perturbative argument. By comparison we can read off

$$G_{s_1', s_1}(B) = \frac{-1}{\epsilon_{s_1}(B) - \epsilon_{s_1'}(B)} \frac{\partial P_{s_1', s_1}(B)}{\partial B}$$

Finally we arrive at the following form of the extension and make the full dependence on the flow parameter B explicit

$$\eta^{(2a)}(B) = \sum_{s_1', s_1, \beta_1} \frac{1}{\epsilon_{s_1'}(B) - \epsilon_{s_1}(B)} \frac{\partial P_{s_1', s_1}(B)}{\partial B} :b_{s_1', \beta_1}^\dagger b_{s_1, \beta_1} : \quad (4.11)$$

The full generator is given by

$$\eta(B) = \eta^{(1)}(B) + \eta^{(2a)}(B) \quad (4.12)$$

4.3 Flow equation for Anderson-like Hamiltonians

In this section we calculate the various contributions to the flow equation of the Hamiltonian. A systematic expansion of the flow equation (cf 3.6) for the Hamiltonian can be written in the following form:

$$\begin{aligned}
 \frac{\partial H(B)}{\partial B} &= [\eta, H] = \quad (4.13) \\
 &= [\eta^{(1)}, H_0] + [\eta^{(1)}, H_{int}^{(1)}] + [\eta^{(2a)}, H_0] + [\eta^{(1)}, H_{int}^{(2)}] + [\eta^{(2a)}, H_{int}^{(1)}] + \dots
 \end{aligned}$$

When we discuss the system of differential flow equations we will notice that this corresponds to an expansion in terms of a perturbative parameter. We restrict to terms up to second order in this parameter which accords to considering the first three commutators only. The last of them has already been fixed by the definition of the extended generator (cf 4.10). The remaining two commutators are evaluated here. This comes along with the calculation of two major operator structures. The $[:4: , 2]$ -commutator has already been presented for a special case in section (10), and the $[:4: , 4]$ -commutator. Both can be found in the appendix in full generality.

Free flow of the Hamiltonian

We call the flow produced by the canonical generator and the free Hamiltonian the free flow of the Hamiltonian. It is first order in the interaction strength U .

$$[\eta^{(1)}, H_0] = - \sum_{s_1' s_2' s_1 s_2} \sum_{\beta_1 \beta_2} U_{s_1' s_1 s_2' s_2 \beta_1 \beta_2}(B) (\epsilon_{s_2' \beta_2} - \epsilon_{s_2 \beta_2} + \epsilon_{s_1' \beta_1} - \epsilon_{s_1 \beta_1})^2 :b_{s_1' \beta_1}^\dagger b_{s_1 \beta_1} b_{s_2' \beta_2}^\dagger b_{s_2 \beta_2}: \quad (4.14)$$

In the Anderson model this represents the leading order of the flows and gives rise to important approximations of the behaviour of the coupling constants. These approximations are commonly used to parametrize coupling constants for higher order calculations.

Second order contributions

Further structures and new aspects are normally introduced by the next order of the flow equation. We note that in particular this order is responsible for the appearance of ground state correlators and therefore accounts for any dependency on temperature or out-of-equilibrium conditions.

$$[\eta^{(1)}, H_{int}^{(1)}] = \sum_{s_1' s_1 s_2' s_2} \sum_{\beta_1 \beta_2} \sum_{s_5' s_5 s_6' s_6} \sum_{\beta_5 \beta_6} (\epsilon_{s_2' \beta_2} - \epsilon_{s_2 \beta_2} + \epsilon_{s_1' \beta_1} - \epsilon_{s_1 \beta_1}) U_{s_1' s_1 s_2' s_2 \beta_1 \beta_2}(B) U_{s_5' s_5 s_6' s_6 \beta_5 \beta_6}(B) :b_{s_1' \beta_1}^\dagger b_{s_1 \beta_1} b_{s_2' \beta_2}^\dagger b_{s_2 \beta_2} :, :b_{s_5' \beta_5}^\dagger b_{s_5 \beta_5} b_{s_6' \beta_6}^\dagger b_{s_6 \beta_6} :]$$

The explicit form of this commutator can be found in the appendix (17). It shows the generation of higher order interactions (operator products of length six) and potential scattering terms (of length two). For a detailed analysis we restrict to the Anderson impurity model in the following chapter. This will fix some multi-indices and therefore reduce the number of non-vanishing contractions.

Chapter 5

Diagonalization of the Anderson Hamiltonian

In the last chapter we have developed the operator structure of the flow equation transformation for Anderson-like Hamiltonians. We now restrict our attention to the well-established Anderson impurity model. We set up the flow equations for the energies and coupling constants of the Hamiltonian and study their behaviour under the flow for small and for large values of the flow parameter analytically. At this point we will, in particular, focus on characteristic features introduced by out-of-equilibrium conditions.

5.1 Reduction to the Anderson Hamiltonian

The Anderson impurity model is already part of the class of Anderson-like Hamiltonians which we have discussed in the last chapter. By specifying the multi-indices involved we can make it explicit; effectively we make some simplifying assumptions to the spin structure of the interaction term. This breaks a spin symmetry which is still present in the Anderson-like Hamiltonian (5.3) and reduces the number of non-vanishing contractions in the flow equation significantly.

In the Anderson impurity model the spin structure of a single interaction term is fixed in the physical basis by

$$H_{int} = U :d_{\uparrow}^{\dagger} d_{\uparrow} d_{\downarrow}^{\dagger} d_{\downarrow}: \quad (5.1)$$

As the pre-diagonalization \mathcal{B} has been chosen spin diagonal, the hybridization does not affect the spin structure of the on-site interaction term. Therefore the same spin orientations hold for the transformed operators in the pre-diagonalized basis. We set $\beta_1 = \uparrow$, $\beta_2 = \downarrow$ in (5.3), observe the collapse of the corresponding spin sums and arrive at the Hamiltonian

$$\begin{aligned} H(B) = & \sum_{s\alpha} \epsilon_s(B) :b_{s\alpha}^{\dagger} b_{s\alpha}: + \sum_{s_1' \neq s_1} \sum_{\alpha} P_{s_1' s_1}(B) :b_{s_1' \alpha}^{\dagger} b_{s_1 \alpha}: + \\ & \sum_{s_1' s_2' s_1 s_2} U_{s_1' s_1 s_2' s_2}(B) :b_{s_1' \uparrow}^{\dagger} b_{s_1 \uparrow} b_{s_2' \downarrow}^{\dagger} b_{s_2 \downarrow}: \end{aligned} \quad (5.2)$$

It is equivalent to the Anderson Hamiltonian for $B = 0$. Then the potential scattering amplitudes $P_{s_1' s_1}$ vanish.

5.2 General flow equation for the Anderson Hamiltonian

In chapter 4 we have already discussed the general splitup of the flow equations in terms of various contributions of the generator and the Hamiltonian. We have found that the flow equation for an Anderson-like Hamiltonian can be written up to second order in a perturbative parameter (which will turn out to be the interaction strength U) as

$$\frac{\partial H(B)}{\partial B} \stackrel{\mathcal{O}(U^2)}{=} [\eta^{(1)}, H_0] + [\eta^{(1)}, H_{int}^{(1)}] \quad (\rightarrow (4.13))$$

Now we will express it as a set of differential equations for its generalised coupling constants. Firstly, we expand the left hand side.

$$\begin{aligned} \frac{\partial H(B)}{\partial B} = & \sum_{s\alpha} \frac{\partial \epsilon_s(B)}{\partial B} :b_{s\alpha}^\dagger b_{s\alpha}: + \sum_{s_1' \neq s_1} \sum_{\alpha} \frac{\partial P_{s_1', s_1}(B)}{\partial B} :b_{s_1', \alpha}^\dagger b_{s_1 \alpha}: + \\ & \sum_{s_1' s_2' s_1 s_2} \frac{\partial U_{s_1' s_1 s_2' s_2}(B)}{\partial B} :b_{s_1' \uparrow}^\dagger b_{s_1 \uparrow} b_{s_2' \downarrow}^\dagger b_{s_2 \downarrow}: \end{aligned} \quad (5.3)$$

The commutators of right hand side of the flow equation have already been evaluated for a more general setup. We now simplify these results by imposing the constraints on the spin structure which we have discussed above. Moreover we neglect any higher order interactions generated under the flow (i.e. all operator products of length six) and the re-definition of the constant energy offset.

Second order contribution

We first consider the commutator $[\eta^{(1)}, H_{int}^{(1)}]$ which is second order in U . The prefactor extends to all operator products shown.

$$\begin{aligned} [\eta^{(1)}, H_{int}] = & \sum_{s_1' s_1 s_2' s_2} \sum_{s_5' s_5 s_6' s_6} (\epsilon_{s_2'} - \epsilon_{s_2} + \epsilon_{s_1'} - \epsilon_{s_1}) U_{s_1' s_1 s_2' s_2}(B) U_{s_5' s_5 s_6' s_6}(B) \\ & + :b_{s_1' \beta_1}^\dagger b_{s_5 \beta_5} b_{s_2' \beta_2}^\dagger b_{s_6 \beta_6}: n^-(s_1) \delta_{s_1}^{s_5'} \delta_{s_2}^{s_6'} \quad (\uparrow\uparrow\downarrow\downarrow) \\ & - :b_{s_1' \beta_1}^\dagger b_{s_5 \beta_5} b_{s_6' \beta_6}^\dagger b_{s_2 \beta_2}: n^-(s_1) \delta_{s_1}^{s_5'} \delta_{s_6}^{s_2'} \\ & - :b_{s_5' \beta_5}^\dagger b_{s_1 \beta_1} b_{s_2' \beta_2}^\dagger b_{s_6 \beta_6}: n^+(s_1') \delta_{s_5}^{s_1'} \delta_{s_2}^{s_6'} \\ & + :b_{s_5' \beta_5}^\dagger b_{s_1 \beta_1} b_{s_6' \beta_6}^\dagger b_{s_2 \beta_2}: n^+(s_1') \delta_{s_5}^{s_1'} \delta_{s_6}^{s_2'} \\ & + :b_{s_1' \beta_1}^\dagger b_{s_5 \beta_5} b_{s_6' \beta_6}^\dagger b_{s_2 \beta_2}: n^-(s_2') \delta_{s_6}^{s_2'} \delta_{s_1}^{s_5'} \\ & - :b_{s_1' \beta_1}^\dagger b_{s_5 \beta_5} b_{s_2' \beta_2}^\dagger b_{s_6 \beta_6}: n^+(s_2) \delta_{s_1}^{s_5'} \delta_{s_2}^{s_6'} \\ & - :b_{s_5' \beta_5}^\dagger b_{s_1 \beta_1} b_{s_6' \beta_6}^\dagger b_{s_2 \beta_2}: n^-(s_2') \delta_{s_5}^{s_1'} \delta_{s_6}^{s_2'} \\ & + :b_{s_5' \beta_5}^\dagger b_{s_1 \beta_1} b_{s_2' \beta_2}^\dagger b_{s_6 \beta_6}: n^+(s_2) \delta_{s_5}^{s_1'} \delta_{s_2}^{s_6'} \end{aligned}$$

While the last terms all show the original spin structure of the on-site interaction in the Anderson impurity model ($\uparrow\uparrow\downarrow\downarrow$), two new couplings are generated under the flow:

$$\begin{aligned} & + :b_{s_1' \beta_1}^\dagger b_{s_1 \beta_1} b_{s_5' \beta_5}^\dagger b_{s_5 \beta_5}: (n^+(s_2') - n^+(s_2)) \delta_{s_6}^{s_2'} \delta_{s_2}^{s_6'} \quad (\uparrow\uparrow\uparrow\uparrow) \\ & + :b_{s_6' \beta_6}^\dagger b_{s_6 \beta_6} b_{s_2' \beta_2}^\dagger b_{s_2 \beta_2}: (n^+(s_1') - n^+(s_1)) \delta_{s_1}^{s_5'} \delta_{s_5}^{s_1'} \quad (\downarrow\downarrow\downarrow\downarrow) \end{aligned}$$

Both terms are suppressed by the Pauli principle as laid out in chapter (4.1.2). We therefore neglect their contribution.

For the operator products of length two we find a symmetry between up- and downspin orientation. Due to the spin degeneracy of the energies and the potential scattering amplitudes our further evaluation will restrict to one class only.

$$\begin{aligned}
& + :b_{s'_1\beta_1}^\dagger b_{s_5\beta_5} : n^-(s_1) (n^+(s_2') - n^+(s_2)) \delta_{s_1}^{s_5'} \delta_{s_6}^{s_2'} \delta_{s_2}^{s_6'} \quad (\uparrow\uparrow) \\
& - :b_{s'_5\beta_5}^\dagger b_{s_1\beta_1} : n^+(s_1') (n^+(s_2') - n^+(s_2)) \delta_{s_5}^{s_1'} \delta_{s_2}^{s_6'} \delta_{s_6}^{s_2'} \\
& + :b_{s'_1\beta_1}^\dagger b_{s_5\beta_5} : n^+(s_2) n^-(s_2') \delta_{s_1}^{s_5'} \delta_{s_2}^{s_6'} \delta_{s_6}^{s_2'} \\
& - :b_{s'_5\beta_5}^\dagger b_{s_1\beta_1} : n^+(s_2) n^-(s_2') \delta_{s_5}^{s_1'} \delta_{s_2}^{s_6'} \delta_{s_6}^{s_2'} \\
\\
& + :b_{s'_6\beta_6}^\dagger b_{s_2\beta_2} : n^-(s_2') (n^+(s_1') - n^+(s_1)) \delta_{s_1}^{s_5'} \delta_{s_5}^{s_1'} \delta_{s_6}^{s_2'} \quad (\downarrow\downarrow) \\
& - :b_{s'_2\beta_2}^\dagger b_{s_6\beta_6} : n^+(s_2) (n^+(s_1') - n^+(s_1)) \delta_{s_1}^{s_5'} \delta_{s_5}^{s_1'} \delta_{s_2}^{s_6'} \\
& + :b_{s'_2\beta_2}^\dagger b_{s_6\beta_6} : n^+(s_1') n^-(s_1) \delta_{s_5}^{s_1'} \delta_{s_2}^{s_6'} \delta_{s_1}^{s_5'} \\
& - :b_{s'_6\beta_6}^\dagger b_{s_2\beta_2} : n^+(s_1') n^-(s_1) \delta_{s_5}^{s_1'} \delta_{s_6}^{s_2'} \delta_{s_1}^{s_5'}
\end{aligned}$$

These terms are responsible for the existence of non-trivial flow equations for the eigenenergies of the Hamiltonian and the potential scattering amplitudes.

First order contribution

Another but simpler contribution is added by the commutator $[\eta^{(1)}, H_0]$. It is the only term in first order of U which is present in the flow equation.

$$[\eta, H_0] = - \sum_{s_1' s_1 s_2' s_2} U_{s_1' s_1 s_2' s_2} (\epsilon_{s_2'} - \epsilon_{s_2} + \epsilon_{s_1'} - \epsilon_{s_1})^2 :b_{s_1'\uparrow}^\dagger b_{s_1\uparrow} b_{s_2'\downarrow}^\dagger b_{s_2\downarrow} :$$

It only affects the flow of the interaction U as it consists of a quartic term (cf. next paragraph). The lack of any quadratic expression implies that there is no first order contribution to the flow of the energies and scattering amplitudes. This is an important result which states that the renormalisation of the energies is an effect in second order of U . Therefore a consistent second order treatment of the flow equations needs to respect a first order approximation for the flowing coupling U only.

In particular this means that a first order parametrization of the eigenenergies which are variables of the generator and of the Hamiltonian can be avoided. Throughout most calculations of this work we will assume that the eigenenergies $\epsilon_s(B) = \epsilon_s(B=0)$ are independent of the flow parameter. On the other hand this result illuminates the fact that analytical calculations beyond second order will grow fast in complexity.

Set of differential flow equations

Now we split up the flow equation by comparing coefficients of the various operator products which are present in its left hand side (5.3) and in the two commutators. Thus we produce

a set of coupled differential equations, one for each generalized coupling constant. This set can be reduced to two different classes of equations: One describes the coefficients of the quartic operator products (the on-site interaction), the other one those of the quadratic ones (energies and scattering amplitudes). We will study both of them in the following sections.

5.3 Flow equation for the interaction U

We begin with an evaluation of the flow equation for the on-site interaction U . It is characterized by its dependences on the flow parameter B and on four points in energy space.

Initial condition and further flow of U

In chapter 2 we have found a functional form of the energy dependence in the initial basis representation which serves as an initial condition.

$$U_{s_1's_1s_2's_2}(B=0) = U W_{s_1's_1s_2's_2} \quad (\rightarrow 2.39)$$

Now we allow for a change of U under the flow and treat the dependence on the hybridization as a constant prefactor.

$$U_{s_1's_1s_2's_2}(B) = \tilde{U}_{s_1's_1s_2's_2}(B) W_{s_1's_1s_2's_2} \quad (5.4)$$

This establishes both the new dependence on the flow parameter and, indirectly, a more detailed energy dependence of the on-site interaction.

Single generalized coupling constant at fixed energy

In the language of generalized coupling constants we understand this as a bulk description for a variety of these constants. Each of them is well-defined by its fixed energy labels. This is a remnant of the mode decomposition performed when a field is quantized in standard quantum field theory. There any creation or annihilation operator is defined with respect to one particular mode, carrying a fixed momentum (or equivalently an energy) index. The only remaining dependence of these generalized coupling constants is on the flow parameter. Practically we only write down a single differential equation for one particular such constant $U_{s_1's_1s_2's_2}(B)$ which describes the behaviour under the flow and note that it holds for arbitrary (but fixed) energy values.

Non-locality of the canonical commutator in energy space

We notice that the canonical generator itself depends on $U_{s_1's_1s_2's_2}$ at *all* energy values. This brings about a strong coupling of the differential equations for the arbitrary but fixed energy values of U .

To solve such a system analytically one has to achieve a decoupling of its equations by introducing reasonable approximations on the energy dependence of the interaction at *all* values of the flow parameter. As the dependences on energy and the flow parameter appear to be closely correlated such approximations are equally referred to as parametrizations with respect to the flow parameter B . A typical method to tackle down such problems is the iterative improvement of an parametrization which has initially been chosen in a very straightforward and simple way. We will follow this path for two steps of the iteration.

5.3.1 Parametrizations of U

We start with a parametrization which assumes a constant value of $\tilde{U}_{s_1's_1s_2's_2}(B) = U$ independent of energy or the flow parameter. It is correct in the limit $B \rightarrow 0$ as we started with a well-defined Coulomb on-site interaction in the Anderson Hamiltonian. The trivial constant energy dependence of $U_{s_1's_1s_2's_2}$, which results from the hybridization (see equation 5.4), is unimportant and finally drops out of the (first order) flow equation.

This choice leads to a reduction of the system of coupled differential equations for the various coupling constants $U_{s_1's_1s_2's_2}$ to a single one describing the behaviour of $U(B)$. Due to the roughness of the approximation we set up the differential flow equation to first order of U only. We call the first order result the free flow of U , as it only refers to the commutator of the generator with the free Hamiltonian. It will serve as a more adequate parametrization for second order calculations.

5.3.2 Flow equation for $U(B)$ to first order in U

The first order result is based on the commutator

$$[\eta^{(1)}, H_0] = -U \sum_{s_1's_1s_2's_2} W_{s_1's_1s_2's_2} (\epsilon_{s_2'} - \epsilon_{s_2} + \epsilon_{s_1'} - \epsilon_{s_1})^2 :b_{s_1'\uparrow}^\dagger b_{s_1\uparrow} b_{s_2'\downarrow}^\dagger b_{s_2\downarrow}: \quad (5.5)$$

By comparing the coefficients in the flow equation, we obtain

$$\frac{\partial U}{\partial B} \approx -U (\epsilon_{s_2'} - \epsilon_{s_2} + \epsilon_{s_1'} - \epsilon_{s_1})^2 \quad (5.6)$$

The differential equation is easily solved

$$U(B) = U_0 e^{-(\epsilon_{s_2'} - \epsilon_{s_2} + \epsilon_{s_1'} - \epsilon_{s_1})^2 B} \quad (5.7)$$

We call this the free parametrization of $\tilde{U}_{s_1's_1s_2's_2}$ and notice a new non-trivial energy dependence. We briefly denote it by $\Delta\epsilon = \epsilon_{s_2'} - \epsilon_{s_2} + \epsilon_{s_1'} - \epsilon_{s_1}$. This first order result is approximately correct for small values of the on-site interaction.

Crucial interpretation

This first order result shows some remarkable features of the diagonalization procedure: Firstly, the overall behaviour of the interaction with growing flow parameter B is an exponential decrease. Diagonal elements alone do not show this falloff. This corresponds to the fact that the Hamiltonian becomes more and more diagonal under the flow.

Secondly, we observe energy scale separation. For any off-diagonal element with $\Delta\epsilon \neq 0$ and an arbitrary suppression factor $1 > a > 0$ we find a smallest value $B(a) = -\ln(a)/(\Delta\epsilon)^2$ such that for all $B > B(a)$ the interaction is suppressed at least by a . The crucial observation is that $B(a)$ depends on the inverse of the energy difference. The further away elements are from the diagonal line the earlier they are suppressed by the flow equation procedure.

Re-inserting this result as an improved parametrization into the Hamiltonian and, in particular, into the generator therefore touches the heart of the flow equation approach. From a RG point of view we could say it in an alternative way: Effectively, this parametrization induces for all values of $B \neq 0$ a smooth natural cut-off to far-away energy correlations into internal energy summations.

5.3.3 Flow equation for $U(B)$ to second order in U

We continue our calculation by starting a second iteration¹. We use the result (5.7) as a new parametrization for U but make the exponential energy dependence explicit. Still we assume a residual dependence of $U(B)$ on the flow parameter.

$$U_{s_1's_1s_2's_2}(B) = U(B)W_{s_1's_1s_2's_2}e^{-(\epsilon_{s_2'} - \epsilon_{s_2} + \epsilon_{s_1'} - \epsilon_{s_1})^2 B} \quad (5.8)$$

The setup of an extended flow equation is done by evaluating the quartic terms of the commutator $[\eta^{(1)}, H_{int}^{(1)}]$. A close look shows that those referring to the Anderson spin structure ($\uparrow\uparrow\downarrow\downarrow$) can be easily combined pairwise. We consider an arbitrary but fixed single generalized coupling constant or, equivalently, the on-site interaction at one particular point of energy $U_{\tilde{s}_1'\tilde{s}_1\tilde{s}_2'\tilde{s}_2}$. In order to avoid too cumbersome notation we omit the label s in the indices. Hence numbers do not refer to particular values of an index but stand for an index itself. We mark all external indices (those which refer to the energy labels of the coupling constant) with a tilde.

Evaluation of the commutator terms

A careful calculation which includes a re-arrangement of the exponentials involved leads to a global pre-factor

$$U_0^2 W_{\tilde{1}'\tilde{1}\tilde{2}'\tilde{2}} e^{-\frac{B}{2}(\epsilon_{\tilde{2}'} - \epsilon_{\tilde{2}} + \epsilon_{\tilde{1}'} - \epsilon_{\tilde{1}})^2} \quad (5.9)$$

and four different contributions which are summed up for the final result:

$$\begin{aligned} & \sum_{s_1 s_2} (W_1)^2 (W_2)^2 [n^-(s_1) - n^+(s_1)] (-\epsilon_1 - \epsilon_2 + \epsilon_{\tilde{2}'} + \epsilon_{\tilde{1}'}) e^{-2B - \epsilon_1 - \epsilon_2 + \frac{\epsilon_{\tilde{2}'} + \epsilon_{\tilde{1}'} + \epsilon_{\tilde{2}'} + \epsilon_{\tilde{1}'}}{2}}^2 \\ & \sum_{s_1 s_2'} (W_1)^2 (W_{2'})^2 [n^-(s_2') - n^-(s_1)] (\epsilon_{2'} - \epsilon_1 + \epsilon_{\tilde{1}'} - \epsilon_{\tilde{2}}) e^{-2B - \epsilon_{2'} - \epsilon_1 + \frac{\epsilon_{\tilde{1}'} - \epsilon_{\tilde{2}} - (\epsilon_{\tilde{2}'} - \epsilon_{\tilde{1}'})}{2}}^2 \\ & \sum_{s_1' s_2} (W_{1'})^2 (W_2)^2 [n^+(s_2) - n^+(s_1')] (\epsilon_{1'} - \epsilon_2 + \epsilon_{\tilde{2}'} - \epsilon_{\tilde{1}}) e^{-2B - \epsilon_{1'} - \epsilon_2 + \frac{\epsilon_{\tilde{2}'} - \epsilon_{\tilde{1}} - (\epsilon_{\tilde{1}'} - \epsilon_{\tilde{2}})}{2}}^2 \\ & \sum_{s_1' s_2'} (W_{1'})^2 (W_{2'})^2 [n^+(s_1') - n^-(s_1')] (\epsilon_{2'} + \epsilon_{1'} - \epsilon_{\tilde{2}} - \epsilon_{\tilde{1}}) e^{-2B - \epsilon_{2'} + \epsilon_{1'} + \frac{\epsilon_{\tilde{1}} + \epsilon_{\tilde{2}} + \epsilon_{\tilde{1}'} + \epsilon_{\tilde{2}'}}{2}}^2 \end{aligned}$$

An interesting feature of these expressions is displayed by the exponential function. Due to its cut-off behaviour it opens a window in energy space which effectively contributes to the flow equation. We simply call it the *cut-off window*. By the choice of the energy observation point at which the flow of the coupling is studied the cut-off window is dynamically shifted into this particular energy regime: It is opened around a mean value of the fixed energies of the creation and annihilation operators, e.g.

$$e^{-2B \left(\epsilon_{1'} - \frac{\epsilon_{\tilde{1}'} + \epsilon_{\tilde{1}}}{2} \right) - \left(\epsilon_2 - \frac{\epsilon_{\tilde{2}'} + \epsilon_{\tilde{2}}}{2} \right)^2}$$

¹We point out that an iterative calculation of a quantity naturally leads to a re-definition of variables in higher orders. The reader should not be confused about notation.

Evaluation at the Fermi energy

Now we choose as our observation point the Fermi energy $\epsilon_F = 0$. At this point the first order result for the interaction (cf. 5.7), $U_{\epsilon_F} = U_{\epsilon_F \epsilon_F \epsilon_F \epsilon_F}$, becomes independent of the flow parameter as the exponential argument vanishes $(\epsilon_{s_2'} - \epsilon_{s_2} + \epsilon_{s_1'} - \epsilon_{s_1})^2|_F = 0$. Hence under the free flow, i.e. to first order in U , the interaction remains constant: $U_{\epsilon_F}(B) = U_0$. This means that the first order parametrization of $U(B)$ becomes only effective for the internal energy summations, playing the role of a true cut-off function which eliminates far energy correlations. By this an energy window around the diagonal line of width $\Delta E \sim \frac{1}{\sqrt{B}}$ is opened, the cut-off window. For solving the flow equation up to second order we have to consider the residual dependence of U_0 on the flow parameter. Hence we replace it by the more explicit form $U_{\epsilon_F}(B)$. Several manipulations of the four contributions (including their common prefactor) lead to a compact form of the second order contribution to the right hand side of the flow equation:

$$U_{\epsilon_F}^2(B)(W_{\epsilon_F})^4 2 \sum_{s_1 s_2} (W_1)^2 [(W_2)^2 - (W_{-2})^2] [n^+(s_1) - n^-(s_1)] (\epsilon_2 - \epsilon_1) e^{-2B(\epsilon_2 - \epsilon_1)^2} \quad (5.10)$$

A negative index refers to an object taken at the negative energy, e.g. $W_{-2} = W(-\epsilon_2)$. We already mentioned that at the Fermi energy the free flow vanishes ($[\eta^{(1)}, H_0]|_F = 0$). Therefore the flow equation has no term in first order of U and the behaviour of the coupling constant is governed by the second order expression.

Second order flow equation for $U(B)$ at the Fermi energy

The left hand side of the flow equation now reads

$$\frac{\partial H_{int}(U(B))}{\partial B} = (W_{\epsilon_F})^4 \frac{\partial U_{\epsilon_F}(B)}{\partial B}$$

Consequently, the factors $(W_{\epsilon_F})^4$ cancel and we obtain the flow equation for the interaction at the Fermi energy

$$\frac{\partial U_{\epsilon_F}(B)}{\partial B} = 2U_{\epsilon_F}^2(B) \sum_{s_1 s_2} (W_1)^2 [(W_2)^2 - (W_{-2})^2] [n^+(s_1) - n^-(s_1)] (\epsilon_2 - \epsilon_1) e^{-2B(\epsilon_2 - \epsilon_1)^2} \quad (5.11)$$

Trivial behaviour for the symmetric Anderson impurity model

In the case of the symmetric Anderson impurity model the impurity level is situated energetically right at the Fermi surface: $\epsilon_d = \epsilon_F \equiv 0$. Hence the hybridization is symmetric with respect to the origin and the flow equation for the interaction vanishes for all values of B . The interaction at the Fermi energy remains constant throughout the flow, renormalization effects just do not show up. This is an exceptional result as in most other models the renormalization of the coupling constant at the Fermi energy is a characteristic and important feature of the flow equation method. It holds both in and out of equilibrium.

All further examinations apply to the asymmetric Anderson impurity model ($\epsilon_d \neq \epsilon_F$, i.e. the hybridization function is asymmetric). For reasons of continuity we do not expect dramatic changes with growing asymmetry. Nonetheless the *asymmetric case* is the generic one which is implemented in most physical systems. For this case we proceed with a detailed analysis of the behaviour of the interaction under the flow.

Integral representation of the flow equation

For all practical purposes, both analytical and numerical evaluations, we prefer to work in energy space. We assume a linear dispersion relation, i.e. a constant density of states ρ_0 , to change between both representations. Moreover we consider the limit of continuous band energies. Altogether, we promote all internal sums in state space to continuous energy integrals.

$$\sum_{s_1 s_2} \rightarrow \rho_0^2 \int d\epsilon_1 \int d\epsilon_2$$

All further studies on the flow equation can then be performed as a discussion of functions in energy space.

5.4 Analytical discussion of the flow of the interaction for the asymmetric Anderson impurity model ($\epsilon_d \neq \epsilon_F$)

The differential equation of the on-site interaction U (5.11) is the most important one with respect to Hamiltonian diagonalization. We study it at the Fermi energy where the most relevant physical processes are located. For simplicity, we restrict to this case only. Our first interest is to integrate this flow equation with respect to the flow parameter and to analyze the behaviour of the flowing coupling constant $U(B)$ under the diagonalization process. We keep an eye out for possible divergences or uncontrolled growth of the coupling as this might spoil the (perturbatively controlled) diagonalization process; the quality of the flow equation approach depends on a well-behaved flow of the dominating coupling constants.

In this section we present analytical approximations for the behaviour of $U(B)$ in the limits of initial ($B \approx 0$) and final ($B \rightarrow \infty$) flow. The main goal of this approach is to illuminate the functioning of the diagonalization process and to name the most important aspects involved in the renormalization of the coupling constant. We therefore present quite a few technical details in order to highlight on the internal nature of the flow equation procedure. Normally we will, firstly, comment on the relevant ideas in a nutshell and then present their full application to the flow of B .

5.4.1 Restrictions on energy contributions

One of these ideas is an approximate but detailed study of the energy contributions to the right hand side of the flow equation (5.11). We observe that –although formally included in the internal integrations– large energy ranges do not contribute to the change of U . In order to sharpen our perception of the origins of such behaviour we focus on the various functional expressions in the flow equation (5.11) separately. In particular we mention the hybridization, the Fermi distribution function and an exponential cutoff function which was implicitly introduced by the free flow parametrization of the on-site interaction. Our analysis is carried out by referring to the interplay of different 'windows' opened by these terms. We will use this language extensively for later discussions but restrict to the two most important aspects here.

Limitations by hybridization and cut-off functions

Two kinds of functional expressions limit the range of all internal energy integrations symmetrically around a mean value: The hybridization and the cut-off function.

For a one-level impurity problem the hybridization is of Lorentz shape and characterized by its width Δ . It depends only on properties of the tunnel coupling between the leads and the impurity as described in chapter 2. It does not change significantly under the flow equation procedure. Instead, the cut-off function is a bell-shaped Gaussian curve which heavily depends on the flow parameter. Its width is given by $B^{-1/2}$, i.e. by the flow parameter directly. Both curves show a fast descent, suppressing energy contributions far away from their mean. But depending on the regime of the flow, their relative importance varies.

- (1) At initial flow, i.e. for small B , we are in the regime of $B^{-1/2} \gg \Delta$. This implies that the hybridization window defines the restriction on the energies, the cut-off is virtually not visible; it is of infinite size.
- (2) With growing flow parameter the cut-off window acquires finite restrictions. For $B^{-1/2} \approx \Delta$ the relative positions of the mean values of both curves determine the effective contributions. We will not consider this case in greater detail.
- (3) For very advanced flow, i.e. for large values of the flow parameter, the situation is characterized by $B^{-1/2} \ll \Delta$. Now the limitations of the cut-off window become the dominating aspect. Inside this window, the hybridization can be assumed to be of limited change and expanded in a Taylor series.

Asymmetric energy restrictions by Fermi distribution functions

A second, but even more important aspect of energy restriction is introduced by the Fermi distribution functions n^+ and n^- which entered the flow equation formalism by normal ordering prescriptions. For zero temperature and in equilibrium, they are characterized by a sharp edge at the Fermi energy, separating occupied from unoccupied energy states of the system. Effectively, the Fermi functions single out one of both classes and eliminate the contributions of the other. This introduces an asymmetry into the model which shows most relevant consequences. In general such asymmetries limit or foster cancellations of functions which are symmetric in energy. In particular such effects become important when the Fermi edge and poles of point symmetric functions coincide. Then they might stir dramatic changes and divergences in final results. From a physical point of view this underlines the outstanding role of the sharp Fermi surface. We admit that very similar effects can emerge at sharp band edges or comparable discontinuities which do not always represent true physical behaviour. In our model instead, the only functions showing such features are Fermi distribution functions. Moreover, we adapt our model to out-of-equilibrium or nonzero temperature conditions by variations in the Fermi functions only. Particularly at the Fermi energy their characteristic signatures are dominant. Therefore it is not unreasonable to expect that a model which combines Fermi distribution functions with a pole structure in energy might exhibit significantly different features in and out of equilibrium (or equivalently for nonzero temperature). This is one of the main motivations for our present inquiry.

5.4.2 Discussion of $U(B)$ for initial flow ($1/\sqrt{B} \gg \Delta$)

In this section we discuss the behaviour of the interaction for small values of the flow parameter. We already mentioned that in this case the cut-off function can be neglected. Therefore it is sufficient to solve an approximate flow equation

$$\frac{\partial U_{\epsilon_F}(B)}{\partial B} = 2\rho_0^2 U_{\epsilon_F}^2(B) \int d\epsilon_{s_1} \int d\epsilon_{s_2} (W_1)^2 [(W_2)^2 - (W_{-2})^2] [n^+(s_1) - n^-(s_1)] (\epsilon_2 - \epsilon_1) \quad (5.12)$$

We observe two major simplifications:

1. The dependence of the flow parameter has been restricted to the coupling constant $U_{\epsilon_F}^2(B)$ itself and the internal integrations just contribute a constant factor c . Hence the differential equation can be integrated easily.

$$U_{\epsilon_F}^{B \approx 0}(B) = \frac{U_{\epsilon_F}(B=0)}{1 - c U_{\epsilon_F}(B=0)B} \xrightarrow{B \rightarrow 0} U_{\epsilon_F}(B=0) \quad (5.13)$$

The sign of the factor c plays a decisive role in the development of the coupling constant. For its computation we make use of a second observation.

2. The internal integrations decouple.

$$\begin{aligned} c &= 2\rho_0^2 \int d\epsilon_1 W_1^2 [n(s_1)^+ - n(s_1)^-] \int d\epsilon_2 \epsilon_2 [W_2^2 - W_{-2}^2] \\ &= 4\rho_0^2 \int d\epsilon_1 W_1^2 [n(s_1)^+ - n(s_1)^-] \int d\epsilon_2 \epsilon_2 W_2^2 = 4\rho_0^2 N \cdot E \end{aligned}$$

Both integrals can be understood as a mean value of occupied sites and energy with respect to the hybridization W^2 . We will find that the product $N \cdot E$ is never positive.

We continue our discussion with an evaluation of the mean values N and E . Firstly we consider the implicit dependences hidden in both objects: Via the hybridization function the energy level of the impurity ϵ_d enters, for the Fermi functions we discuss the dependence on the external voltage bias applied to the system.

The *mean value of the energy* is calculated in a straightforward way. We recall that the hybridization is symmetric with respect to the impurity energy. Therefore we substitute the integration variable $\epsilon_2 \rightarrow \epsilon = \epsilon_2 - \epsilon_d$.

$$E = \int d\epsilon_2 \epsilon_2 W^2(\epsilon_2) = \underbrace{\int d\epsilon \epsilon W^2(\epsilon + \epsilon_d)}_0 + \underbrace{\epsilon_d \int d\epsilon W^2(\epsilon + \epsilon_d)}_1 = \epsilon_d \quad (5.14)$$

The first integral vanishes due to the symmetry, the second one equals one as the square of the hybridization function is normalised.

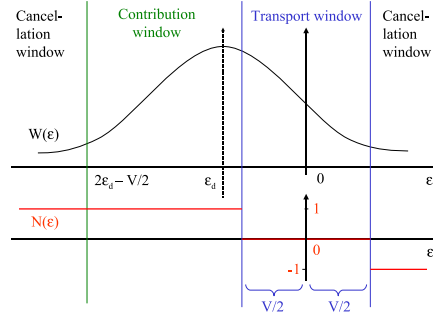


Figure 5.1: Thumbsketch of the hybridization and the Fermi distribution function for the regime of *initial flow*. The transport window (blue) is opened around the Fermi energy. Symmetry arguments applied to the product of both functions easily explain the windows of cancellation and of effective contribution.

Technique of graphical evaluation

To evaluate the *mean value of the Fermi functions* N we introduce a technique which is very suitable to analyse such and similar expressions. The idea is to make use of the symmetry of the functions involved and the simple form of the zero temperature Fermi functions to include their contributions fully in the choice of limits of an integration independent of the Fermi functions. Effectively, this moves the dependence on the external voltage bias from the Fermi function into the integration limits and makes it explicit. For this graphical motivation is a very helpful tool. The illustrative strength of the method comes along with a discussion of different 'windows' which are –for this purpose– disjunct subsets of the integration domain. We already mentioned windows opened by the hybridization and the cut-off function which were rough estimations of the width of these functions. Instead of these handwaving visualisations we focus on the well-defined boundaries of the following ones:

- The *transport window* is opened around the Fermi energy. Its width is determined by the external voltage bias V . We only consider the case of vanishing difference between the Fermi functions $n_T = [n^+ - n^-] \equiv 0$ inside the transport window. Hence the transport window does not contribute to any mean value itself. Our point of interest is that it provides precise boundary values for all relevant windows. If, furtheron, the aspect of a nonzero value of n_T , i.e. a feature which results from significant differences in the hybridization couplings of the left and the right lead (cf. 1.5), should be included, another contribution from the transport window has to be added to all evaluations.
- By the term *cancellation window* we understand an -possibly unconnected- domain which finally does not affect the value of an integral due to cancellations of the (various) terms involved. The antisymmetry of the difference of the Fermi functions together with the (shifted) symmetry of the hybridization bring about the cancellation of its long-range 'tails'.
- The only subset which effectively produces a non-vanishing contribution to the integral may be called *contribution window*. We are particularly interested in the upper and lower limits of this domain.

Evaluating the graphics we find

$$\begin{aligned}\epsilon_d < 0 & : N = + \int_{2\epsilon_d - V/2}^{-V/2} d\epsilon W^2(\epsilon) > 0 \\ \epsilon_d > 0 & : N = - \int_{V/2}^{2\epsilon_d + V/2} d\epsilon W^2(\epsilon) < 0\end{aligned}$$

The actual value of the mean N therefore depends primarily on the position of the impurity energy level. For the symmetric Anderson model with $\epsilon_d = \epsilon_F = 0$ sitting at the Fermi surface this contribution vanishes - an obvious result under the coinciding symmetries of the Fermi functions and the hybridization. Limiting our view to the sign of the result we can write $\text{sign}(N) = -\text{sign}(\epsilon_d)$.

We want to remark that this kind of analysis is capable of producing exact analytical results in the case of zero temperature. We therefore will use this method again to study the influence of non-equilibrium conditions on the advanced flow of the interaction.

Comment on the initial flow of $U(B)$

Taking the results for both mean values N and E into account we see that the constant $c \sim NE \sim -\text{sign}(\epsilon_d)^2 \sim -1$ is always a negative number or zero. This implies that for initial flow the interaction $U(B)$ does not grow (5.13). Backed by the constant behaviour of $U(B)$ in the symmetric case we in particular we do not expect a divergence of the coupling under the flow. Therefore we assume that the solution

$$U_{\epsilon_F}^{B \approx 0}(B) = \frac{U_{\epsilon_F}(B=0)}{1 + 4\rho_0^2 |\epsilon_d N| U_{\epsilon_F}(B=0)B} \quad (\rightarrow 5.13)$$

which can be trusted for $B \ll \Delta^2$ extends approximately up to values of $B \approx 1/\Delta^2$. Thus we obtain a rough approximation for the value of the coupling when the flow parameter corresponds with characteristic energy scales of the system.

$$U_{\Delta} \stackrel{\text{def}}{=} U_{\epsilon_F}(B = 1/\Delta^2) \approx \frac{U_{\epsilon_F}(B=0)}{1 + 4\frac{\rho_0^2}{\Delta^2} |\epsilon_d N| U_{\epsilon_F}(B=0)} \quad (5.15)$$

We will use this result as an initial condition for the solution of the flow of $U(B)$ in the regime of large values of the flow parameter which we will study in the following sections. In order to do so we need to reformulate the flow equation.

5.4.3 Re-arrangement of the flow equation of $U(B)$ at the Fermi energy

In order to proceed with an analytical evaluation of the flow equation (5.11), we have to re-arrange it in a more accessible form. In the advanced flow regime the most relevant limitations on internal integrations result from the Gaussian cut-off function. We therefore apply an integral transformation such that the argument of the exponential depends on a single variable only.

2-D-integral transformation

By this demand the new variable x is already fixed, for the second new variable we choose an orthogonal one. The old variables are easily expressed in terms of the new ones.

$$\begin{pmatrix} x \\ y \end{pmatrix} = \begin{pmatrix} \epsilon_2 - \epsilon_1 \\ \epsilon_2 + \epsilon_1 \end{pmatrix} \iff \begin{pmatrix} \epsilon_1 \\ \epsilon_2 \end{pmatrix} = \frac{1}{2} \begin{pmatrix} y - x \\ y + x \end{pmatrix} \quad (5.16)$$

This transformation is not normalized and leads to a rescaling of the integration. We therefore compute the Jacobian:

$$\left\| \frac{\partial \epsilon}{\partial \mathbf{x}} \right\| = \frac{1}{4} \left\| \begin{pmatrix} -1 & 1 \\ 1 & 1 \end{pmatrix} \right\| = -\frac{1}{2}$$

We express the flow equation for $U(B)$, (5.11) in the new variables and note that the (absolute) value of the Jacobian and the prefactor cancel.

$$\frac{\partial U_{\epsilon_F}(B)}{\partial B} = -U_{\epsilon_F}^2(0) \rho_0^2 \int_{-\infty}^{\infty} dy \int_{-\infty}^{\infty} dx \quad W^2 \left(\frac{y-x}{2} \right) N_y(x) x e^{-2Bx} \left[W^2 \left(\frac{y+x}{2} \right) - W^2 \left(-\frac{y+x}{2} \right) \right] \quad (5.17)$$

For the transformed Fermi function we introduced a shorthand notation

$$N_y(x) := \left[n^+ \left(\frac{y-x}{2} \right) - n^- \left(\frac{y-x}{2} \right) \right] \quad (5.18)$$

Hence the cut-off function already acquired a simple form. In the next step we will discuss the two remaining structures, namely the modified Fermi function $N_y(x)$ and the difference of the hybridization functions.

Transformed Fermi function

Firstly we examine the effects of the integral transformation on the Fermi function $N_y(x)$ defined in (5.18) for arbitrary but fixed values of y . By inserting (5.16) into (A.14) we find

$$N_y(x) = \begin{cases} -1 & \text{for } x < y - 2\epsilon_U \\ n_T & \text{for } y - 2\epsilon_U \leq x \leq y - 2\epsilon_L \\ 1 & \text{for } x > y - 2\epsilon_L \end{cases} \quad (5.19)$$

which we consider for the case of a vanishing Fermi function inside the transport window only ($n_T = 0$). Then this function is point symmetric around $x = y$.

Effectively, the transformation stretches the transport window to double size in the (x, y) -space and changes the orientation of the curve (now depending on $-x$) by 180 degrees. This corresponds to a change of limits: formerly upper bounds are turned into lower bounds and vice versa. To keep the notation intuitive for graphical evaluation we make the following definitions: for all fixed values of y we define the transformed limits of the transport window

$$\begin{pmatrix} x_U \\ x_L \end{pmatrix} = \begin{pmatrix} y - 2\epsilon_L \\ y - 2\epsilon_U \end{pmatrix} \stackrel{\text{sym}}{=} \begin{pmatrix} y + V \\ y - V \end{pmatrix} \quad (5.20)$$

In the symmetric case, we work with the function

$$N_y(x) = \begin{cases} -1 & \text{for } x < y - V \\ 0 & \text{for } y - V \leq x \leq y + V \\ 1 & \text{for } x > y + V \end{cases} \quad (5.21)$$

In the remaining part of this section we simply refer to this function as *the* Fermi function.

Taylor-Expansion of the hybridization factors

Secondly, we treat the two factors in (5.17) which depend on the hybridization function W^2 . As we aim at evaluating the flow equation in the regime of advanced flow we know that the dominating restriction will be the cut-off window. Inside of it we can approximate the hybridization by the linear term of a Taylor expansion as only a small sector of its Lorentzian shape is seen.

We expand around the Fermi energy

$$W^2(\epsilon) = W^2(\epsilon_F) + \frac{\partial W^2}{\partial \epsilon} \Big|_{\epsilon=\epsilon_F} (\epsilon - \epsilon_F) + \dots \quad (5.22)$$

which we set zero. Expressing the expansion in terms of the transformed variables we obtain up to linear order for the hybridization functions in the flow equation

$$W^2(\epsilon_2) = W^2(0) + \frac{\partial W^2}{\partial \epsilon} \Big|_{\epsilon_F} \frac{y-x}{2} \quad \text{and} \quad (5.23)$$

$$W^2(\epsilon_2) - W^2(-\epsilon_2) = 2 \frac{\partial W^2}{\partial \epsilon} \Big|_{\epsilon_F} \epsilon_2 = \frac{\partial W^2}{\partial \epsilon} \Big|_{\epsilon_F} (y+x) \quad (5.24)$$

Multiplying both contributions we obtain the hybridization factor to the flow equation

$$W_1^2 (W_2^2 - W_{-2}^2) = W^2(0) \frac{\partial W^2}{\partial \epsilon} \Big|_{\epsilon_F} (x+y) + \frac{1}{2} \left(\frac{\partial W^2}{\partial \epsilon} \Big|_{\epsilon_F} \right)^2 (y^2 - x^2) \quad (5.25)$$

The separate discussions of the summands will be the main task when studying the advanced flow regime. The flow equation reads now

$$\frac{\partial U_{\epsilon_F}(B)}{\partial B} = -U_0^2 \rho_0^2 \int_{-\infty}^{\infty} dy \int_{-\infty}^{\infty} dx \ N_y(x) \ x \ e^{-2Bx} \left[W^2(0) \frac{\partial W^2}{\partial \epsilon} \Big|_{\epsilon_F} (x+y) + \frac{1}{2} \left(\frac{\partial W^2}{\partial \epsilon} \Big|_{\epsilon_F} \right)^2 (y^2 - x^2) \right] \stackrel{!}{=} U_0^2 (F) \quad (5.26)$$

For simplicity we introduce a symbolic abbreviation (F) for the algebraic term of the right hand side.

$$(F) = -\rho_0^2 \int_{-\infty}^{\infty} dy \int_{-\infty}^{\infty} dx \ N_y(x) \ x \ e^{-2Bx} \left[W^2(0) \frac{\partial W^2}{\partial \epsilon} \Big|_{\epsilon_F} (x+y) + \frac{1}{2} \left(\frac{\partial W^2}{\partial \epsilon} \Big|_{\epsilon_F} \right)^2 (y^2 - x^2) \right] \quad (5.27)$$

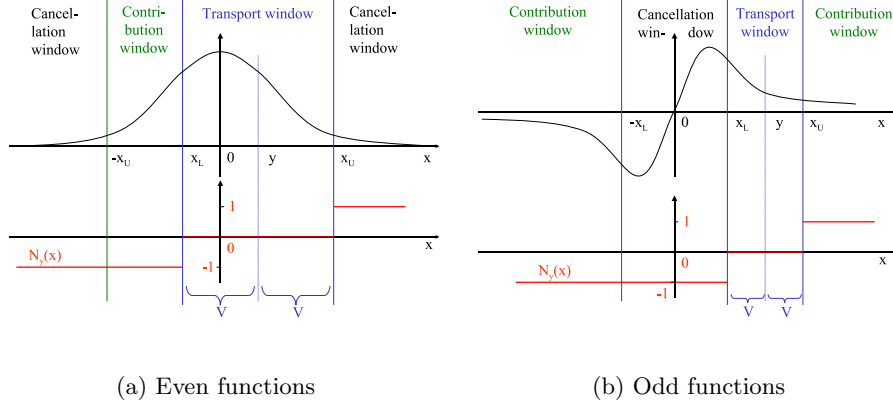


Figure 5.2: Thumbsketch of even and odd variations of the Gaussian function and of the Fermi distribution function for the regime of *advanced flow*. The integral transformation (5.16) has already been applied.

5.4.4 Discussion of Advanced Flow ($1/\sqrt{B} \ll \Delta$) at zero Temperature

In this regime, the Gaussian cut-off function determines the effective range of contributions to the dx -integral which we discuss in a first step. Inside the cut-off window the first order Taylor expansion of the hybridization is a sufficient approximation. The most relevant aspects for an evaluation of the integrations are introduced by the Fermi function. According to the general philosophy of our approach we will express its effects by explicit restrictions on the integration domain. For this procedure we again apply symmetry considerations and use graphical motivations.

Our further discussion will follow the following line: Noticing that either even or odd functions are present in the argument of the dx -integration, we separately consider these cases to make use of obvious symmetries and calculate the value of the integral. This will lead to a functional expression which still depends on y . In a second step we apply the dy -integration. Then symmetry considerations come into operation again.

Even functions in x

Even functions in the integrand can be assumed to be of the form $x^{2k}e^{-2Bx^2}$ for arbitrary integer numbers k . They are axial symmetric with respect to $x = 0$ and show an exponential decay.

Their axial symmetry combined with the point symmetry of the Fermi function leads to the opening of a cancellation window for large absolute values of x as contributions in the tails of the function $]-\infty, -x_C]$ and $[x_C, \infty[$ compensate for each other. Depending on the position of the transport window, $x_C = x_U$ (for $y > 0$) or $x_C = -x_L$ (for $y \leq 0$).

The effective contribution depends in a similar way on the asymmetry of the position of the transport window with respect to the symmetry of the Gaussian curve. It might open a contribution window of length $2|y|$, either $[-x_U, x_L]$ (for $y > 0$) or $[x_U, -x_L]$ (for $y < 0$). The

effective dx -integration is performed over this window only.

$$\int_{-\infty}^{\infty} dx N_y(x) x^{2k} e^{-2Bx^2} = -\Theta(y) \int_{-y-V}^{y-V} dx x^{2k} e^{-2Bx^2} + \Theta(-y) \int_{y+V}^{-y+V} dx x^{2k} e^{-2Bx^2} \quad (5.28)$$

Integrations over even arguments in x and y vanish:

An important observation shows that for fixed external voltage bias the result must be point symmetric in y . The relative position of the symmetry centres ($x = 0$ for the even functions and $x = y$ for the Fermi function) decides on the position of the contribution window which vanishes completely in the case of their coincidence. Therefore the contribution window is symmetrically opened on both sides for corresponding values of y , but the Fermi function induces different signs.

This implies that the dy -integration vanishes whenever the dy integrand consists of an even weight in y and the result of the dx -integration. Hence terms of the form

$$\int dy y^{2l} \int dx N_y(x) x^{2k} e^{-2Bx^2} = 0 \quad (5.29)$$

do not contribute to the flow of the interaction for any integer values l, k .

Odd functions in x

We start with a similar analysis for a class of odd functions in x characterized by the argument $x^{2k+1} e^{-2Bx^2}$ for arbitrary integer values of k . The interesting situation for these terms arises with $|y| > V^b$. In this case a cancellation window of length $2(|y| - V^b)$ is opened around the zero point. Now the contribution window is split into two parts containing the tails of the function. We consider both cases $y > 0$ and $y < 0$ explicitly which differ by the position of the windows only.

$$\begin{aligned} \int_{-\infty}^{\infty} dx N_y(x) x^{2k+1} e^{-2Bx^2} &= \\ &= \left[\Theta(-y) \left(- \int_{-\infty}^{x_L} dx + \int_{-x_U}^{\infty} dx \right) + \Theta(y) \left(- \int_{-\infty}^{-x_L} dx + \int_{x_U}^{\infty} dx \right) \right] x^{2k+1} e^{-2Bx^2} \\ &= \left[\Theta(-y) \left(- \int_{-\infty}^{-|y|-V} dx + \int_{|y|-V}^{\infty} dx \right) + \Theta(y) \left(- \int_{-\infty}^{-|y|+V} dx + \int_{|y|+V}^{\infty} dx \right) \right] \\ &\quad x^{2k+1} e^{-2Bx^2} \quad (5.30) \end{aligned}$$

Integrations over odd arguments in x produce axial symmetric result in y :

We observe that the contributions are axial symmetric for corresponding values of y , i.e.

$$\int_{-\infty}^{\infty} dx N(y; x) x^{2k+1} e^{-2Bx^2} = \int_{-\infty}^{\infty} dx N(-y; x) x^{2k+1} e^{-2Bx^2} \quad (5.31)$$

Integrations over odd arguments in x and y vanish:

Consequentially, the dy -integration vanishes if an odd weight in y is applied, i.e. for arbitrary integer values k and l

$$\int dy y^{2l+1} \int dx x^{2k+1} N_y(x) e^{-2Bx^2} = 0 \quad (5.32)$$

Restriction of integration for arguments of the form $y^{2l} x^{2k+1}$:

Moreover, we can simplify all further calculations which involve odd functions in x and even weights in y by restricting the dy -integration to half of the axis and doubling the obtained result.

$$\int_{-\infty}^{\infty} dy y^{2l} \int_{-\infty}^{\infty} dx N_y(x) x^{2k+1} e^{-2Bx^2} = 2 \int_{-\infty}^0 dy y^{2l} \int_{-\infty}^{\infty} dx N_y(x) x^{2k+1} e^{-2Bx^2} \quad (5.33)$$

for arbitrary integer values k and l .

Discussion of the terms in the flow equation

Now we apply our analysis of the integrals to the different terms in the right hand side of (5.26) which originated from the Taylor expansion of the hybridization. They show different behaviour depending on their parity in x and y . The linear term vanishes because of symmetries already discussed: $y x e^{-2Bx^2}$ is an odd term in x and y and does not contribute according to (5.32), for the even term $x^2 e^{-2Bx^2}$ we can apply the result (5.29).

$$\int_{-\infty}^{\infty} dy \int_{-\infty}^{\infty} dx N_y(x) (x + y) x e^{-2Bx^2} = 0 \quad (5.34)$$

Only the quadratic terms $\sim (y^2 - x^2) x e^{-2Bx^2}$ produce nonvanishing contributions. Again we make use of the symmetries and restrict the range of integration according to (5.33) to values $y < 0$. We calculate both terms independently using standard Gaussian integrals which can be found in the appendix.

Calculation of the term $\sim y^2 x e^{-2Bx^2}$

$$\begin{aligned} \int_{-\infty}^{\infty} dy y^2 \int_{-\infty}^{\infty} dx N_y(x) x e^{-2Bx^2} &= \\ &= 2 \int_{-\infty}^0 dy y^2 \left[(-1) \int_{-\infty}^{y-V} dx + \int_{-y-V}^{\infty} dx \right] x e^{-2Bx^2} \\ &= 2 \int_{-\infty}^0 dy y^2 \frac{1}{4B} \left[e^{-2B(y-V)^2} + e^{-2B(y+V)^2} \right] \\ &= \underbrace{\frac{1}{2B} \int_{-\infty}^0 dy y^2 e^{-2B(y-V)^2}} + \underbrace{\frac{1}{2B} \int_{-\infty}^0 dy y^2 e^{-2B(y+V)^2}} \end{aligned}$$

The two underbraced terms differ in a sign only and are treated in a similar way. We introduce new variables $z = y \pm V$, substitute and separately calculate the integrals.

$$\begin{aligned}
&= \frac{1}{2B} \int_{-\infty}^0 dy \quad [(y-V)^2 + 2V(y-V) + V^2] e^{-2B(y-V)^2} + \\
&\quad \frac{1}{2B} \int_{-\infty}^0 dy \quad [(y+V)^2 - 2V(y+V) + V^2] e^{-2B(y+V)^2} \\
&= \frac{1}{2B} \left\{ \int_{-\infty}^{-V} dz \quad [z^2 + 2Vz + V^2] e^{-2Bz^2} + \int_{-\infty}^V dz \quad [z^2 - 2Vz + V^2] e^{-2Bz^2} \right\} \\
&= \frac{1}{2B} \left[\frac{-1}{4B} (-Ve^{-2BV^2}) + \frac{1}{4B} \int_{-\infty}^{-V} dz \quad e^{-2Bz^2} - \frac{V}{2B} e^{-2BV^2} + V^2 \int_{-\infty}^{-V} dz \quad e^{-2Bz^2} \right] + \\
&\quad \frac{1}{2B} \left[\frac{-1}{4B} (Ve^{-2BV^2}) + \frac{1}{4B} \int_{-\infty}^V dz \quad e^{-2Bz^2} + \frac{V}{2B} e^{-2BV^2} + V^2 \int_{-\infty}^V dz \quad e^{-2Bz^2} \right]
\end{aligned}$$

Using the symmetry of the Gaussian, $\int_{-\infty}^{-V} dz \quad e^{-2Bz^2} = \int_V^{\infty} dz \quad e^{-2Bz^2}$ the integrals can be combined to full Gaussian integrals and evaluated. In total one obtains the following result:

$$\int_{-\infty}^{\infty} dy \quad y^2 \int_{-\infty}^{\infty} dx \quad N_y(x) \quad x e^{-2Bx^2} = \frac{1}{2B} \left(\frac{1}{4B} + V^2 \right) \sqrt{\frac{\pi}{2B}} \quad (5.35)$$

Calculation of the term $\sim x^3 e^{-2Bx^2}$: Using similar techniques we calculate the second nonvanishing contribution to the flow equation. As a detailed presentation of the calculation would not shed new light on the topic we just state the result:

$$\int_{-\infty}^{\infty} dy \quad \int_{-\infty}^{\infty} dx \quad N_y(x) \quad x^3 e^{-2Bx^2} = \frac{3}{8B^2} \sqrt{\frac{\pi}{2B}} \quad (5.36)$$

We remark that this result is independent of the voltage bias. Therefore we can expect specific out-of-equilibrium changes to the flow of the interaction only by the first contribution.

Flow equation in the advanced flow regime

Now we insert the results (5.34), (5.35) and (5.36) into (5.26). Hence the flow equation for the interaction $U(B)$ is given by the difference of both terms calculated above:

$$\frac{dU_F(B)}{U_F^2(B)} = -\rho_0^2 \frac{1}{2} \left(\frac{\partial W^2}{\partial \epsilon} \Big|_{\epsilon_F} \right)^2 \left(\frac{V^2}{2B} - \frac{1}{4B^2} \right) \sqrt{\frac{\pi}{2B}} \quad dB \quad (5.37)$$

Solution for the flow equation

In order to approximately evaluate the flow equation we assume that the solutions for initial and advanced flow coincide at $B = 1/\Delta^2$ which delivers an initial value $U_{\Delta} = U(B = 1/\Delta^2)$ (cf. 5.15). Now the differential equation can be integrated easily and produces the following result:

$$U_F^{B \rightarrow \infty}(B) = \frac{U_{\Delta}}{1 - \frac{1}{12} \sqrt{\frac{\pi}{2}} \rho_0^2 \left(\frac{\partial W^2}{\partial \epsilon} \Big|_{\epsilon_F} \right)^2 U_{\Delta} [-B^{-3/2} + 6 V^2 B^{-1/2} + \Delta^3 - 6\Delta V^2]} \quad (5.38)$$

Here we notice that for $B \rightarrow \infty$, i.e. in the case of diagonal Hamiltonian, there is a renormalization of the interaction which depends on the voltage bias applied to the system. The derivative of the hybridization function at the Fermi level amounts to $\frac{\partial W^2}{\partial \epsilon}|_{\epsilon_F} = 2\pi\rho_0 \frac{\epsilon_d}{\Delta} W^2(\epsilon_F) < 2\rho_0 \frac{\epsilon_d}{\Delta}$ and we know from the result (5.15) that $U_\Delta < U(B=0)$.

Now a more detailed discussion of this result for various regimes is possible. Depending on the parameters there is a configuration such that with increasing outer voltage the on-site interaction is reduced. This may correspond to results obtained in other models² where out of equilibrium conditions provoke a suppression of correlation effects. Further inquiries could be of interest.

5.4.5 Interaction as suitable perturbative parameter

In section 5.4.2 we have found for the regime of initial flow that the change of the interaction $U(B)$ under the flow is positive, decreasing and bounded from above by its initial value $U(B=0)$. This is a reliable estimation of the behaviour of the coupling for small values of the flow parameter. The last lines have shown that for large values of the flow parameter the interaction constant grows towards an asymptotic value. Comparing both results we conclude that there must be a minimal coupling strength $U_{min} := U(B_{min})$ which is obtained during the renormalization procedure in between of both regimes. Assuming a certain well-behaved continuity in the change of the coupling –which may be justified from experiences with the flow equations approach applied to other models– we expect that the coupling does not diverge under the flow for some common parameter regimes. Yet for impurity levels far off the Fermi energy or strong correlations divergences could appear. Therefore a detailed analysis of any application is indispensable.

A proper and detailed study of the flowing coupling constant for all regimes of the flow parameter is, of course, subject to a full numerical treatment of the flow equation (5.11). Nonetheless we believe that even in the asymmetric Anderson impurity model the on-site interaction U will be for many carefully chosen parameter regimes a controllable flowing quantity. Whenever chosen small initially it will not change its order of magnitude or character dramatically under the flow. Therefore we expect that it will be a suitable perturbative parameter in the sense of section (3.2.2) and that a perturbative expansion in terms of the coupling constant $U(B)$ holds throughout the flow equation procedure. On the other hand, a further analysis of the result could show where it fails and indicate limits of a perturbative approach.

Perturbative parameter for the symmetric model

Without any doubt the on-site interaction is a suitable perturbative parameter for the symmetric model. This choice is a natural one, as there is only one coupling involved in the initial Hamiltonian. In contrast to some other applications of the flow equations (e.g. the Kondo model), which have shown that expansion parameters might be different from the bare couplings of the model, this is not the case here.

Further on we will discuss the importance of various contributions to the flow equations and their solutions by their order in U , as we have already done for the setup of the flow equation of U itself. Our calculation will include all terms up to second order in U and neglect higher order structures.

²Notably the Kondo model studied by Stefan Kehrein

5.5 Flow equation for the energies and scattering amplitudes

We already examined the flow equation for the on-site interaction in a fairly extended way. We now want consider the flow equation for one-particle energies (ϵ_s) and potential scattering amplitudes ($P_{s's}$). This can be done in a joint formalism as both refer to the same operator structures. We will find that the change of these constants is a typical second order effect in U .

5.5.1 Flow equations for the renormalised energies and the potential scattering term

Obviously, the band energies ϵ_s are subject to renormalization changes, which will be expressed by flow equations for $\epsilon_s(B)$. Additionally, similar new terms, describing potential scattering, might arise with increasing flux although they were not present in the original Hamiltonian. In order to absorb both into a common formalism, we consider the flow of the constant $P_{s_1's_1}$ appearing in the free part of the Hamiltonian

$$H_0(B) = \sum_{s_1's_1} P_{s_1's_1} :b_{s_1'}^\dagger b_{s_1}: \quad (5.39)$$

where $P_{s_1s_1} = \epsilon_{s_1}$ with coinciding indices represents the band energies. For initial flow, we have non-vanishing band energies ($P_{s_1s_1}(B=0) \neq 0$) but no scattering terms are present ($P_{s_1's_1}(B=0) = 0$).

Evaluation of the commutator terms

As the commutator $[\eta^{(1)}, H_0]$ does not contain any operator product of length two, all these products result from the commutator $[\eta^{(1)}, H_{int}^{(1)}]$ which is quadratic in U . Hence energy renormalization and potential scattering are second order effects only. The results are degenerated for both spin orientations ($\uparrow\uparrow$) and ($\downarrow\downarrow$), so we only consider the first one. Single spin flips are forbidden by spin conservation. Combining four relevant terms by substituting internal indices we finally arrive at the following flow equation.

$$\frac{\partial P_{s_1's_1}(B)}{\partial B} = \{U_0^2 W_{\bar{1}\bar{1}}\} \sum_{s_1s_2's_2} W_{12'2}^2 e^{-B(\epsilon_{\bar{1}'} + \epsilon_{2'} - \epsilon_1 - \epsilon_2)^2} e^{-B(\epsilon_{\bar{1}} + \epsilon_{2'} - \epsilon_1 - \epsilon_2)^2} 2 \left(\frac{\epsilon_{\bar{1}'} + \epsilon_{\bar{1}}}{2} + \epsilon_{2'} - \epsilon_1 - \epsilon_2 \right) Q_{12'2} \quad (5.40)$$

We remind the reader of the definition of $Q_{12'2}$ in (A.15) where it is introduced as a quadratic combination of Fermi distribution functions at different points in energy. Furthermore we mention that the right hand side is symmetric in the external indices $s_{\bar{1}'}$ and $s_{\bar{1}}$. The following discussion of this equation will be done separately for the one-particle energies and the potential scattering amplitudes.

Renormalisation of the one-particle energies

The renormalisation of the one-particle energies is a fundamental effect of Hamiltonian diagonalization and cannot be avoided. It incorporates a part of the spectral weight which is

flowing from the off-diagonal into the diagonal elements of the Hamiltonian. Nonetheless it is of lower-ranking interest as in all observable results one-particle energies appear next to factors of the interaction. As the energy corrections are of the kind $\epsilon(B) = \epsilon(0) + U^2 \Delta\epsilon$ they are not visible in second order calculations.

$$U\epsilon(B) = U\epsilon(0) + U^3 \Delta\epsilon \stackrel{O(U^2)}{\approx} U\epsilon(0) \quad (5.41)$$

Therefore we neglect all aspects of energy renormalization and treat the one-particle energies in good approximation as constants under the flow.

Potential scattering amplitudes and extended generator

A different perspective should be taken on the issue of the potential scattering term. It is generated under the flow and corrupts the diagonal shape of the Hamiltonian. An extension of the generator has been defined in equation (4.11) which fully compensates for these contributions. Using the explicit flow equation for the scattering amplitudes we make this extension explicit:

$$\begin{aligned} \eta^{(2a)}(B) = & U_0^2(B) \sum_{s_{\bar{1}'} s_{\bar{1}}} W_{s_{\bar{1}'} s_{\bar{1}}} \frac{1}{\epsilon_{s_{\bar{1}'}} - \epsilon_{s_{\bar{1}}}} \sum_{s_1 s_2 / s_2} W_{s_1 s_2 / s_2}^2 Q_{s_1 s_2 / s_2} \\ & e^{-B(\epsilon_{s_{\bar{1}'}} + \epsilon_{s_2'} - \epsilon_{s_1} - \epsilon_{s_2})^2} e^{-B(\epsilon_{s_{\bar{1}}} + \epsilon_{s_2'} - \epsilon_{s_1} - \epsilon_{s_2})^2} \\ & 2 \left(\frac{\epsilon_{s_{\bar{1}'}} + \epsilon_{s_{\bar{1}}}}{2} + \epsilon_{s_2'} - \epsilon_{s_1} - \epsilon_{s_2} \right) :b_{s_{\bar{1}'}}^\dagger b_{s_{\bar{1}}}: \end{aligned} \quad (5.42)$$

This part of the generator is clearly antihermitian as the coefficients of the operator products are antisymmetric under interchange of the labels $s_{\bar{1}}$ and $s_{\bar{1}'}$.

The effect of the extension on the Hamiltonian diagonalization has been the cornerstone of its definition and has improved the diagonalization method. Hence we expect that it –loosely speaking– re-distributes the effects which potential scattering has and inserts additional terms into the flow equations of other observables. We will study this as an aspect of the transformation of observables in the next chapter.

Chapter 6

Transformation of the observables

In chapter 3 we have learned that according to the general framework of the flow equation formalism the infinitesimal unitary transformations applied to the Hamiltonian simultaneously affect the appearance of all observables. With increasing flow higher order terms of their basis representation are generated and change their behaviour. In this chapter we study the transformation of the creation and of the annihilation operator which we will need to express a one-particle Greens function in the final basis representation.

6.1 Ansatz for the transformation of fundamental operators

Before we progress to the transformation of a composed observable we study the transformation of a one-particle creation or annihilation operator under the flow equation procedure. Following the general outline of chapter (3) we choose a truncation scheme for the fundamental operator itself and represent it in terms of generalised coupling constants, then we derive their flow equations. The analysis of these flow equations will show that it is more convenient and sufficient to study a linear superposition of operators.

6.1.1 Creation operator

As a first step we consider the creation operator. As it is an ordinary object of the multi-particle operator space it undergoes the same unitary transformations as any other observable. Therefore we start with defining its basis representation which is trivial for initial flow but will acquire a more complex structure furtheron. Hence we need to discuss a suitable truncation scheme.

Choice of a truncation scheme

Physical demands impose constraints on the unitary transformations and allow for a reasonable restriction of the truncation scheme. As particle number and spin conservation is assumed the mixing of certain subsets is forbidden. Particle number conservation ensures that only subsets with the same numeral difference of creation and annihilation operators mix, spin conservation excludes some spin parameter regimes within the remaining subsets.

This implies that the number of creation operators minus the number of annihilation operators equals one in any term which is generated under the flow. In principle, arbitrarily high excitations may contribute. In an approximative restriction we only admit those of first

order particle excitations, i.e. operator products up to length three. Thus we start with the following ansatz

$$b_{s_{9'}}^\dagger(\gamma_{s_{5'}}^{s_{9'}}(B), M_{s_{5'}s_{6'}s_5}^{s_{9'}}(B)) = \sum_{s_{5'}} \gamma_{s_{5'}}^{s_{9'}}(B) b_{s_{5'}}^\dagger + \sum_{s_{5'}s_{6'}s_5} M_{s_{5'}s_{6'}s_5}^{s_{9'}}(B) :b_{s_{5'}}^\dagger b_{s_{6'}}^\dagger b_{s_5}: \quad (6.1)$$

Initial conditions

The initial conditions are set by physical plausibilities. At initial flow the original observable has not yet been changed, so

$$\gamma_{s_{5'}}^{s_{9'}}(B=0) = \delta_{s_{5'}}^{s_{9'}} \quad \text{and} \quad M_{s_{5'}s_{6'}s_5}^{s_{9'}}(B=0) = 0.$$

The newly introduced constants $\gamma_{s_{5'}}^{s_{9'}}(B)$ and $M_{s_{5'}s_{6'}s_5}^{s_{9'}}(B)$ are subject to a renormalization change under the flow induced by the sequence of infinitesimal transformations.

The obvious next steps are the setup of the flow equations by evaluating various commutators. We postpone this analysis for a short glimpse at the transformation of annihilation operators.

6.1.2 Annihilation operator

As creation and corresponding annihilation operators are related by hermitian conjugation we can regress to more general aspects of the transformation of hermitian conjugate observables.

Transformation of hermitian conjugate observables

According to the definition of the canonical generator and of its extension $\eta^{(2a)}$ the full generator is anti-hermitian ($\eta^\dagger(B) = -\eta(B)$). Thus the flow equation of the conjugate operator is simply given by the conjugated flow equation of the operator.

$$[\eta(B), b(b)] \stackrel{a.h.}{=} (b(B)\eta^\dagger(B) - \eta^\dagger(B)b(B)) = [\eta(B), b^\dagger]^\dagger$$

For the flow equation, this means

$$\frac{\partial b(B)}{\partial B} \stackrel{\text{FEqu}}{=} [\eta(B), b(B)] = [\eta(B), b^\dagger(B)]^\dagger \stackrel{\text{FEqu}}{=} \left(\frac{\partial b^\dagger(B)}{\partial B} \right)^\dagger$$

Consequentially, the same constants γ and M describe the behaviour of the annihilation operator under the transformation.

$$b_{s_9}(\gamma(B)M(B)) = \sum_{s_{5'}} \left(\gamma_{s_{5'}}^{s_9}(B) \right)^* b_{s_{5'}} + \sum_{s_{5'}s_{6'}s_5} \left(M_{s_{5'}s_{6'}s_5}^{s_9}(B) \right)^* :b_{s_5}^\dagger b_{s_{6'}}^\dagger b_{s_{5'}}:$$

All generalised coupling constants are real numbers. We re-label the internal summations to keep a correspondence between primed indices and creation operators

$$b_{s_9}(\gamma_{s_5}^{s_9}(B)M_{s_5s_6s_{5'}}^{s_9}(B)) = \sum_{s_5} \gamma_{s_5}^{s_9}(B) b_{s_5} + \sum_{s_{5'}s_6s_5} M_{s_5s_6s_{5'}}^{s_9}(B) :b_{s_5}^\dagger b_{s_6}^\dagger b_{s_5'}: \quad (6.2)$$

Thus we find that it is sufficient to treat the transformation of the creation operator to set up and solve the differential equations for the generalized couplings γ and M . No other structure will be needed.

6.1.3 Ansatz for the transformation of a composite object

It will turn out to be advantageous for solving the flow equations and calculating the spectral function of the impurity to consider a particular linear superposition of creation operators which all share a common spin orientation and are weighted by the hybridization.

As all our results are independent of the particular spin orientation we arbitrarily choose (\uparrow) . We establish the convention that whenever a spin index is made explicit the corresponding multi-index does not contain a spin part any more. This shall apply equally to indices of internal summations.

We define the composite object

$$O^\dagger(B=0) = \sum_{s_{5'}} W(s_{5'}) b_{s_{5'}\uparrow}^\dagger \quad (6.3)$$

and note that the same structural ansatz and truncation scheme can be used as for the creation operator itself (6.1). Yet the generalized coupling constants are re-defined and loose the formerly explicit outer energy dependence.

$$\gamma_{s_{5'}}(B) = \sum_{s_{9'}} W(s_{9'}) \gamma_{s_{5'}}^{s_{9'}}(B) \quad (6.4)$$

$$M_{s_{5'}s_{6'}s_5}(B) = \sum_{s_{9'}} W(s_{9'}) M_{s_{5'}s_{6'}s_5}^{s_{9'}}(B) \quad (6.5)$$

Effectively, this leads to an analogue ansatz for a new observable O defined by the new constants. and their initial conditions at $B=0$. Due to spin conservation, the spin of the first term is already fixed, while the second one contains two possible spin structures $(\uparrow\uparrow\uparrow)$ and $(\uparrow\downarrow\downarrow)$ which both represent a single net spin \uparrow .

$$O^\dagger(\gamma_{s_{5'}}(B), M_{s_{5'}s_{6'}s_5}(B)) = \sum_{s_{5'}} \gamma_{s_{5'}}(B) b_{s_{5'}\uparrow}^\dagger + \sum_{s_{5'}s_{6'}s_5} M_{s_{5'}s_{6'}s_5}(B) :b_{s_{5'}\uparrow}^\dagger b_{s_{6'}\uparrow}^\dagger b_{s_5}^\dagger: \quad (6.6)$$

The initial conditions are chosen as

$$\gamma_{s_{5'}}(B=0) = W(s_{5'}) \quad \text{and} \quad M_{s_{5'}s_{6'}s_5}(B=0) = 0 \quad (6.7)$$

6.2 Flow equations for the observable O^\dagger

We now will set up the flow equations for the observable O^\dagger and their generalised coupling constants. In a first step we limit our view on those terms which are generated by the canonical generator $\eta^{(1)}$. A discussion of the perturbative orders in terms of powers of the on-site interaction will answer the question what contributions of the extended generator $\eta^{(2a)}$ have to be taken into account. Lateron we will include these corrections into the flow equation

Recapitulation of canonical generator and parametrization of the coupling constant

We briefly remind the reader of the explicit form of the canonical commutator including the specific spin structure of the Anderson impurity model

$$\eta^{(1)} = \sum_{s_1's_1s_2's_2} U_{s_1's_1s_2's_2}(B) (\epsilon_{s_2'} - \epsilon_{s_2} + \epsilon_{s_1'} - \epsilon_{s_1}) :b_{s_1'\uparrow}^\dagger b_{s_1\uparrow}^\dagger b_{s_2'\downarrow}^\dagger b_{s_2\downarrow}^\dagger: \quad (\rightarrow 4.7)$$

where we use the first order ('free flow') parametrization of the interaction

$$U_{s_1's_1s_2's_2}(B) = U_0 W_{s_1's_1s_2's_2} e^{-(\epsilon_{s_2'} - \epsilon_{s_2} + \epsilon_{s_1'} - \epsilon_{s_1})^2 B} \quad (\rightarrow 5.8)$$

For the following calculation we make use of the fixed spin structure of the generator.

6.2.1 Contributions to the flow equation by the canonical generator

Following the general rules for the transformation of observables (cf 3.14) we easily write down the flow equation for the observable O^\dagger .

$$\begin{aligned} \frac{\partial O^\dagger(B)}{\partial B} &= [\eta^{(1)}(U(B)), O^\dagger(B)] = \\ &= U_0 \sum_{s_1's_1s_2's_2} W_{s_1's_1s_2's_2} (\epsilon_{s_2'} - \epsilon_{s_2} + \epsilon_{s_1'} - \epsilon_{s_1}) e^{-B(\epsilon_{s_2'} - \epsilon_{s_2} + \epsilon_{s_1'} - \epsilon_{s_1})^2} \cdot \\ &\quad \left[\sum_{s_5'} \gamma_{s_5'} [:b_{s_1'\uparrow}^\dagger b_{s_1'\uparrow} b_{s_2'\downarrow}^\dagger b_{s_2'\downarrow} : , b_{s_5'\uparrow}^\dagger] + \right. \\ &\quad \left. \sum_{s_5's_6's_5} M_{s_5's_6's_5} [:b_{s_1'\uparrow}^\dagger b_{s_1'\uparrow} b_{s_2'\downarrow}^\dagger b_{s_2'\downarrow} : , :b_{s_5'}^\dagger b_{s_6'}^\dagger b_{s_5} :] \right] \end{aligned} \quad (6.8)$$

The main task of this calculation is the evaluation of both commutators involved. The results can be found in the appendix.

We observe that including both spin conserving spin structures $\uparrow\uparrow\uparrow$ and $\uparrow\downarrow\downarrow$ in the ansatz (6.6) is sufficient to end up with a set of operator products which is cyclic (closed) under commutation with the canonical generator. This means that the truncation scheme is complete up to length three in the sense that no other operator products of length three are generated under the flow.

Differential flow equations for the generalized coupling constants

We evaluate the various terms in the commutators and finally arrive at a set of three coupled differential equations for the generalized coupling constants γ , $M_{\uparrow\uparrow\uparrow}$ and $M_{\uparrow\downarrow\downarrow}$ of the observable O .

$$\begin{aligned} \frac{\partial \gamma_{\tilde{5}'\uparrow}(B)}{\partial B} &= U_0 \sum_{s_1s_2's_2} W_{\tilde{5}'12'2} (\epsilon_{\tilde{5}'} - \epsilon_2 + \epsilon_{2'} - \epsilon_1) e^{-B(\epsilon_{\tilde{5}'} - \epsilon_2 + \epsilon_{2'} - \epsilon_1)^2} \\ &\quad Q_{12'2} M_{122'\uparrow\downarrow} \end{aligned} \quad (6.9)$$

$$\begin{aligned} \frac{\partial M_{\tilde{5}'6'\tilde{5}\uparrow\uparrow}(B)}{\partial B} &= -U_0 \sum_{s_2's_2} W_{\tilde{5}'\tilde{5}2'2} (n^+(2') - n^+(2)) M_{\tilde{6}'22'\uparrow\downarrow} \\ &\quad (\epsilon_{\tilde{5}'} - \epsilon_{\tilde{5}} + \epsilon_{2'} - \epsilon_2) e^{-B(\epsilon_{\tilde{5}'} - \epsilon_{\tilde{5}} + \epsilon_{2'} - \epsilon_2)^2} \end{aligned} \quad (6.10)$$

$$\begin{aligned}
\frac{\partial M_{\tilde{5}'\tilde{6}'\tilde{5}\uparrow\downarrow}(B)}{\partial B} &= U_0 \sum_{s_1} W_{\tilde{5}'1\tilde{6}'\tilde{5}} \gamma_{1\uparrow} (\epsilon_{\tilde{6}'} - \epsilon_{\tilde{5}} + \epsilon_{\tilde{5}'} - \epsilon_1) e^{-B(\epsilon_{\tilde{6}'} - \epsilon_{\tilde{5}} + \epsilon_{\tilde{5}'} - \epsilon_1)^2} \\
&+ U_0 \sum_{s_1 s_2'} W_{\tilde{5}'12'\tilde{5}} (\epsilon_{\tilde{5}'} - \epsilon_{\tilde{5}} + \epsilon_{2'} - \epsilon_1) e^{-B(\epsilon_{\tilde{5}'} - \epsilon_{\tilde{5}} + \epsilon_{2'} - \epsilon_1)^2} \\
&\quad [n^-(2') - n^-(1)] M_{1\tilde{6}'2'\uparrow\downarrow} \\
&+ U_0 \sum_{s_1 s_2} W_{\tilde{6}'1\tilde{5}'2} (\epsilon_{\tilde{5}'} + \epsilon_{\tilde{6}'} - \epsilon_2 - \epsilon_1) e^{-B(\epsilon_{\tilde{5}'} + \epsilon_{\tilde{6}'} - \epsilon_2 - \epsilon_1)^2} \\
&\quad [n^-(1) - n^+(2)] M_{12\tilde{5}\uparrow\downarrow} \\
&+ U_0 \sum_{s_1' s_1} W_{1'1\tilde{6}'\tilde{5}} (\epsilon_{\tilde{6}'} - \epsilon_{\tilde{5}} + \epsilon_{1'} - \epsilon_1) e^{-B(\epsilon_{\tilde{6}'} - \epsilon_{\tilde{5}} + \epsilon_{1'} - \epsilon_1)^2} \\
&\quad [n^+(1') - n^+(1)] [M_{1\tilde{5}1'\uparrow\uparrow} - M_{\tilde{5}'11'\uparrow\uparrow}]
\end{aligned} \tag{6.11}$$

6.2.2 Discussion of the flow equations

We continue with an analysis of the perturbative orders of the various terms present in the flow equations. Again, we use the on-site interaction U as an expansion parameter. To start with we refer to the initial values of the generalized coupling constants: $\gamma(B=0) = 1$ is obviously of order one; it does not vanish for zero on-site interaction. The other constants are generated under the flow and do not show an offset at $B=0$.

The first term in equation (6.11) expresses the generation of $M_{\uparrow\downarrow}$ which is –due to the pre-factor– first order in U . Consequentially, the second and third term of this equation, which describe the backaction of $M_{\uparrow\downarrow}$ onto itself, are second order in U .

The same holds for the constant $M_{\uparrow\uparrow}$ which is also generated in second order of U (see 6.10). Therefore the backaction of $M_{\uparrow\uparrow}$ onto $M_{\uparrow\downarrow}$ which is represented by the last term of (6.11) is of order U^3 .

Finally, we have a look at equation (6.13). We observe that corrections to γ are second order in U , as the pre-factor and $M_{\uparrow\downarrow}$ contribute one power in U each. We summarize our results:

Generation properties in orders of U

$$\begin{aligned}
\gamma &\sim 1 + \mathcal{O}(U^2) \\
M_{\uparrow\downarrow} &\sim \mathcal{O}(U) + \mathcal{O}(U^2) + \mathcal{O}(U^3) \\
M_{\uparrow\uparrow} &\sim \mathcal{O}(U^2)
\end{aligned}$$

For a consistent evaluation of the impurity Greens function we need γ up to second order but the constants M to first order only. Thus we fully neglect the generation of the constant $M_{\uparrow\uparrow}$. Instead, we need to include another contribution which results from the extended generator $\eta^{(2a)}$. In chapter (5) we have seen that the extended generator is second order in U (5.42). Therefore we expect a contribution to the flow equations of the observable O in second order of U . We will notice that it acts as a kind of backaction of γ onto itself and has to be considered in our further examinations.

6.2.3 Amendments to the flow equations by the extended generator

In chapter (4) we defined the extension of the generator and in equation we made it explicit. For now, we deal with it in the following form:

$$\eta^{(2a)}(B) = \sum_{s_{\uparrow'} s_{\downarrow}} \frac{1}{\epsilon_{s_{\uparrow'}} - \epsilon_{s_{\downarrow}}} \frac{\partial P_{s_{\uparrow'} s_{\downarrow}}(B)}{\partial B} :b_{s_{\uparrow'}}^\dagger b_{s_{\downarrow}}: \quad (\rightarrow (4.11))$$

Commutation of this generator with terms proportional to the constants $M_{\uparrow\downarrow}$ and $M_{\uparrow\uparrow}$ are already at least third order in U and do not need to be considered in second order calculations. Hence the only second order contribution is given by

$$[\eta^{(2a)}, \sum_{s_{\uparrow'}} \gamma_{s_{\uparrow'}} b_{s_{\uparrow'}}^\dagger] = \sum_{s_{\uparrow'} s_{\downarrow}} \frac{1}{\epsilon_{s_{\uparrow'}} - \epsilon_{s_{\downarrow}}} \frac{\partial P_{s_{\uparrow'} s_{\downarrow}}(B)}{\partial B} \gamma_{s_{\downarrow}} b_{s_{\uparrow'}}^\dagger \quad (6.12)$$

This term clearly contributes to the flow equation of γ in second order of U . It can be re-written in the following form:

Extended flow equation for γ

$$\begin{aligned} \frac{\partial \gamma_{s_{\uparrow'} s_{\downarrow}}(B)}{\partial B} &= U_0 \sum_{s_1 s_2'} W_{s_1 s_2'} (\epsilon_{s_1'} - \epsilon_2 + \epsilon_2' - \epsilon_1) e^{-B(\epsilon_{s_1'} - \epsilon_2 + \epsilon_2' - \epsilon_1)^2} \\ &\quad Q_{12'2} M_{122'\uparrow\downarrow} \\ &\quad + \sum_{s_1} \frac{1}{\epsilon_{s_1'} - \epsilon_1} \frac{\partial P_{s_{\uparrow'} s_1}(B)}{\partial B} \gamma_{s_1} \end{aligned} \quad (6.13)$$

As the newly introduced correction is proportional to γ it induces a kind of back-action of γ onto itself. This makes the system of differential equations more complicated, such that for analytical approximations we need to approximate this back-action by a constant value. We expect this approximation to return good results in a regime of not too strong coupling as for small interactions the corrections to γ are small in second order of U . The effective corrections to the flow equation due to this approximation in the back action would be of order four and thus efficiently suppressed. But for growing coupling strength we will need to apply more accurate (potentially numerical) tools.

6.3 Approximate analytical solutions to the flow equations of the observable

We now aim at analytical solutions for the flow of the generalized coupling constants. We start with a first-order evaluation of the equation (6.11) which gives a first-order result for $M_{\uparrow\downarrow}$.

6.3.1 Parametrization of γ

Similarly to the treatment of the flow equation for the on-site interaction we firstly choose a parametrization for the flowing constants involved. This parametrization could –in principle– be improved by an iterative calculation. For first order results this is, of course, not necessary.

Thus we choose a constant parametrization of $\gamma(\epsilon) = W(\epsilon) \quad \forall 0 \leq B < \infty$ which is zeroth order in U and hence not subject to any changes under the flow equation procedure.

6.3.2 First order solution for $M_{\uparrow\downarrow}$

For a first order solution to equation (6.11) we can restrict its right hand side to its first term. Inserting the constant parametrization of γ we obtain a simple differential equation which can be integrated in a straightforward way.

$$\frac{\partial M_{s_{\tilde{5}'}, s_{\tilde{6}'}, s_{\tilde{5}} \uparrow \downarrow}(B)}{\partial B} = U_0 W_{\tilde{5}' \tilde{6}' \tilde{5}} \sum_{s_1} W_1^2 (\epsilon_{\tilde{6}'} - \epsilon_{\tilde{5}} + \epsilon_{\tilde{5}'} - \epsilon_1) e^{-B(\epsilon_{\tilde{6}'} - \epsilon_{\tilde{5}} + \epsilon_{\tilde{5}'} - \epsilon_1)^2}$$

Integration is between $\int_{M(B=0)=0}^{M(B)} dM'$ and $\int_0^B dB'$ and introduces on the right hand side a nontrivial integration constant which fully describes the limit $B \rightarrow \infty$. Finally, we obtain

$$M_{s_{\tilde{5}'}, s_{\tilde{6}'}, s_{\tilde{5}} \uparrow \downarrow}(B) \stackrel{\mathcal{O}(U)}{=} -U_0 W_{\tilde{5}' \tilde{6}' \tilde{5}} \sum_{s_1} W_1^2 \frac{e^{-B(\epsilon_{\tilde{6}'} - \epsilon_{\tilde{5}} + \epsilon_{\tilde{5}'} - \epsilon_1)^2} - 1}{\epsilon_{\tilde{6}'} - \epsilon_{\tilde{5}} + \epsilon_{\tilde{5}'} - \epsilon_1} \quad (6.14)$$

We call this solution the "free" parametrization of $M_{\uparrow\downarrow}$ as it does not contain any kind of backaction of other flowing constants; it is obviously of order U .

Evaluation of the internal summation

We introduce the short-hand notation

$$\xi \stackrel{def}{=} \epsilon_{\tilde{6}'} - \epsilon_{\tilde{5}} + \epsilon_{\tilde{5}'} \quad (6.15)$$

and transform the internal summation in momentum space into an energy integral which we split up into two contributions.

$$M_{s_{\tilde{5}'}, s_{\tilde{6}'}, s_{\tilde{5}} \uparrow \downarrow}(B) = U_0 W_{\tilde{5}' \tilde{6}' \tilde{5}} \left[\underbrace{\rho \int d\epsilon W^2(\epsilon) \frac{1}{\xi - \epsilon}}_{K(\xi)} + \underbrace{\rho \int d\epsilon W^2(\epsilon) \frac{e^{-B(\xi - \epsilon)^2}}{\epsilon - \xi}}_{I(\xi; B)} \right] \quad (6.16)$$

The first integral represents the Kramers-Kronig transform of the hybridization which we have calculated in (2.35). The second one is a correction which depends on the flow parameter. We make the hybridization explicit (2.32) and apply the following substitution.

$$z = \sqrt{B}(\epsilon - \xi) \quad (6.17)$$

Note that a linear shift of the integration variable does not change the value of the integral.

$$I(\xi; B) = \rho \int dz \frac{e^{-z^2}}{z} W^2(z/\sqrt{B} + \xi) \quad (6.18)$$

Discussion in the limit of accomplished flow

For obvious reasons our special interest is in the limit of accomplished flow, because it corresponds to the appearance of an observable in the (approximate) eigenbasis of the Hamiltonian. In this limit, $B \rightarrow \infty$, the hybridization function decouples from the integral I which becomes anti-symmetric in the integration variable. Hence it vanishes.

$$I(\xi; B \rightarrow \infty) = W^2(\xi) \rho \int dz \frac{e^{-z^2}}{z} = 0 \quad (6.19)$$

Thus we arrive at the first order result

$$M_{s_{\tilde{\gamma}'}, s_{\tilde{\gamma}'}, s_{\tilde{\gamma}'}}^{\uparrow\downarrow}(B \rightarrow \infty) \stackrel{O(U)}{=} U_0 W_{\tilde{\gamma}'\tilde{\gamma}'\tilde{\gamma}'} K(\epsilon_{\tilde{\gamma}'} - \epsilon_{\tilde{\gamma}} + \epsilon_{\tilde{\gamma}'}) \quad (6.20)$$

6.3.3 Second order solution for γ

As a second step, we calculate corrections to γ which is up to now simply assumed as a constant offset. We learned from perturbation analysis that we do not need to expect a first order contribution. To calculate the second order behavior of γ accurately we need to solve the extended flow equation (6.13) which includes potential scattering effects.

Equation (6.14) provides a parametrization for the coupling constant $M_{\uparrow\downarrow}$. It is first order in U and thus -because of its prefactor- sufficient for second order calculations. Just as well we include the explicit flow equation for the scattering amplitudes (5.40) into (6.13) and thereby make the flow equation explicit. A systematic relabelling of indices is sufficient to deal with the expressions involved; further assumptions are not needed.

Explicit form of the extended flow equation for γ

$$\begin{aligned} \frac{\partial \gamma_{s_{\tilde{\gamma}'}, \uparrow}(B)}{\partial B} &= U_0^2 W_{s_{\tilde{\gamma}'}} \sum_{s_1 s_2' s_2} W_{s_1 s_2' s_2}^2 Q_{s_1 s_2' s_2} e^{-B(\epsilon_{s_{\tilde{\gamma}'}} - \epsilon_{s_2} + \epsilon_{s_2'} - \epsilon_{s_1})^2} \\ &\quad \sum_{s_3} W_{s_3}^2 \frac{\epsilon_{s_{\tilde{\gamma}'}} - \epsilon_{s_2} + \epsilon_{s_2'} - \epsilon_{s_1}}{\epsilon_{s_3} - \epsilon_{s_2} + \epsilon_{s_2'} - \epsilon_{s_1}} \left(e^{-B(\epsilon_{s_2} - \epsilon_{s_2'} + \epsilon_{s_1} - \epsilon_{s_3})^2} - 1 \right) \\ &+ U_0^2 W_{s_{\tilde{\gamma}'}} \sum_{s_1 s_2' s_2} W_{s_1 s_2' s_2}^2 Q_{s_1 s_2' s_2} e^{-B(\epsilon_{s_{\tilde{\gamma}'}} + \epsilon_{s_2'} - \epsilon_{s_1} - \epsilon_{s_2})^2} \sum_{s_3} \frac{\gamma_{s_3} W_{s_3}}{\epsilon_{s_{\tilde{\gamma}'}} - \epsilon_{s_3}} \\ &\quad 2 \left(\frac{\epsilon_{s_{\tilde{\gamma}'}} + \epsilon_{s_3}}{2} + \epsilon_{s_2'} - \epsilon_{s_1} - \epsilon_{s_2} \right) e^{-B(\epsilon_{s_3} + \epsilon_{s_2'} - \epsilon_{s_1} - \epsilon_{s_2})^2} \end{aligned} \quad (6.21)$$

For the internal integration we can parametrize γ consistently by its zeroth order result.

$$\begin{aligned} \frac{\partial \gamma_{s_{\tilde{\gamma}'}, \uparrow}(B)}{\partial B} &= U_0^2 W_{s_{\tilde{\gamma}'}} \sum_{s_1 s_2' s_2} W_{s_1 s_2' s_2}^2 Q_{s_1 s_2' s_2} e^{-B(\epsilon_{s_{\tilde{\gamma}'}} - \epsilon_{s_2} + \epsilon_{s_2'} - \epsilon_{s_1})^2} \\ &\quad \sum_{s_3} W_{s_3}^2 \left\{ \frac{\epsilon_{s_{\tilde{\gamma}'}} - \epsilon_{s_2} + \epsilon_{s_2'} - \epsilon_{s_1}}{\epsilon_{s_3} - \epsilon_{s_2} + \epsilon_{s_2'} - \epsilon_{s_1}} \left(e^{-B(\epsilon_{s_2} - \epsilon_{s_2'} + \epsilon_{s_1} - \epsilon_{s_3})^2} - 1 \right) + \right. \\ &\quad \left. \frac{2}{\epsilon_{s_{\tilde{\gamma}'}} - \epsilon_{s_3}} \left(\frac{\epsilon_{s_{\tilde{\gamma}'}} + \epsilon_{s_3}}{2} + \epsilon_{s_2'} - \epsilon_{s_1} - \epsilon_{s_2} \right) e^{-B(\epsilon_{s_3} + \epsilon_{s_2'} - \epsilon_{s_1} - \epsilon_{s_2})^2} \right\} \end{aligned}$$

Change of notation and decoupling of internal sums

In order to simplify our notation, we re-name the energy variables and introduce the energy sum a .

$$\begin{pmatrix} x \\ y \\ a \end{pmatrix} \stackrel{\text{def}}{=} \begin{pmatrix} \epsilon_{s_3} \\ \epsilon_{s_{\bar{s}'}} \\ -\epsilon_{s_2} + \epsilon_{s_{2'}} - \epsilon_1 \end{pmatrix} \quad \text{and} \quad \sum_{s_2 s_3} \rightarrow \sum_{xa} \quad (6.22)$$

This allows for a decoupling of internal summations. We recapitulate that in our notation indices on functions correspond to the energy index of their argument. We write $\epsilon_2 = \epsilon_{s_{2'}} - \epsilon_1 - a$ and treat this as an energy argument of the hybridization or the Q function. We make the definition

$$T(a) \stackrel{\text{def}}{=} \sum_{s_1 s_{2'}} W_{s_1 s_{2'}(s_{2'} - s_2 - a)}^2 Q_{s_1 s_{2'}(s_{2'} - s_2 - a)} \quad (6.23)$$

The extended differential equation for γ reads now

$$\begin{aligned} \frac{\partial \gamma(y; B)}{\partial B} &= U_0^2 W(y) \sum_{ax} W_x^2 T(a) \cdot \\ &\left\{ \left[\frac{y+a}{x+a} + \frac{2a+x+y}{y-x} \right] e^{-B[(y+a)^2 + (x+a)^2]} - \frac{y+a}{x+a} e^{-B(y+a)^2} \right\} \end{aligned} \quad (6.24)$$

Calculation of the second order result for γ

We perform the simple summation

$$\frac{y+a}{x+a} + \frac{2a+x+y}{y-x} = \frac{(x+a)^2 + (y+a)^2}{(x+a)(y-x)}$$

and integrate with respect to B to obtain the second order correction to γ :

$$\gamma(y; B) = \gamma(y; B=0) + \Delta\gamma(y; B) \quad (6.25)$$

$$\Delta\gamma(y; B) = U_0^2 W(y) \sum_{ax} W_x^2 T(a) \left[\frac{1 - e^{-B[(y+a)^2 + (x+a)^2]}}{(x+a)(y-x)} + \frac{e^{-B(y+a)^2} - 1}{(y+a)(x+a)} \right] \quad (6.26)$$

6.3.4 Discussion of γ in the limit of accomplished flow

Again, our first priority is to study the appearance of γ in the limit $B \rightarrow \infty$. In contrast to the easily taken limit in the treatment of the constant M above we have to face some complications. Therefore we approach the result from two different points of view.

Naive performance of the limit

A naive way to perform the limit $B \rightarrow \infty$ is to neglect all exponential factors which should simply die away. We would obtain

$$\begin{aligned}
\Delta\gamma(y; B \rightarrow \infty) &\stackrel{?}{=} U_0^2 W(y) \sum_{ax} W_x^2 T(a) \underbrace{\left[\frac{1}{(x+a)(y-x)} - \frac{1}{(y+a)(x+a)} \right]}_{\frac{1}{(y-x)(y+a)}} \\
&\stackrel{?}{=} U_0^2 W(y) \underbrace{\left[\sum_x W_x^2 \frac{1}{y-x} \right]}_{K(y)} \sum_a \frac{T(a)}{y+a} \\
&\stackrel{?}{=} U_0^2 W(y) K(y) \sum_a \frac{T(a)}{y+a} \tag{6.27}
\end{aligned}$$

This naive limit is not fully correct, but already includes the most important part of the final solution. Nonetheless we will find a non-vanishing correction term.

Rescaling transformation

In a second approach we promote the internal sums in (6.26) to integrations and rescale the integration parameters. This eliminates the explicit emergence of the flow parameter in the exponential functions.

$$\begin{pmatrix} z_1 \\ z_1 \end{pmatrix} \stackrel{\text{def}}{=} \begin{pmatrix} \sqrt{B}(y+a) \\ \sqrt{B}(x+a) \end{pmatrix} \iff \begin{pmatrix} a \\ x \end{pmatrix} = \begin{pmatrix} \frac{z_1}{\sqrt{B}} - y \\ \frac{z_2 - z_1}{\sqrt{B}} + y \end{pmatrix} \tag{6.28}$$

$$\begin{aligned}
\Delta\gamma(y; B) &= U_0^2 W(y) \rho^2 \int dz_1 \int dz_2 W^2\left(\frac{z_2 - z_1}{\sqrt{B}} + y\right) T\left(\frac{z_1}{\sqrt{B}} - y\right) \cdot \\
&\quad \left[\frac{1 - e^{-(z_1^2 + z_2^2)}}{z_2(z_1 - z_2)} + \frac{e^{-z_1^2} - 1}{z_1 z_2} \right] \tag{6.29}
\end{aligned}$$

Discussion of the integral in the limit of accomplished flow

We perform the limit $B \rightarrow \infty$ which, again, leads to a decoupling of the functions $W^2(y)$ and of $T(-y)$. Then two integrals remain.

$$I_1 = \int dz_1 \int dz_2 \frac{e^{-z_1^2}}{z_1 z_2} \tag{6.30}$$

$$I_2 = \int dz_1 \int dz_2 \frac{e^{-[z_1^2 + z_2^2]}}{z_2(z_1 - z_2)} \tag{6.31}$$

While the integral I_1 is asymmetric in its argument and vanishes, I_2 introduces a non-vanishing contribution. This leads to a pole correction term which has to be inserted into the expression of $\Delta\gamma$.

Pole-correction term

A proper treatment and a profound analysis of the integral I_2 is, unfortunately, beyond the scope of this work. Its difficult pole structure and the missing regularization might suggest that it produces a divergent contribution. This is not correct as the straightforward promotion of the summation in (6.26) to an integration (6.29) neglected important constrictions which have been implicitly assumed. For instance, we introduce the extension of the canonical generator, $\eta^{(2a)}$, as a potentially divergent object in (4.11). Naturally, this requires the implicit assumption to treat this divergence as a regularized structure and to apply a principal value integration. Further investigations in the correct treatment of these structures is necessary. We proceed with an effective solution of this problem for the symmetric Anderson impurity model. Then the functions $W(y)$ and $T(-y)$ are symmetric in y and there is very good reason to believe (cf. 7.3.4) that the pole correction (PC) term is of the following form:

$$\Delta\gamma_{PC}(y) = -U_0^2 \frac{\pi^2}{2} W^3(y)T(y) \quad (6.32)$$

The most convincing justification for this choice of the pre-factor is the fact that it ensures the conservation of spectral weight. We will study this feature in detail in the following section. Moreover, we remark that the correction term depends –via the function $T(y)$ – on the Fermi distribution function and, in consequence, on the outer voltage bias. Therefore we expect it to make a significant contribution to the out-of-equilibrium properties of γ .

Full expression for γ in the limit of accomplished flow

Collecting the results (6.25), (6.27) and (6.32) the correct expression for the flowing coupling constant in the limit $B \rightarrow \infty$ is of the following form:

$$\begin{aligned} \gamma(y; B \rightarrow \infty) &= W(y) + \Delta\gamma(y; B \rightarrow \infty) \\ &= W(y) + U_0^2 W(y) \left[K(y) \sum_a \frac{T(a)}{y+a} - \frac{\pi^2}{2} W^2(y)T(y) \right] \\ &= W(y) + U_0^2 \Delta\gamma^{(2)}(y) \end{aligned} \quad (6.33)$$

In the last line we have made the dependence on the on-site interaction explicit and defined the second order correction $\Delta\gamma^{(2)}(y)$. We will make use of this result lateron.

Chapter 7

Derivation of the impurity spectral density

Until now we have presented the development of the flow equation formalism for the Anderson impurity model. We have studied the flow of generalized coupling constants under unitary transformations for the Hamiltonian and the creation operator. As we aim to produce physically relevant and –more or less directly– observable predictions we focus on the impurity spectral density. There are various suggestions to measure this quantity experimentally. In a quantum dot experiment, for instance, a third lead which is weakly coupled to the dot could act as a probing device. [33]

The impurity density of states is directly related to the retarded impurity Greens function. Its calculation will be performed in the (approximately) diagonal basis of the Hamiltonian, i.e. for $B \rightarrow \infty$. In this basis the equilibrium ground state of the system is well-known; it can be written down as a simple Fermi distribution of quasiparticles, thus correlators can be evaluated easily. The characteristic features of the system are carried by the transformed observables which enter into the Greens function. Therefore we need to express the retarded impurity Greens function in terms of the diagonal basis of the Hamiltonian.

7.1 Greens function formalism for transformed observables

7.1.1 Definition and ansatz

We start with a canonical definition (see, for instance, [34]) of the retarded Greens function and apply it to the impurity of an Anderson impurity model. Firstly, we represent its operators in the pre-diagonalized basis. By this we extract all effects caused by the hybridization, i.e. the tunnel coupling between the impurity and the metallic leads, from the description of the ground state and include them in the explicit form of new hybridized operators.

$$iG_d^R(t) = \left\langle \left\{ d_H(t), d_H^\dagger(0) \right\} \right\rangle \Theta(t) = \sum_{s',s} B_{s'd}^\dagger B_{sd} \langle IGS | \left\{ b_{Hs}(t), b_{Hs'}^\dagger(0) \right\} | IGS \rangle \Theta(t)$$

But the main problem of this representation, the unknown interacting ground state of the correlator, remains. Due to the on-site interaction, the Hamiltonian is not a diagonal operator and even the equilibrium ground state cannot be described as a Fermi sea.

Therefore we apply as a second step another unitary transformation and change to the diagonal basis of the Hamiltonian. Now the interacting ground state is –in equilibrium– easily written down as a Fermi sea ($|GS\rangle = U^{-1} |IGS\rangle$) of quasiparticles defined w.r.t. the diagonal Hamiltonian.

$$iG_d^R(t) = \sum_{s',s} B_{s'd}^\dagger B_{sd} \langle IGS | U U^{-1} \{ b_{Hs}(t), b_{Hs'}^\dagger(0) \} U U^{-1} |IGS\rangle \Theta(t)$$

In the flow equation framework this corresponds to a transformation of all particle operators into more complicated quasiparticle structures according to the rules of the transformation of the observables. To change into a diagonal basis of the Hamiltonian the flow equation transformation has to be applied to full extend, i.e. the flow parameter extends to infinity.

$$iG_d^R(t) = \sum_{s',s} B_{s'd}^\dagger B_{sd} \langle GS | \left\{ \mathcal{F}_{B \rightarrow \infty} [b_{Hs}(t)], \mathcal{F}_{B \rightarrow \infty} [b_{Hs'}^\dagger(0)] \right\} |GS\rangle \Theta(t) \quad (7.1)$$

For the creation and annihilation operator we work with the truncation scheme introduced in (6.1). We quote this result for the annihilation operator and note that in the case of a single operator the constants of the expansion γ and M do carry an additional outer energy dependence.

$$\mathcal{F}_B \left[b_{s_9} (\gamma_{s_5}^{s_9}(0) M_{s_5 s_6 s_5'}^{s_9}(0)) \right] = \sum_{s_5} \gamma_{s_5}^{s_9}(B) b_{s_5} + \sum_{s_5' s_6 s_5} M_{s_5 s_6 s_5'}^{s_9}(B) : b_{s_5'}^\dagger b_{s_6} b_{s_5} : \quad (\rightarrow 6.2)$$

Inserting this ansatz into the Greens function (7.1) makes the multiparticle character of an interacting Greens function more explicit; it was primarily hidden in the nature of the Heisenberg operators. Expressing them in terms of Schroedinger operators would have made the influence of the non-diagonal, multiparticle Hamiltonian more obvious.

7.1.2 Evaluation of time dependence

Before we insert this ansatz into the Greens function (7.1) we evaluate the time dependence of the annihilation operator. As for $B \rightarrow \infty$ the Hamiltonian is diagonal up to second order in U it is sufficient to consider the commutators of a diagonal one-particle Hamilton operator defining the time evolution of the system and the annihilation operator in its truncation scheme. The relevant commutators can be found in the appendix. Their cyclic nature allows for an easy application of the Baker-Hausdorff-formula in the limit $B \rightarrow \infty$.

$$\begin{aligned} \mathcal{F}_{B \rightarrow \infty} [b_{Hs}(t)] &= e^{iH(B \rightarrow \infty)t} \mathcal{F}_{B \rightarrow \infty} [b_s] e^{-iH(B \rightarrow \infty)t} \\ &= e^{iHt} \left(\sum_{s_5} \gamma_{s_5}^s b_{s_5} + \sum_{s_5' s_6 s_5} M_{s_5 s_6 s_5'}^s : b_{s_5'}^\dagger b_{s_6} b_{s_5} : \right) e^{-iHt} \\ &= \sum_{s_4 s_5 s_6 s_5'} \left(\gamma_4^s e^{-i\epsilon_4 t} b_4 + M_{565'}^s e^{i(\epsilon_{5'} - \epsilon_5 - \epsilon_6)t} : b_5^\dagger b_6 b_5 : \right) \end{aligned} \quad (7.2)$$

The time evolution of the creation operator is trivial and does not effect the appearance of the Greens function.

7.1.3 Evaluation of the Greens function

We now insert (7.2) into the retarded impurity Greens function (7.1) and re-arrange the terms involved.

$$iG_d^R(t) = \sum_{s',s} B_{s'd}^\dagger B_{sd} \sum_{s_4 s_5 s_6 s_{5'}} \sum_{s_7' s_8' s_7 s_9'} \Theta(t) \left\langle \left\{ \gamma_4^s e^{-i\epsilon_4 t} b_4 + M_{565'}^s e^{i(\epsilon_{5'} - \epsilon_5 - \epsilon_6)t} : b_5^\dagger b_6 b_5 : , \gamma_{9'}^{s'} b_{9'}^\dagger + M_{7'8'7}^{s'} : b_7^\dagger b_8^\dagger b_7 : \right\} \right\rangle \quad (7.3)$$

Restrictions by the operator structure

Firstly we mention that correlators of the form $\langle \{b, :b^\dagger b^\dagger b:\} \rangle$ vanish. This is easily seen because after contraction of the single operator with a corresponding one in the product only one-particle expectation values would remain; but these were already eliminated by the normal ordering prescription.

Approximations according to perturbative arguments

In chapter (6) we have seen that due to the specific spin structure of the Anderson impurity model only two spin structures for the constant M do contribute, namely $M_{\uparrow\uparrow\uparrow}$ and $M_{\uparrow\downarrow\downarrow}$. Moreover we have learned that both constants behave under the flow like $M_{\uparrow\downarrow\downarrow} \sim \mathcal{O}(U)$ and $M_{\uparrow\uparrow\uparrow} \sim \mathcal{O}(U^2)$. This implies that mixed terms of the form $M_{\uparrow\downarrow\downarrow} M_{\uparrow\uparrow\uparrow} \sim \mathcal{O}(U^3)$ or terms quadratic in $M_{\uparrow\uparrow\uparrow} \sim \mathcal{O}(U^4)$ can be dropped in a calculation of order U^2 . We therefore neglect such contributions wherever they occur.

Re-arrangement of hybridization

For one-level impurity models (like the Anderson impurity model) we already know that the hybridization function is given by

$$B_{sd}^\dagger = B_{sd} = W(\epsilon_s) \quad (7.4)$$

Hence we can formally include all hybridization effects into new generalized coupling constants which represent just those composite objects which we have already discussed in section (6.1.3). In particular, we have derived the flow equations for generalized coupling constants.

$$\gamma_{s_4} = \sum_s B_{sd} \gamma_{s_4}^s = \sum_s W(\epsilon_s) \gamma_{s_4}^s \quad \text{and} \quad (7.5)$$

$$M_{s_5 s_6 s_{5'}} = \sum_s B_{sd} M_{s_5 s_6 s_{5'}}^s = \sum_s W(\epsilon_s) M_{s_5 s_6 s_{5'}}^s \quad (7.6)$$

with the initial conditions

$$\gamma_{s_4}(B=0) = W(\epsilon_{s_4}) \quad \text{and} \quad M_{s_5 s_6 s_{5'}}(B=0) = 0 \quad (7.7)$$

Fourier transform of the step function

In order to discuss the energy dependence of the retarded Greens function explicitly, we express the $\Theta(t)$ -function in terms of its Fourier representation:

$$\Theta(t) = - \int_{-\infty}^{\infty} \frac{d\omega}{2\pi i} \frac{e^{-i\omega t}}{\omega + i\eta} \quad (7.8)$$

As all other time dependence is in the argument of exponentials this allows for an easy Fourier transform of the retarded Greens function by a linear shift of the Fourier variable. This is a standard approach and can be found in the literature (e.g. [34]).

7.1.4 Contributions to the Greens function in $\mathcal{O}(U^2)$

Finally, two structures quadratic in the constants γ and $M_{\uparrow\downarrow}$ remain in the retarded impurity Greens function of the Anderson impurity model. We discuss their contributions separately.

Contribution by γ

The evaluation of the correlator $\langle \{b, b^\dagger\} \rangle$ results in a straightforward contraction

$$iG_d^{R(\gamma)}(t) = \sum_s e^{-i\epsilon_s t} |\gamma_s|^2 \Theta(t)$$

or, expressed in energy space,

$$G_d^{R(\gamma)}(\omega) = \sum_s |\gamma(\epsilon_s)|^2 \frac{1}{\omega - \epsilon_s + i\eta} \quad (7.9)$$

Contribution by $M_{\uparrow\downarrow}$

This contribution to the Greens function arises from the term

$$iG_d^{R(M)}(t) = \Theta(t) \sum_{s_5 s_6 s_5'} \sum_{s_7' s_8' s_7} e^{i(\epsilon_{s_5'} - \epsilon_{s_5} - \epsilon_{s_6})t} M_{s_5 s_6 s_5' \uparrow\downarrow} M_{s_7' s_8' s_7 \uparrow\downarrow} \langle \{ :b_{s_5'\downarrow}^\dagger b_{s_6\downarrow} b_{s_5\uparrow} : , :b_{s_7'\uparrow}^\dagger b_{s_8'\downarrow}^\dagger b_{s_7\downarrow} : \} \rangle \quad (7.10)$$

where we made the spin structure explicit. The non-trivial correlator can be found in a more general form in the appendix. In this place we impose the specific spin structure which reduces the number of nonzero contractions. Finally, a single term remains.

$$iG_d^{R(M)}(t) = \Theta(t) \sum_{s_5 s_6 s_5'} e^{i(\epsilon_{s_5'} - \epsilon_{s_5} - \epsilon_{s_6})t} M_{565'\uparrow\downarrow}^2 Q_{55'6}, \quad (7.11)$$

We briefly remind the reader that the combination of Fermi functions Q was defined in (A.15). Again we can read off the M^2 - contribution to the Fourier transformed retarded Green's function

$$iG_d^{R(M)}(\omega) = \sum_{s_5 s_6 s_5'} \frac{M_{565'\uparrow\downarrow}^2 Q_{55'6}}{\omega + \epsilon_{s_5'} - \epsilon_{s_5} - \epsilon_{s_6} + i\eta} \quad (7.12)$$

7.1.5 Spectral density and Greens function of the impurity

The spectral density of the impurity and its retarded Greens function are directly related by the following relation:

$$\rho_d(\omega) = -\frac{1}{\pi} \Im(G_d^R(\omega)) \quad (7.13)$$

In order to calculate the imaginary part of the Fourier transformed retarded Greens function, we refer to the symbolic identity which is valid for real ω

$$\frac{1}{\omega \pm i\eta} = P \frac{1}{\omega} \mp i\pi\delta(\omega) \quad (7.14)$$

Again we can split up the result in two contributions, originating from the two terms which form the retarded impurity Green's function up to second order, equations (7.9) and (7.12), respectively. For the impurity density of states we obtain

$$\rho_d^\gamma(\omega) = \sum_{s_4} |\gamma(\epsilon_{s_4})|^2 \delta(\omega - \epsilon_{s_4}) \rightarrow \rho |\gamma(\omega)|^2 \quad (7.15)$$

$$\rho_d^M(\omega) = \sum_{s_5 s_6 s_{5'}} M_{s_5 s_6 s_{5'} \uparrow \downarrow}^2 Q_{s_5 s_{5'} s_6} \delta(\omega + \epsilon_{s_{5'}} - \epsilon_{s_5} - \epsilon_{s_6}) \quad (7.16)$$

and finally write

$$\rho_d(\omega) = \rho_d^\gamma(\omega) + \rho_d^M(\omega) \quad (7.17)$$

Limit of non-interacting system

In the limit of vanishing on-site interaction the flow equation for γ and M vanish and only the initial conditions (7.7) remain. Now we observe a characteristic feature of the pre-diagonalising transformation already mentioned in (2.2.2): Its matrix elements, which couple the impurity to band states, are directly related to the impurity density of states.

$$\rho_d^{U \rightarrow 0}(\omega) = \sum_s |B_{sd}(\epsilon_s)|^2 \delta(\omega - \epsilon_s) \rightarrow |B_{sd}(\omega)|^2 \stackrel{OLS}{=} W^2(\omega) \quad (7.18)$$

Thus the 'free' spectral density of a one-level impurity is a Lorentian distribution peaked at the impurity level and described by $W^2(\omega)$.

7.2 Analytical solution for the spectral density

Our interest is to study the spectral density of the impurity at the end of the flow procedure, i.e. for $B \rightarrow \infty$. For this regime we have found approximate solutions for the coefficients of the transformation γ and $M_{\uparrow\downarrow}$ up to second order in U in chapter (6). For this case we make the contributions to the spectral density explicit.

7.2.1 Calculation of the second order correction to the impurity spectral density

Again, we discuss the corrections to the spectral density separately for both generalized coupling constants.

Contribution by γ

Firstly, we study the approximate solution for γ which consists of a constant off-set and corrections in second order of U .

$$\gamma(\omega; B \rightarrow \infty) = W(\omega) + U_0^2 \Delta\gamma^{(2)}(\omega) \quad (\rightarrow 6.33)$$

The contribution by γ to the spectral density of the impurity is given by

$$\begin{aligned} \rho_d^{(\gamma)}(\omega)/\rho &= |\gamma(\omega; B \rightarrow \infty)|^2 \\ &= W^2(\omega) + 2U_0^2 W(\omega) \Delta\gamma^{(2)}(\omega) + U_0^4 \left[\Delta\gamma^{(2)}(\omega) \right]^2 \end{aligned} \quad (7.19)$$

In this form it is obvious that $\rho_d^{(\gamma)}(\omega)$ is a positive quantity. But as we restrict all calculations to be consistent up to second order in U its positivity might be lost. This suggests but does not prove that the appearance of negative values in the impurity spectral density is an effect which typically results from second order limitations (see 7.2.2 for further details).

Contribution by $M_{\uparrow\downarrow}$

We insert the result (6.20) into (7.16) and continue with the calculation of the corrections which result from the generation of the higher order multiparticle contributions to the transformed creation operator.

$$\rho_d^M(\omega) = U_0^2 \sum_{s_5 s_6 s_5'} [W_{s_5 s_6 s_5'} K(\epsilon_{s_6} - \epsilon_{s_5'} + \epsilon_{s_5})]^2 Q_{s_5 s_5' s_6} \delta(\omega + \epsilon_{s_5'} - \epsilon_{s_5} - \epsilon_{s_6}) \quad (7.20)$$

We promote one summation in momentum space to an integration over energy and evaluate the constraint imposed by the delta function ($\epsilon_6 = \epsilon_{5'} - \epsilon_5 + \omega$). This allows for a rather simple result

$$\rho_d^M(\omega)/\rho = U_0^2 K^2(\omega) T(\omega) \quad (7.21)$$

Here we have used the definition (6.23) for $T(\omega)$. Note that it contains two internal summations and is solely responsible for any dependences on temperature or outer voltages which enter the impurity spectral density via the combined Fermi function Q .

In the case of zero temperature it is easy to see that the combined Fermi function Q is a positive quantity even under out-of-equilibrium conditions. Thus the contribution to the impurity spectral density by the constant $M_{\uparrow\downarrow}$ is always a positive correction.

Full spectral function

In total, the spectral function consists of the following contributions: The free spectral function $\rho_u^0(\omega) = W^2(\omega)$ and two corrections in order U_0^2 , resulting from the flow of the constants γ and $M_{\uparrow\downarrow}$, respectively. The term in order U_0^4 is neglected. We write

$$\rho_d(\omega)/\rho = W^2(\omega) + U_0^2 \mathcal{C}(\omega) \quad (7.22)$$

We call $\mathcal{C}(\omega)$ the (second order) *correction function*.

It is an important observation that there is no first order correction to the impurity spectral density. Thus a single correction function $\mathcal{C}(\omega)$, which incorporates –via the Fermi functions–

all dependences on temperature or outer voltages, defines the structural change of the impurity spectral function. We present its explicit form:

$$\mathcal{C}(\omega) = 2W^2(\omega) K(\omega) \sum_a \frac{T(a)}{\omega + a} - \pi^2 W^4(\omega)T(\omega) + W^2(\omega)K^2(\omega)T(\omega) \quad (7.23)$$

Increasing the correlation strength continuously reshapes the spectral density and makes the new structures more clearly visible.

7.2.2 Discussion of the correction function

It is an interesting and very helpful aspect of equation (7.22) that we can easily separate between any dependence of the outer parameters (which are included in the correction function) and the correlation strength. Moreover, it will simplify numerical evaluations and accompany our future work. Therefore we start with a discussion of the correction function without referring to the on-site interaction strength.

Confirmation of the Luttinger theorem for the symmetric Anderson impurity model in equilibrium

Referring to equation (7.23) we observe that two terms of the correction function contain $K(\omega)$ as a prefactor. Its explicit expression is given in equation (2.35) which makes obvious that it vanishes at the energy of the impurity level. For the symmetric Anderson model this coincides with the Fermi energy ($\epsilon_d = \epsilon_F = 0$). Moreover, the third term is proportional to the object $T(\omega)$. In equilibrium, an easy discussion of the combined Fermi function $Q_{12'2}$ shows that at the Fermi energy it gives exactly zero, so $T(\omega)$ has to vanish at the Fermi level, too. Thus we conclude that for a symmetric Anderson impurity model the impurity spectral function at the Fermi surface is independent of the interaction: $\rho_d(\omega = \epsilon_F = 0) = \text{const } \forall U$. As the free spectral density is a Lorentian peaked at the impurity level we expect under equilibrium conditions an invariant peak height.

This reproduces a result which has been derived by Luttinger [35][36] for a general class of systems. Afterwards, it has been proven for the Anderson impurity model explicitly. For further reference, we recommend [15] where an exact solution for the impurity spectral density at the Fermi surface is given in simple form and has been applied to the symmetric Anderson impurity model. Note the assumption of particle-hole symmetry at the Fermi surface. We remark that out of equilibrium the combined Fermi function $Q_{12'2}$ changes and we cannot expect $T(\epsilon_F) = 0$ any more. Thus we assume that the Luttinger theorem does not generally hold under out-of-equilibrium situations.

Artifacts of second order calculation

We already mentioned that in equation (7.19) ρ_d is given by a full square and always positive. For a consistent evaluation we restrict to terms up in second order of U and loose the strict positivity of the spectral density.

Later in this chapter we will show that the spectral weight is normalized throughout the flow procedure. Then the correction $\mathcal{C}(\omega)$ only re-distributes it under the influence of the on-site interaction. Thus we expect that $\mathcal{C}(\omega)$ differs in sign for different parameter regimes. As the contribution of the coupling constant M is positive we know that negative values of the correction function have their origin in the behaviour of the constant γ .

In the case of $\Delta\gamma^{(2)}(\epsilon) < 0$ and strong coupling ($U_0 \gg \Delta$) it might happen that the spectral density $\rho(\epsilon)$ becomes negative. We will observe such behaviour in numerical evaluations. Nonetheless we stress that such negative values seem to come as an artifact of second order calculations. Hence the appearance of negative values in the spectral function is a true sign of transgression of the limits of second order approximation and renders all results unreliable. We will learn that due to numerically small values of $\mathcal{C}(\omega)$ this argument only applies for comparatively large values of U_0 in a medium correlation regime ($U \approx 5 - 7\Delta$) which are –frankly spoken– already beyond a plausible perturbative approximation.

Integral of correction function

In the following section we will prove the –physically expected– conservation of spectral weight under increased interaction strength. As a plain consequence we expect the correction function to vanish under spectral integration.

$$\int d\omega \mathcal{C}(\omega) = 0 \quad (7.24)$$

We note that the argument of the integration is not the exact variation of the spectral density any more but an approximative expression in second order of U . This might introduce an error $\Delta\mathcal{C}$ which in the density of states scales with U^2 . Thus we expect that the approximate analytical solution of the set of differential equation does not extend easily into the regime of strong coupling. We will study this error numerically.

7.3 Conservation of spectral weight

The impurity spectral density is a normalised function which describes the relative distribution of spectral weight with respect to energy. Thus we expect that its normalisation should not change under the influence of interactions. We will prove the conservation of spectral weight both for the system of differential flow equations (6.11 and 6.13) and for their approximate analytical solution (6.14 and 6.25) up to second order in U in a mathematically precise way. We start with the general examination of the set of differential flow equations for the creation operator and study the retarded Greens function at a zero time.

7.3.1 Spectral integration and zero time retarded Greens function

Calculating the normalisation of the spectral function clearly means integrating over its energy dependence. This integral can be related to the retarded Greens function if it is evaluated at zero time. Using the relation (7.13) we write

$$\int d\omega \rho_d(\omega) = -\frac{1}{\pi} \int d\omega \Im(G_d^R(\omega)) = G_d^R(t = 0_+, B) \quad (7.25)$$

So we can check the conservation of spectral weight throughout the full flow equation transformation (i.e. for all B) by studying the change of the retarded Greens function at zero time under the flow.

7.3.2 Stability of Greens function at zero time

The following calculation will show that the retarded Greens function at zero time does not change under the flow.

In the case of final flow we have expressed the correlator in terms of the generalized coupling constants of an transformed observable. We assume that this expression holds in good approximation generically for arbitrary values of the flow parameter. This assumption corresponds to the neglect of any change of the ground state under the flow which we consider to be –in equilibrium– a Fermi sea. Hence the change of the operators becomes the only relevant effect caused by the unitary transformations; it is described by the flowing coupling constants γ and M . Note that the time dependent Greens function is more complicated for arbitrary values of time and of the flow parameter. This is due to the fact that for arbitrary values of B the Hamiltonian is not diagonal and the time evolution of the Heisenberg operators is nontrivial.

$$\begin{aligned} iG_d^R(t=0_+, B) &= \sum_{j'j} B_{j'd}^\dagger B_{jd} \langle \Psi_0(B) | \left\{ \mathcal{F}_B [b_j], \mathcal{F}_B [b_{j'}^\dagger] \right\} | \Psi_0(B) \rangle \\ &\approx \sum_{s_5} |\gamma_{s_5}(B)|^2 + \sum_{s_5' s_5 s_6} |M_{s_5 s_6 s_5' \uparrow \downarrow}(B)|^2 Q_{s_5 s_5' s_6} \end{aligned} \quad (7.26)$$

We make use of the flow equations for the generalized coupling constants as expressed in (6.11) and (6.13).

$$i \frac{\partial}{\partial B} G_d^R(t=0_+, B) = 2 \sum_{s_5} \gamma_{s_5} \frac{\partial \gamma_{s_5}}{\partial B} + 2 \sum_{s_5' s_5 s_6} M_{s_5 s_6 s_5' \uparrow \downarrow} Q_{s_5 s_5' s_6} \frac{\partial M_{s_5 s_6 s_5' \uparrow \downarrow}}{\partial B} \quad (7.27)$$

Inserting the flow equations and a suitable relabelling of the various terms involved shows that all terms which originated from the canonical generator cancel each other directly. Moreover, even the contribution of the extended generator to the flow equation of γ vanishes due to a symmetry argument. In the following excursion we briefly present the calculation. Inserting the flow equations leads to

$$\begin{aligned} i \frac{\partial}{\partial B} G_d^R(t=0_+, B) &= 2 \sum_{s_5 s_1} \gamma_{s_5} \gamma_{s_1} \frac{1}{\epsilon_{s_5} - \epsilon_{s_1}} \frac{\partial P_{s_5 s_1}(B)}{\partial B} + \\ &2 \sum_{s_5} \gamma_{s_5} U_0 \sum_{s_1 s_2' s_2} W_{s_1 s_2' s_2} (\epsilon_5 - \epsilon_2 + \epsilon_2' - \epsilon_1) e^{-B(\epsilon_5 - \epsilon_2 + \epsilon_2' - \epsilon_1)^2} Q_{s_1 s_2' s_2} M_{s_1 s_2' s_2 \uparrow \downarrow} + \\ &2 \sum_{s_5' s_5 s_6} M_{s_5 s_6 s_5' \uparrow \downarrow} Q_{s_5 s_5' s_6} U_0 \sum_{s_1} W_{s_1 s_5' s_6} \gamma_1 (\epsilon_6 - \epsilon_5' + \epsilon_5 - \epsilon_1) e^{-B(\epsilon_6 - \epsilon_5' + \epsilon_5 - \epsilon_1)^2} \end{aligned}$$

Relabelling the internal indices in the second summand according to the scheme $(5, 1, 2, 2') \rightarrow (1, 5, 6, 5')$ clearly shows the cancellation of the second and third term such that only the contribution induced by the extension of the generator (the first term) remains. In chapter (5.5.1) we have observed that the flow equation of the scattering amplitudes $P_{s_1' s_1}$ is symmetric in its indices. This implies that in total the argument of the summation in the potential scattering term is asymmetric under index permutation $s_5 \leftrightarrow s_1$. Consequently, the potential scattering contribution also vanishes and we read off

$$i \frac{\partial}{\partial B} G_d^R(t=0_+, B) = 0$$

Note that this result holds generically for all values of outer parameters, i.e. (in the usual ground state approximation) even under out-of-equilibrium conditions. It is a feature of the set of differential flow equations and does not refer to any assumptions made for an approximate analytic evaluation. Therefore we expect it to hold in principle even for a more detailed, e.g. numerical solution of the set of flow equations.

Confirmation of unitarity

We add the remark that the analysis is completely the same for a single ground state correlator of the anticommutator between an annihilation and a creation operator (i.e. if no matrix elements of the pre-diagonalising transformation would be present in the Greens function). The only difference then is in the meaning of the generalized coupling constants. Such an approach would show more clearly that the canonical anticommutator itself does not change under the flow equation procedure. Hence we confirm that up to second order in U a unitary transformation has been implemented (cf. 2.2.2).

7.3.3 Conservation of spectral weight by the flow equations

The invariance of the time zero retarded Green's function under the flow reflects the conservation of spectral weight by the flow equations in the chosen truncation scheme and up to second order in the perturbative parameter U . Thus we can write

$$\frac{\partial}{\partial B} \int d\omega \rho_d(\omega) = 0 \quad (7.28)$$

Hence a calculation which provides an exact solution of the set of differential flow equations which we have set up in chapter 6 conserves the invariance of the spectral density under the flow.

7.3.4 Conservation of spectral weight by the approximate analytical solution

In a similar calculation we can prove the invariance of the spectral weight under the flow even for the approximate analytical solution. We show that the right hand side of equation (7.27) is zero if we insert the explicit solutions (6.14 and 6.25) and their explicit derivatives with respect to the flow parameter.

$$0 \stackrel{?}{=} \sum_{s_5} \gamma_5 \frac{\partial \gamma_5}{\partial B} + \sum_{s_5' s_5 s_6} M_{565'\uparrow\downarrow} Q_{55'6} \frac{\partial M_{565'\uparrow\downarrow}}{\partial B} \quad (7.29)$$

We note that the derivative $\frac{\partial \gamma_s(B)}{\partial B} \sim \mathcal{O}(U^2)$. For a consistent calculation in second order of U we only need to consider the constant term of $\gamma_5(B) = \gamma_5(0) + \mathcal{O}(U^2)$ in the first summand. In the second summand both M and its derivative $\frac{\partial M(B)}{\partial B}$ contribute in first order of U and cannot be neglected.

Basic idea of the proof and comments

A striking feature of the following proof is that only symmetry arguments are used to show that equation (7.29) does hold. Therefore it is independent of a correct treatment of the pole

structure which we have discussed in (6.3.4). Thus we can refer to this result for a meaningful implementation (or correction) of the emerging, formally diverging integrals.

Moreover we directly see that the symmetry holds for all values of the flow parameter and the conservation of spectral weight cannot be violated for any finite value of B , i.e. anywhere within the transformation process. The fact that the approximate analytical solutions respects this important sum rule suggests that it is a reliable approach to study the out-of-equilibrium behaviour of the Anderson impurity model within its perturbatively defined validity.

For the interested reader we briefly present the explicit form of the terms involved.

Aspects of the calculation*

Again we make use of the short-hand notation introduced in (6.3.3) and explicitly denote the analytical expressions and their derivatives. In order to maintain the full symmetry of the terms we refer to their crude form, including all summations.

$$\begin{aligned} \gamma_{\tilde{5}'}(B) &= \gamma_{\tilde{5}'}(B=0) + \\ & U_0^2 W_{\tilde{5}'} \sum_{12'23} W_{12'23}^2 Q_{12'2} \left[\frac{1 - e^{-B[(y+a)^2+(x+a)^2]}}{(x+a)(y-x)} + \frac{e^{-B(y+a)^2} - 1}{(y+a)(x+a)} \right] \\ \frac{\partial \gamma_{\tilde{5}'}(B)}{\partial B} &= U_0^2 W_{\tilde{5}'} \sum_{12'23} W_{12'23}^2 Q_{12'2} \left[\frac{(x+a)^2 + (y+a)^2}{(x+a)(y-x)} e^{-B[(y+a)^2+(x+a)^2]} \right. \\ & \quad \left. - \frac{y+a}{x+a} e^{-B(y+a)^2} \right] \\ M_{s_{\tilde{5}'} s_{\tilde{6}'} s_{\tilde{5}} \uparrow \downarrow}(B) &\stackrel{O(U)}{=} -U_0 W_{\tilde{5}' \tilde{6}' \tilde{5}} \sum_{s_1} W_1^2 \frac{e^{-B(\epsilon_{\tilde{6}'} - \epsilon_{\tilde{5}} + \epsilon_{\tilde{5}'} - \epsilon_1)^2} - 1}{\epsilon_{\tilde{6}'} - \epsilon_{\tilde{5}} + \epsilon_{\tilde{5}'} - \epsilon_1} \\ \frac{\partial M_{s_{\tilde{5}'} s_{\tilde{6}'} s_{\tilde{5}} \uparrow \downarrow}(B)}{\partial B} &= +U_0 W_{\tilde{5}' \tilde{6}' \tilde{5}} \sum_{s_2} W_2^2 (\epsilon_{\tilde{6}'} - \epsilon_{\tilde{5}} + \epsilon_{\tilde{5}'} - \epsilon_2) e^{-B(\epsilon_{\tilde{6}'} - \epsilon_{\tilde{5}} + \epsilon_{\tilde{5}'} - \epsilon_2)^2} \end{aligned}$$

We insert these expressions into (7.29) and make the following replacements of index labels in the second term:

$$\begin{aligned} (\tilde{5}' \tilde{6}' \tilde{5} 1 2) &\longrightarrow (1, 2, 2' xy) \\ \epsilon_{\tilde{6}'} - \epsilon_{\tilde{5}} + \epsilon_{\tilde{5}'} &\longrightarrow -a \end{aligned}$$

This relabelling is nothing else but a change of notation.

We observe that the terms $\sim e^{-B(y+a)^2}$ cancel each other directly and the remaining term $\sim e^{-B[(x+a)^2+(y+a)^2]}$ can be written in the following form

$$0 \stackrel{?}{=} U_0^2 \sum_{x,y} W_{xy}^2 \sum_{12'2} W_{12'2}^2 Q_{12'2} \frac{y+x+2a}{y-x} e^{-B[(x+a)^2+(y+a)^2]} \quad (7.30)$$

We note that the argument of these summations is asymmetric under interchange of x and y . Thus the right hand side vanishes for all values of the flow parameter if unlimited bandwidth is assumed.

Chapter 8

Numerical implementation of the impurity spectral density

8.1 General approach

The final goal of this chapter is the visualisation of the impurity spectral density in terms of a function plotted against energy. As this cannot be done in closed analytical way we modify the spectral function to turn it into a form suitable for numerical evaluation on a digital computer. Then we will study the shape of the spectral function in dependence of outer parameters like an externally applied voltage and of various correlation strength, i.e. for different values of the on-site interaction. We present the details of the numerics in the following sections.

8.1.1 Separation of dependences

The examination of the spectral density will be split up into two independent parts which are –for convenience– implemented in two different programmes; those are only linked by data export/import.

- A Firstly, the correction function $\mathcal{C}(\omega)$ is calculated using numerical methods. This is the numerically most expensive part. The correction function depends via the combined Fermi function Q on the outer conditions like temperature and outer voltage bias. Hence this calculation has to be performed for all situations characterised by such boundary conditions individually.
- B The behaviour of the density of states for an arbitrary but fixed such situation under different on-site interaction on the impurity is studied in a second step. The result of (A), i.e. the correction function, is used.

In the following section we will map the functional expression for the correction function, which is given in discrete momentum space, via a limiting procedure onto a discretized energy space. Then we implement the structures in the commonly used language C^{++} . Firstly, we will present a full numerical evaluation of the correction function before we address the computation of the density of states.

8.1.2 Processing of the correction function

We briefly recapitulate the explicit form of the correction function which we have derived in chapter 7.

$$\mathcal{C}(\omega) = 2W^2(\omega) K(\omega) \sum_a \frac{T(a)}{\omega + a} - \pi^2 W^4(\omega)T(\omega) + W^2(\omega)K^2(\omega)T(\omega) \quad (\rightarrow 7.23)$$

We observe that the function depends in both in a local and in a non-local way on the object $T(\epsilon)$. This suggests a decomposition into a two-step procedure. At first we evaluate the function $T(\epsilon)$ for all values in energy space, then the full evaluation of the remaining structures is possible by simply recalling these results.

8.2 Discretization

All numerical approaches are in principle restricted to countable situations. Due to the limitations of computer technology we have to confine ourselves to discrete models of fairly small size. Nonetheless, for our calculation this shows up to be sufficient for adequate results. We will set up a discrete framework for all calculations which is defined from the perspective of the final result. Our interest is in the energy dependence of the impurity spectral density. Thus it comes natural to perform all computations in a discretized energy space.

8.2.1 Transfer into discrete energy space

Therefore all analytical expressions have to undergo a three-step process of re-formulation:

1. All summations, which are given in a discrete momentum space are promoted to continuous integrals in momentum space. This eliminates the special features introduced by the choice of a discrete energy level structure of the conduction bands. Mathematically, we apply the limit of vanishing level spacing $\Delta_L \rightarrow 0$ and $\Delta_L \sum_k \rightarrow \int dk$
2. Secondly, we apply a linear dispersion relation to change from momentum to energy space: $dk = \rho d\epsilon$ with ρ being the density of states of the electronic system. We assume ρ to be constant; for all numerical evaluations we set it equal to one. It is suitable to choose an intrinsic energy scale which is given by the width of the hybridization, $\Delta = V^2 \rho \pi$. Fixing $\Delta = 1$ defines a natural energy unit of the extension of the spectral function in energy space.
3. Finally, all integrals in energy space are discretized to allow numerical calculations. We do so on a lattice containing up to 2401 sites¹. This needs some further modelling.

8.2.2 Discrete modelling

We already fixed the number of lattice sites S and the numerical values of some constants. The constant electronic density of states has been chosen one, similarly we have set up an energy scale by a normalized hybridization $\Delta = 1$. Still we need to define the size of the energy window which we open for our calculations symmetrically around the Fermi energy ($\epsilon_F = 0$). We choose the same interval for the internal summation and denote it by $\mathcal{I} = [-I\Delta, I\Delta]$; its

¹Because of technical details of the implementation we have always chosen odd numbers of lattice sites.

length is obviously $2I$. This induces a correlation between the numerical stepsize on the lattice and the physical energy difference between two discrete positions. Assuming energetically equally spaced lattice points we get a physical stepsize SW of $SW = 2I\Delta/S$. All numerical summations are defined with respect to an integer ('loop') parameter (e.g. k) which takes values between zero and $S-1$. They are performed as finite Riemann sums over step functions. The length of their basis is given by the physical stepsize. We denote these details of the numerical summation briefly by $\sum_{N_I^S(k)}$.

8.2.3 Discrete quantities

The analytic functions $W(\omega)$, $K(\omega)$ and Q are easily evaluated at the physical energy values of the lattice sites and restricted to this set of values. Their index ϵ now represents a function which maps a lattice position k onto the physical energy of this lattice site. It is given by

$$\epsilon(k) = -I\Delta + 2kI\Delta/S \quad (8.1)$$

The numerically calculated functions (\mathcal{C} , T , Y) are defined on the lattice sites only and implemented as vectors of dimension S .

$$\begin{aligned} T[k] &= T(\epsilon(k)) = \sum_{N_I^S(k_1) N_I^S(k_{2'})} W_{\epsilon(k_1)\epsilon(k_{2'})}^2 Q_{\epsilon(k_1)\epsilon(k_{2'})} Q_{\epsilon(k)-\epsilon(k_1)+\epsilon(k_{2'})} \\ Y[k] &= Y(\epsilon(k)) = \sum_{N_I^S(k_1)} \frac{1}{\epsilon(k) - \epsilon(k_1)} T[k_1] \\ \mathcal{C}[k] &= \mathcal{C}(\epsilon(k)) = 2W^2(\epsilon(k)) K(\epsilon(k)) Y[k] + T[k] [K^2(\epsilon(k)) - \pi^2 W^4(\epsilon(k))] \end{aligned}$$

8.2.4 Principal value integration

Numerics shows that the function T is a rather smooth, well behaved one. Thus the evaluation of Y contains summation over an possibly divergent expression. Therefore a discrete version of the principal value integration is needed. We implemented two very rough approximate schemes:

- (a) Whenever the absolute value of the denominator falls beyond a certain limit, the so-called principal value cut-off, the contribution of the term is excluded from the total sum. In particular this scheme excludes an exact pole. The numerical value of the cut-off was roughly optimized and found to be below the scale of numerical resolution (here 10^{-14}).
- (b) The second approach aims at an approximate analytical solution of the principal value integral around the pole. As the accompanying function is rather smooth it can be linearized in a neighbourhood of a few lattice sites around the pole. Then the principal value integral can be performed exactly and only depends on the gradient of T at the pole, denoted by m .

$$\int_{-\delta}^{\delta} dz \frac{a - mz}{z} = 2 \delta m$$

Both schemes have been implemented in the context of this calculation and their relative quality has been estimated. As a quantitative measure the numerical violation of the conservation of spectral weight has been used (8.6.2).

We have found that in the parameter regimes of interest the first scheme produces more accurate results. Hence we note that the pole structure of the summations is -in the lengthscales of the discrete model- a very local effect which is best dealt with by the correction of a single site.

8.3 Numerical complexity

The correction function $\mathcal{C}(\omega; B)$ contains -in general- four internal summations. Various decouplings in the limit $B \rightarrow \infty$ have made it more accessible for numerical treatment. The detachment of the analytically solvable structure $K(\omega)$ and the restructuring of the calculation in (8.1.2) have reduced the numerical complexity tremendously.

The evaluation of the correction function $\mathcal{C}(\omega)$ decomposes into the addition and multiplication of substructures. While some of them are given by analytic expressions and easily evaluated, the calculation of $T(\epsilon)$ and $Y(\omega)$ demand more numerical efforts. The dominating structure of the problem is the calculation of the function $T(\omega)$. Due to two internal summations and one external evaluation it is of order $\mathcal{O}(S^3)$, i.e. it scales with the third power of the number of lattice sites S . The final evaluation of $Y(\omega)$ is of lower order ($\mathcal{O}(S^2)$) and does not touch the total complexity.

8.4 Implementation in C++

The discretized model which we described above has been implemented in an C++-environment. The analytically given functions $W(\omega)$, $K(\omega)$ and Q have been defined as real functions. Q is a composition of Fermi functions which have been implemented as step functions, i.e. at zero temperature, and an extension towards finite temperature would be straightforward. Out-of-equilibrium boundary conditions have been considered by the definition of a transport window. For the numerically given functions $\mathcal{C}(\omega)$, $Y(\omega)$ and $T(\omega)$ vectors of size S have been initialised. Subroutines include the principal value scheme as well as some basic calculations. The main programme itself starts with a computation of T which is stored in an easily accessible vector variable. Afterwards the function Y is calculated recalling to these values. Finally, the full correction function is composed and the result written to a file.

8.5 Calibration of numerical parameters

Various tests are performed to determine the appropriate numerical parameters of the discrete model and to understand the numerical behaviour of the system. They all rely on the comparison with exact results.

8.5.1 Choice of energy window size

A comparison of the numerical normalisation of the hybridization ($\sum_{N_I^S(k)} W^2(\epsilon(k))$) with its analytic value one suggests suitable choices for the size of the energy window. Within a symmetric interval of 15Δ more than 95 % of the spectral weight of the hybridization is contained. We believe that this is a sufficiently broad interval for reliable evaluations of the impurity spectral density.

8.5.2 Calibration of principal value evaluation

Secondly, we calibrate the principle value evaluation by numerically implementing the Kramers-Kronig transformation of the hybridization (cf 2.35). It relates the exact expression $K(\omega)$ to a principle value integration. Performing this integration numerically we can test the accuracy of the numerical treatment and roughly optimize the value of the cut-off which regulates the exclusion of contributions to the principal value integral.

Using a satisfactory cut-off we observe particularly for values of ω close to the boundaries of the interval \mathcal{I} deviations of up to 12 percent of the analytic result which rapidly improve within a few steps. Again the relative error reaches a local maximum at zero energy of about 1.6 percent but is considerably smaller than one percent for large regimes of the interval. Nonetheless we state that whenever sharp edges like boundaries of integration domains, band edges or jumps in (Fermi) distribution functions coincide with a pole we expect significant contributions. Often they describe the true physical behaviour of the system which is, for instance, in many cases dominated by effects at the Fermi surface. But equally such structures are a source of numerical inexactness and need to be discussed carefully.

8.6 Numerical quality

The tests presented in the last section focus on the numerical procedures by evaluating 'experimental' situations, while the one dealt with here allow for an estimation of errors in the final results. We evaluate the quality of a numerical approach by a two-fold criterion. On the one hand we expect a convergence of the computational results under increasing size of the lattice, on the other we calculate conserved quantities which are well-known.

8.6.1 Test of numerical stability

We have performed the calculation of the equilibrium correction function on lattices of various sizes, among them $S = 301, 601, 1201$ and 2401 . This has shown that for most points in energy space convergence is rapidly achieved and even small lattice sites generate acceptable results (cf. 8.1(a)). Nonetheless we observe that few features like the depth of valleys (cf. 8.1(b)) depend weakly on the resolution. Graphical evaluation points out that even those do converge quickly. Thus we find strong justification for working with a lattice size of 2401 sites.

8.6.2 Estimation of numerical errors

Two features of the equilibrium correction function are known exactly and allow for an estimation of numerical errors.

Local error evaluation by means of the Luttinger theorem

Firstly, due to the Luttinger theorem the equilibrium correction function should vanish at the Fermi energy. The actual computed values can be taken from figure 8.1(c). We note that the error at this particular point in energy is for the equilibrium correction function below the limit of $1.0 \cdot 10^{-05}$.

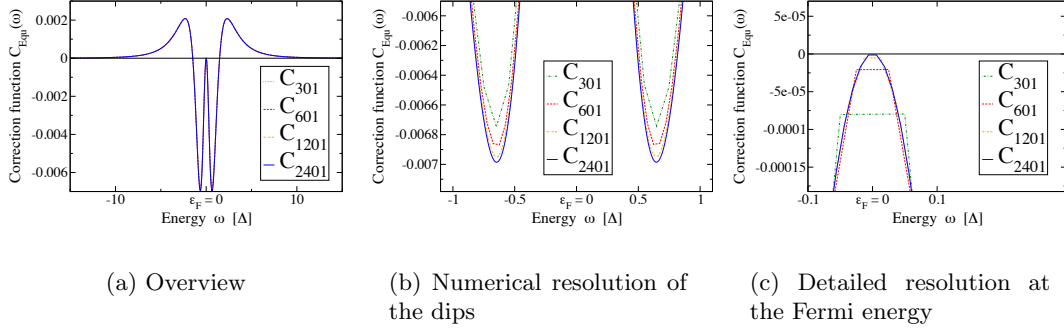


Figure 8.1: Results for the correction function in equilibrium for different lattice sizes. The number of sites ranges between 301 and 2401 and is denoted as an index.

Violation of spectral weight conservation

A second check is possible by the full spectral integral of the correction function. It should vanish to ensure the conservation of spectral weight, which is normalised to one. This provides an integrative, non-local estimation of the numerical error. Again we find a similar value of approximately $1.5 \cdot 10^{-05}$. It directly represents an relative numerical error.

Numerical resolution

Both observations found our opinion that this value should be regarded as the numerical resolution limit. Under out-of-equilibrium conditions, the first criterion does not hold more. Fortunately we observe that the spectral integral does not significantly change. Again, a limit on the derivations is given by $2.5 \cdot 10^{-05}$, in many cases it is clearly below.

Therefore we assume that no artifacts or significant distortions enter because of the numerical evaluation. Hence all such aspects will be attributed to the limitations of the approach, most remarkably to the breakdown of perturbative arguments.

Remark on the voltage implementation

The implementation of the voltage bias in the Fermi functions has been done with respect to a symmetric opening of the transport window. This leads to a slight re-definition of the voltage variable $V \rightarrow 2V$. Furtheron V represents only one half of the total outer voltage which has been applied to the impurity. The evaluation of all numerical results is done with respect to this definition of the voltage. Therefore it is necessary to differ between the total outer voltage $2V$ and the symmetrically applied voltage V in the following chapter.

Chapter 9

Evaluation of the impurity spectral density

In the following chapter we will present numerical evaluations of the spectral density for various parameter regimes. They constitute important results of this work. All plots show situations for a symmetric Anderson impurity model, the impurity energy level coincides with the Fermi surface ($\epsilon_d = \epsilon_F \equiv 0$).

9.1 Equilibrium impurity spectral density

Figure (9.1) shows the change of the impurity spectral function in equilibrium, i.e. for vanishing voltage bias V . We observe that the flow equation method reproduces some well-known facts from other calculations:

9.1.1 Expected observations

- (a) With increasing interaction strength U , the quasi-particle resonance at the Fermi energy is sharpened. Simultaneously, side peaks, commonly referred to as Hubbard side bands, arise and are approximately located at energies $\omega = \pm U/2$.
- (b) In the invariance of the peak height of the resonance under a change of U , i.e. in the stability of the value of the spectral density at the Fermi surface, we re-discover the Luttinger theorem (cf. 7.2.2).

9.1.2 Artifacts and obvious limitations

Some artifacts due to the restriction of all calculations to second order in U should be mentioned. First of all, the curve for $U = 6\Delta$ takes negative values for some parts of the energy spectrum. As the spectral density is a positive weight function this is truly an unphysical result (cf 7.2.2). It restricts the applicability of the second order calculation to values of U significantly below this limit. This indicates that the regime of strong correlations cannot be accessed by this approach.

Moreover, we observe two common intersection points of all graphs away from the Fermi surface. They are generated by the linear influence of the correction function on all plots ($\rho_{Equ}(\omega) = \rho_0(\omega) + U^2 \mathcal{C}_{Equ}(\omega)$). At the zero points of the correction function no changes

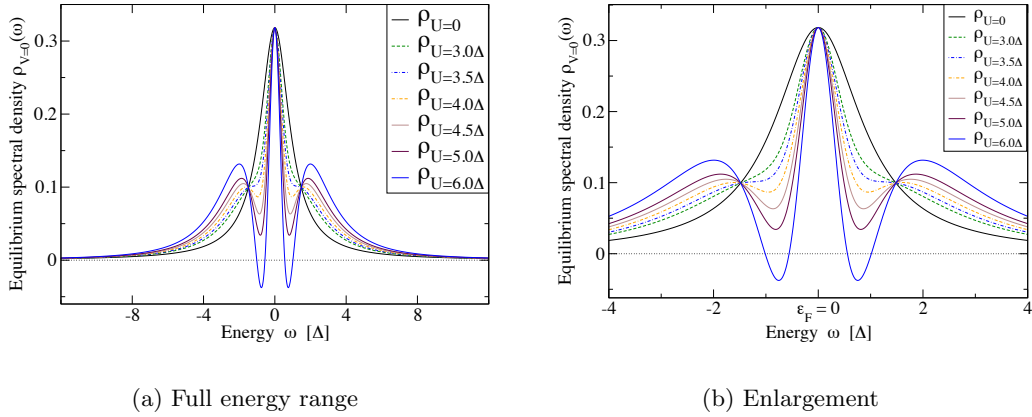


Figure 9.1: Equilibrium impurity spectral function

can be expected for any interaction strength. There is no indication that these points carry any physical relevance and we do not believe that this result should extend to higher order calculations.

9.2 Dependence of the correction function $\mathcal{C}(\omega)$ on the voltage bias

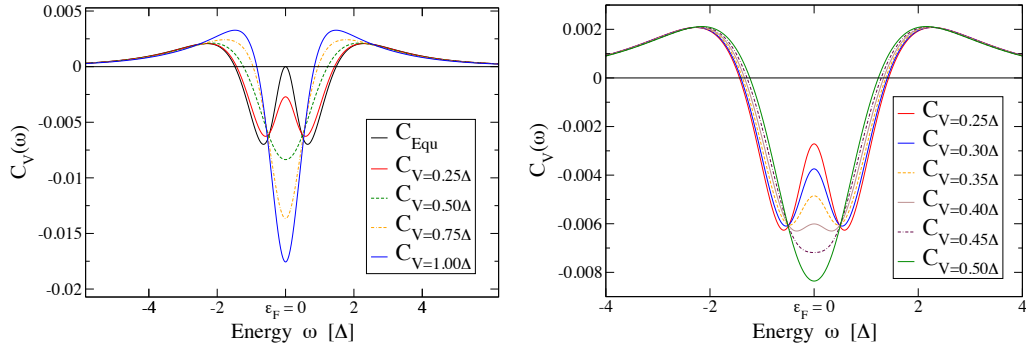
Before we discuss the general dependence of the impurity spectral density on both the interaction strength U and the voltage V we study the development of the correction function under increased bias voltage. This highlights the actual changes which are induced by out-of-equilibrium conditions as other dependencies have already been separated off. We repeat that all results presented here are for zero temperature only.

Decoherence effects in out-of-equilibrium

Dramatic differences appear between the correction function in equilibrium and out-of-equilibrium. While in the first case a double-dip structure allows for a sharpening of the resonance located at the Fermi level, both dips merge at a critical value of the voltage bias. The resulting effects could be described as plain decoherence of the resonance. Then the spectral weight is even faster re-distributed from the resonance into the side bands. As the maxima of the correction functions (which generate the Hubbard side bands in the spectral density) are shifted towards the Fermi surface we expect a further loss of structural resolution.

The hybridization scale regime

Figure (9.2(b)) shows the continuous 'crossover' from re-sharpening effects of the Fermi resonance (which dominate the equilibrium behaviour) to the decoherence regime. It is reached for a symmetrically applied total voltage bias of $2 \cdot V \approx 2 \cdot 0.45\Delta \approx \Delta$. We call this parameter configuration the *hybridization scale regime* and expect typical out-of-equilibrium behaviour when the total voltage bias is of order of the hybridization scale.



(a) General behaviour

(b) Hybridization scale regime

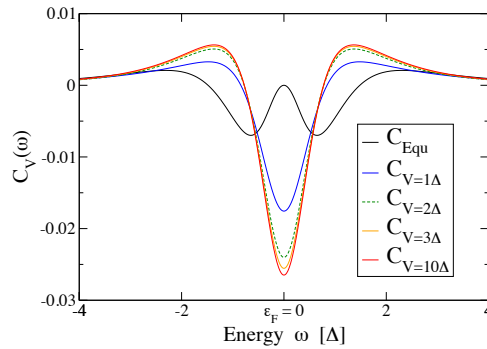
(c) Convergence can be seen for voltages beyond the value of $V = 2\Delta$

Figure 9.2: Correction function for different voltage regimes. If the total voltage bias approaches the hybridization scale, decoherence effects dominate and the characteristic behaviour of the correlation is suppressed. This crossover is depicted in figure (9.2(b)). For large values of the voltage bias, i.e. for far non-equilibrium, convergence of the correction function is observed.

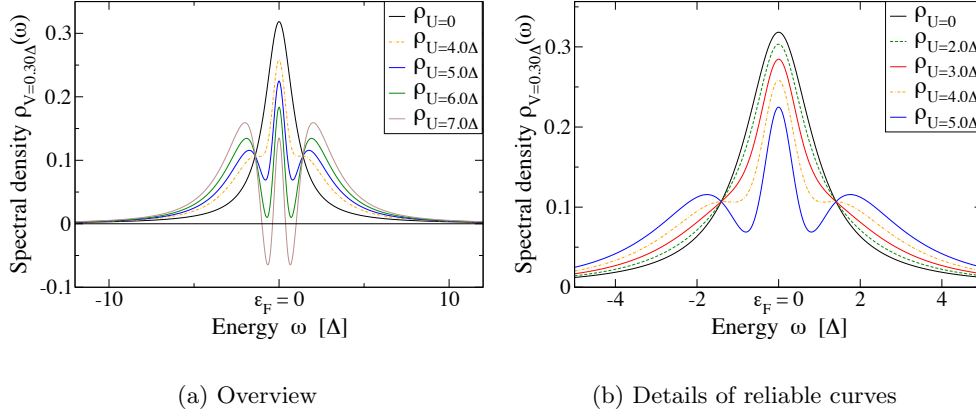


Figure 9.3: Impurity spectral density close to equilibrium ($V = 0.3\Delta$) for various values of the interaction. One easily observes the decoherence of the resonance with *increased* correlation strength.

Convergence of the correction function for far out-of-equilibrium

In figure (9.2(c)) we observe convergence of the correction function for far out-of-equilibrium conditions. It is reached at an external voltage bias of $2V \approx 6\Delta$. In this regime the transport window dominates all other energy structures which effectively 'see' only the constant value of the Fermi distribution function inside the window. Now a further enlargement of the voltage bias cannot change the conditions any more and $\mathcal{C}(\omega)$ approaches a limiting function.

Violation of the Luttinger theorem for non-equilibrium

It is easily seen that the Luttinger theorem is strongly violated in non-equilibrium, as decoherence does effect the shape of the impurity spectral function particularly at the Fermi energy.

9.3 Impurity spectral function out of equilibrium

In a second step, we visualize the behaviour of the impurity spectral function for various values of the interaction strength and the voltage bias. This opens space for interpretation of some physical features of the out-of-equilibrium Anderson impurity model.

9.3.1 Evaluations for constant voltage

Varying the on-site interaction, i.e. the correlation strength, for fixed voltage bias shows interesting but not unexpected behaviour: Due to the linear impact of the correction function onto the spectral density which comes with a prefactor quadratic in the correlation strength we find that the decoherence of the resonance at the Fermi level is proportional to the square of the on-site interaction.

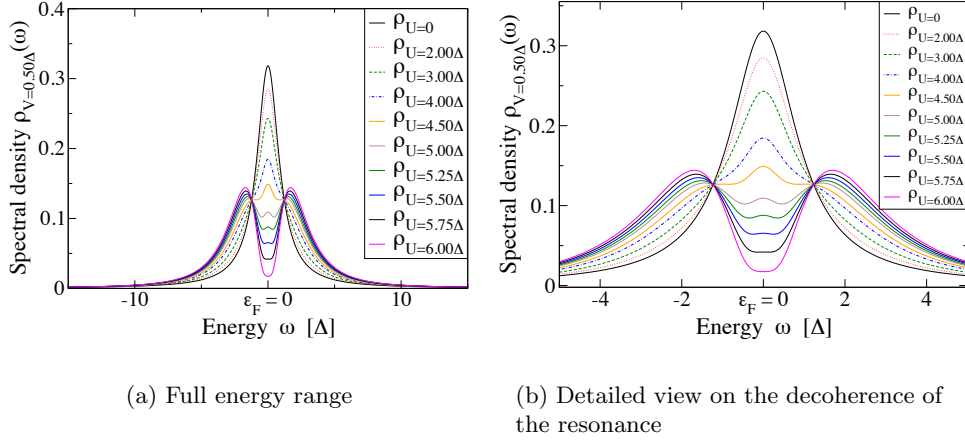


Figure 9.4: Impurity spectral density when the total voltage bias $2V$ equals the hybridization. The decay of the resonance and the shift of its spectral weight into the Hubbard side bands with increased interaction is clearly displayed.

Proportionality of decoherence of the resonance and on-site interaction strength

The results show that under moderate out-of-equilibrium conditions correlation and decoherence effects are directly related. In equilibrium, increased correlation strength causes a sharpening of the Fermi resonance and preserves the peak height of the resonance. The width of the resonance is reduced and spectral weight redistributed into emerging Hubbard side bands. Out of equilibrium, the same effect accounts for increased decoherence. This can be seen as a reduced width of the resonance still faces the same voltage. The decoherence scale is expected to be proportional to the (inverse) ratio of both. Hence contrary to a naive view, increased correlation strength cannot compensate for decoherence effects and the peak height is suppressed with growing interaction even faster.

Due to the limited applicability of this approach (which is restricted to medium-size interaction strength) we need to exclude the curve for $U = 7\Delta$ in figure (9.3(a)) and carefully doubt on the reliability of the predictive power of the graph for $U = 6\Delta$. Therefore we cannot observe a full decay of the resonance in the case of $V = 0.3\Delta$ (figure 9.3).

Hybridization scale regime

Hence we study the same situation for an outer total voltage bias $2V$ which equals the hybridization. Now a full decay of the resonance is within the resolution of the method. Finally, all of its spectral weight has been transferred to well-separated Hubbard side bands (see figure 9.4 for details).

Further out-of-equilibrium situation

Finally we analyse the situation for larger out-of-equilibrium conditions. We note that in such cases one cannot observe a clear generation of Hubbard side bands as they strongly overlap

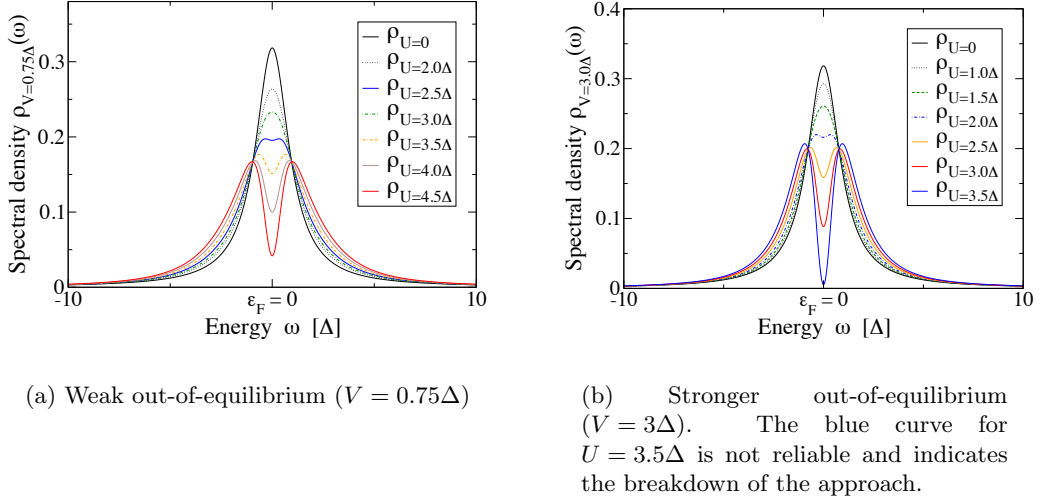


Figure 9.5: Impurity spectral density for larger but fixed voltage bias. We observe a faster decay of the resonance with growing interaction strength. This is explained by the fact that the width of the resonance is reduced under increased correlation. Hence the relative importance of the fixed voltage bias grows.

with the remaining foot¹ of the original Lorentzian.

Moreover we observe that the breakdown of our perturbative approach occurs for growing out-of-equilibrium at even smaller values of the correlation.

9.3.2 Spectral density for fixed correlation strength

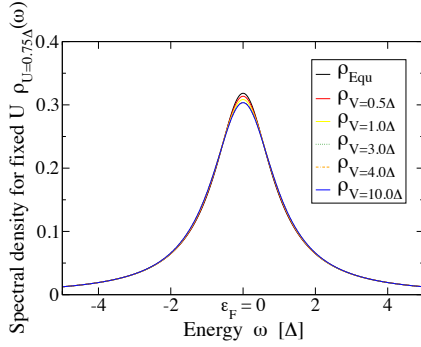
Now we discuss the spectral function for fixed correlation and variable outer voltage. This corresponds the standard implementation of quantum dot experiments where the voltage can be varied easily, while the correlation strength is usually determined by fixed parameters.

Convergence regime

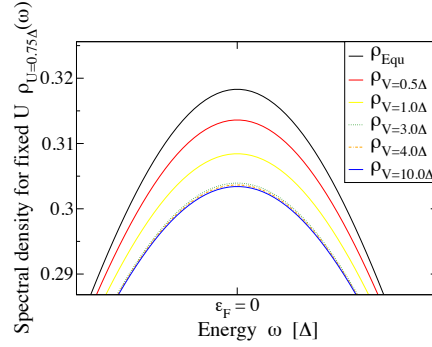
For rather weak correlation strength convergence can be observed under increased voltage bias. Effectively, the peak height of the Lorentzian-shaped hybridization function is reduced until strongly overlapping Hubbard side bands remain. While figure (9.6) shows only marginal reductions of a uniform peak height, in figure (9.7) two distinguishable maxima indicate the presence of correlation effects. Hence we observe that in this example out-of-equilibrium conditions foster the exprimation of robust aspects of correlated system, e.g. the Hubbard side bands.

Moreover we note that in the case of vanishing interaction the hybridization is unaffected by the voltage bias. No out-of-equilibrium effects can be seen in our approach for zero correlation strength. This makes the important role of the on-site interaction visible in a clear way: it is responsible for the emergence of a rich structure in the Anderson impurity model.

¹We call the part of a single-peaked curve which lies significantly between its resonance and its tail the *foot* of the curve.

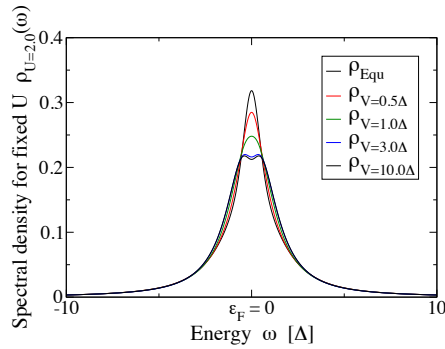


(a) The dominating structure is the Lorentzian hybridization function. It is subject to limited decoherence effects.

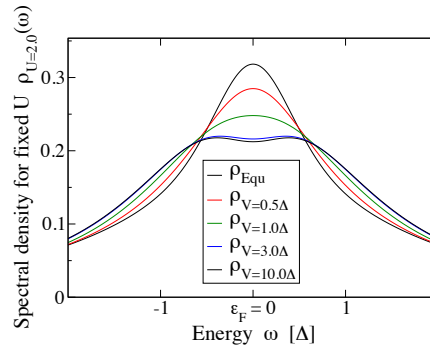


(b) Details of the peak height reduction due to decoherence. Convergence is reached at $V = 3\Delta$.

Figure 9.6: Impurity spectral density for fixed small correlation strength $U = 0.75\Delta$ and variable voltage bias. In this regime correlation effects are unimportant and cannot be observed. Instead we see a slight decoherence of the hybridization function which is the only visible structure. We note that in our approach the interaction-free Anderson Hamiltonian is robust against out-of-equilibrium conditions. Hence a non-zero correlation strength is needed to observe any non-equilibrium effects.

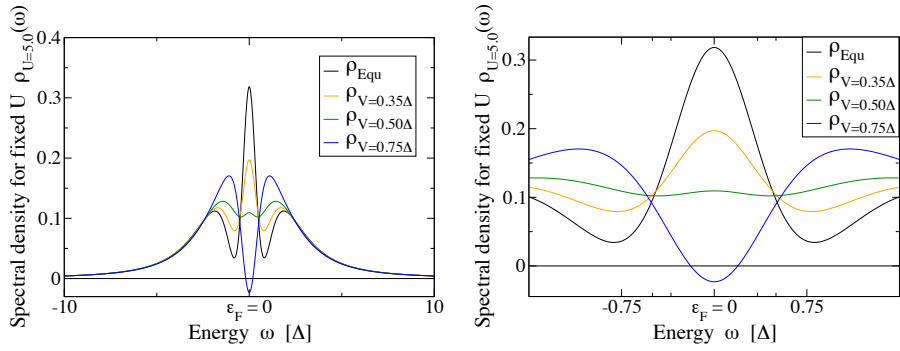


(a) View of the full energy regime.



(b) Details of the convergence.

Figure 9.7: Impurity spectral density for fixed correlation strength $U = 2\Delta$. We observe convergence under increasing outer voltage and note that the limitations of our approach in this regime result from the out-of-equilibrium description.



(a) The medium correlation regime ($U = 5\Delta$) shows a dramatic decay of the resonance at low values of the voltage bias, a significant shift of the Hubbard side bands away from the Fermi energy and an early breakdown of the perturbative approach at already $V = 0.75\Delta$.

(b) Detailed view on the transport window (window sizes are indicated). The integrated spectral weight within the transport window may even drop for increased voltage in this regime.

Figure 9.8: Impurity spectral density for fixed on-site interaction strength in the strong correlation regime ($U = 5\Delta$). We observe a dramatic decay of the resonance at low values of the voltage. This shows that the spectral weight which is accumulated within the transport window does not grow linearly for increased voltage bias; even more, it suggests that it might decrease. Thus non-linear effects should be found in the current-voltage-characteristic.

No observation of strong correlations

Of much more interest is the regime of stronger correlations. We refer to an interaction strength of $U = 5\Delta$ as a medium interaction strength to clearly distinguish it from more typical strongly correlated systems. We briefly mention that characteristic features of such systems under out-of-equilibrium like the splitting of the Kondo resonance cannot be seen in our approach. This does not come as a surprise as, effectively, perturbation theory in the interaction has been implemented up to second order.

Interesting non-linear behaviour for medium correlation

Yet in the regime of medium correlations interesting observations can be made. Then even for small values of the voltage bias a significant decay of the spectral density around the Fermi energy takes place. In figure 9.8(a) this regime is displayed for the full relevant energy range. As the Hubbard side bands are sufficiently shifted to higher and lower energies respectively the decay of the resonance induces important new features.

The integrated spectral weight within the small transport window does no longer grow linearly with increased voltage bias but may even be reduced (cf. 9.8(b)). Therefore we expect the current through the impurity to show a strongly non-linear behaviour. Potentially even a negative current-voltage characteristic may be observable. We point out that for such predictions a more detailed non-perturbative numerical solution of the flow equations is necessary. Particularly for small values of the spectral function, i.e. for an almost completely decayed resonance, the results, which are based on an approximate analytical solution of the flow equations, may serve as an important motivation but should not be over-stressed.

If only very little spectral weight remains within the transport window for certain choices of parameters, the impurity might behave like an insulator. This opens the perspective for an observation of metal-insulator transitions similar to the Mott-Hubbard insulator. We do not expect such behaviour for the Anderson impurity model. But similar models which include additional self-consistency conditions, e.g. the Hubbard model, might show this kind of physics. A further inquiry of all these ideas could be an fascinating continuation of this work.

Chapter 10

Conclusions and outlook

Summary

In this work we have approached the steady state of the out-of-equilibrium Anderson impurity model by a two-step approach. Firstly, the hybridization has been dealt with by an exact pre-diagonalization procedure following the equation of motion technique. Then the flow equation method has been applied to treat the on-site interaction. By an approximate analytical solution of the differential flow equations non-perturbative aspects of this method have been neglected and second order perturbation theory in the on-site interaction strength has been consistently implemented. Finally, evaluations of the impurity spectral density sketched the behaviour of the symmetric model in the regime of medium correlation strength and comparable outer voltage. Due to the Coulomb on-site interaction we observe both the appearance of Hubbard side bands and of a sharp resonance at the Fermi energy which is subject to decoherence under out-of-equilibrium conditions. In the regime of medium correlation strength non-linear transport properties can be expected.

Possible extensions and further points of interest

Some *straightforward extensions* of this work could be easily achieved: As the detailed transformation properties of operators are known, higher correlation functions could be easily evaluated. The simple impact of the hybridization function onto all results allows for a study of the dependence on the hybridization coupling. Moreover, a quantitative comparison of the results with numerical methods would be of particular interest.

For an examination of the *asymmetric Anderson impurity model* a deeper understanding of divergences and their regularisation is necessary and a better founded pole correction has to be established.

A *non-perturbative approach* could be implemented by a detailed numerical solution of the flow equation. This may access characteristic features of higher order calculations by a renormalized resummation of the perturbation series.

A more detailed understanding of the out-of-equilibrium interacting steady state would be necessary for a *calculation of the current* through the impurity and similar observables and could constitute an interesting field of research. Examinations of non-linear transport properties in correlated materials could be relevant applications.

Last but not least it was pointed out that a very different application of this calculation could show up in *dynamical mean field theory* where formally similar structures appear.

Acknowledgments

At the end of this diploma thesis I would like to thank

Prof. Dr. Jan von Delft for granting me the privilege of working with him. His continuous interest in this work has been a driving motivation for me throughout the year and I'm very grateful for his effort to make himself available for uncounted inspiring, supportive and fruitful discussions. His various commitments for his group created an open, communicative and stimulating environment which I have very much enjoyed.

Prof. des. Dr. Stefan Kehrein for his detailed and patient supervision which took place in terms of a collaboration with the University of Augsburg. His profound explanations made me familiar with many aspects of the flow equation method, soon he became the guiding spirit of this work. I'm very thankful for his open ear, his continuous support throughout the last year, some important problem solving and many friendly and warm welcomes to Augsburg. It is my great pleasure to congratulate him for his recent appointment to a professorship at the Ludwig-Maximilians-University. Wholeheartedly I wish him good luck and a challenging and satisfying profession. *Ad multos annos!*

All members of the group at the chair for condensed matter physics¹. I've enjoyed their cheerful company and their helping hands wherever some practical tricks have been needed. My special thanks are directed to Dr. Florian Marquardt and Dr. Michael Sindel for some valuable discussions which are reflected in some aspects of this work. Johannes Ferber's extended help and assistance in all matters related to the use of computers will not be forgotten.

Moreover I gratefully acknowledge the support by many grant-awarding bodies. Scholarships by the Maximilianeum Foundation, the State of Bavaria and the National German Scholarship Foundation have provided me with excellent opportunities, a variety of broad intellectual stimulations, valuable contacts and financial independence.

Last but not least I want to express my deep gratitude towards my parents Siegfried and Brigitte and all members of my family for their continuous love and support, their understanding and patience with me.

¹PD Frank Wilhelm, Florian Marquardt, Andreas Weichselbaum, Benjamin Abel, Udo Hartmann, Theresa Hecht, Hamed Saberi, Ioana Serban, Markus Storz, Johannes Ferber, formerly Henryk Gutmann and Michael Sindel, IT-administrator Ralph Simmler and secretary Stephane Schoonover

Part III

Appendix

Appendix A

Normal ordering and Fermi distribution functions

A.1 Technical aspects of normal ordering

In this section we want to provide the reader with a formal background of the normal ordering procedure and lay down some notation. The specific physical aspects of normal ordering in the context of the flow equations approach are dealt with in section (3.2.5).

Normal ordering procedures are commonly used in quantum field theory (see, for instance, [34]) and conventionally defined as a shift of all creation operators to the right of all annihilation operators. Its important applications, e.g. Wick's theorem, are virtually omnipresent in the respective literature. In this work we follow the spirit and the notation as been established by F. Wegner [37]. His approach sheds some more light on the abstract foundations of this ordering procedure.

Definition of normal ordering

Following Wegner, normal ordering with respect to a ground state $|GS\rangle$ in the commonly used form can always be introduced if the following connection between ground state correlators and the commutator holds:

$$\{a_k, a_l\} = \langle GS| a_k a_l |GS\rangle + \langle GS| a_l a_k |GS\rangle \quad (\text{A.1})$$

a_k, a_l are arbitrary (fermionic) creation or annihilation operators¹ defined with respect to a quadratic Hamiltonian (i.e. for a free theory). A similar constriction could be formulated for bosonic operators, too.

This condition is easily fulfilled for fermionic operators describing condensed matter systems. In particular, we focus on electronic multiparticle systems. Then the correlators are defined by Fermi functions $n^+(k)$ and $n^-(k)$ which describe the occupation of approximate one-particle electronic states by the electrons of the system. The correlators are defined to vanish for all operator products unrelated to

$$\langle GS| a_k^\dagger a_l |GS\rangle = n^+(k') \delta_l^{k'} \quad (\text{A.2})$$

$$\langle GS| a_k a_l^\dagger |GS\rangle = n^-(k) \delta_k^{l'} = \delta_k^{l'} - n^+(k) \delta_k^{l'} \quad (\text{A.3})$$

¹We sometimes refer to creation and annihilation operators as *fundamental* operators.

Normal ordering is now defined as a linear procedure (A.5) on operators which is trivial for single operators and extends to higher order operator products by a recurrence relation (A.4 and A.6).

$$:1: = 1 \quad (\text{A.4})$$

$$:\alpha A(a) + \beta B(a): = \alpha :A(a): + \beta :B(a): \quad (\text{A.5})$$

$$a_k :A(a): = :a_k A(a): + \sum_l \langle GS | a_k a_l | GS \rangle : \frac{\partial A(a)}{\partial a_l} : \quad (\text{A.6})$$

$A(a)$ and $B(a)$ are arbitrary products of fundamental operators, α and β are numbers. To describe the fermionic nature of the operators correctly, both the fundamental operators (a_k) and the differential operators $\frac{\partial}{\partial a_l}$ are considered as (odd) elements of a joint Grassmann algebra. Commutation of two of them produces a minus sign which has to be considered whenever derivatives are calculated. All conventional rules of calculus hold, including the chain rule.

Properties of fermionic normal ordered products

As shown by Wegner, this definition generates the commonly known properties of normal ordered products.

1. Ground state expectation values vanish for arbitrary normal ordered products.

$$\langle GS | :A(a): | GS \rangle = 0 \quad \text{for any operator product } A(a). \quad (\text{A.7})$$

2. Commutation of two fundamental operators inside normal ordering creates a minus sign

$$:a_1 a_2 a_3 a_4: = - :a_1 a_3 a_2 a_4: \quad (\text{A.8})$$

3. Wick's theorem can be written in the following form which will be found very helpful to systematically write down all contractions involved in a re-arrangement of normal ordered products. We refer to it as *Wegner's formula*.

$$:A(a): :B(b): = \exp \left(\sum_{k,l} \langle GS | a_k b_l | GS \rangle \frac{\partial^2}{\partial b_l \partial a_k} \right) A(a) B(b) |_{b=a} \quad (\text{A.9})$$

Re-arrangements of that kind are needed to compute commutators and correlators of higher, normal ordered operator products. Such calculations are the analytical backbone of the flow equation formalism and account for a significant part of the effort involved with this technique.

A.2 Fermi distribution functions

Due to normal ordering Fermi functions are present in most of the relevant flow equations. They take in a significant place in the theory as they incorporate important electronic properties. We assume that they are fully responsible for any dependence on temperature and external voltage which is applied to bring the system into out-of-equilibrium. By the way we

stress that in our theoretical setup no other quantities (like coupling constants, etc.) should depend on such outer conditions.

Fermi distribution functions describe the occupation of states in a fermionic multi-particle system in terms of a one-particle approximation. At zero temperature and in equilibrium they simply reflect the complete filling up to a maximal energy, the Fermi energy ϵ_F . A sharp Fermi edge is formed.

Equilibrium Fermi function

For zero temperature, the Fermi distribution in equilibrium is defined simply by

$$n^+(\epsilon) = \begin{cases} 1 & \text{for } \epsilon \leq \epsilon_F \\ 0 & \text{for } \epsilon > \epsilon_F \end{cases} \quad (\text{A.10})$$

For convenience, we also define its complement $n^-(\epsilon) = 1 - n^+(\epsilon)$ and mention the point symmetry of their difference with respect to the Fermi energy

$$[n^+ - n^-](\epsilon) = \begin{cases} 1 & \text{for } \epsilon < \epsilon_F \\ 0 & \text{for } \epsilon = \epsilon_F \\ -1 & \text{for } \epsilon > \epsilon_F \end{cases} \quad (\text{A.11})$$

The regular appearance of this difference in the flow equation formalism makes the Fermi energy a preferred point in energy for symmetry considerations.

Out-of-equilibrium Fermi function

We now consider the case where an external voltage drop is applied across the impurity. Our description uses two different chemical potentials for the left lead (μ_L) and the right lead (μ_R) of the setup; they are related by the voltage bias $\mu_L - \mu_R = V$ and measured with respect to the Fermi energy. This puts forth the emergence of two sharp Fermi edges at the chemical potentials. Figuratively speaking, the voltage bias opens a 'window' in between, further on called the transport window. Within this window, a coexistence of occupied and unoccupied electronic states fosters electron transport.

We roughly approximate the energy level occupation inside the transport window by a flat filling factor n_T between zero and one, depending on the asymmetry of the couplings involved. The Fermi distribution function acquires the following form:

$$n^+(\epsilon) = \begin{cases} 1 & \text{for } \epsilon < \epsilon_L \\ n_T & \text{for } \epsilon_L \leq \epsilon \leq \epsilon_U \\ 0 & \text{for } \epsilon > \epsilon_U \end{cases} \quad (\text{A.12})$$

To keep the notation intuitively, we denote the limits of the transport window by a lower and an upper energy. For the classical case of $\mu_L > \mu_R$, i.e. for a net current from the left to the right lead, this trivially implies $\epsilon_L = \epsilon_F + \mu_R$ and $\epsilon_U = \epsilon_F + \mu_L$.

For most of our discussions we refer to the *symmetric case* and set the Fermi energy zero. Then the transport window is opened symmetrically around the Fermi energy

$$[\epsilon_L, \epsilon_U] = [-V/2, V/2] \quad (\text{A.13})$$

and the filling factor takes the value $n_T = 0.5$. The difference of the complementary Fermi functions retains its point symmetry and vanishes within the transport window completely.

$$[n^+ - n^-](\epsilon) = \begin{cases} 1 & \text{for } \epsilon < \epsilon_L \\ 0 & \text{for } \epsilon_L \leq \epsilon \leq \epsilon_U \\ -1 & \text{for } \epsilon > \epsilon_U \end{cases} \quad (\text{A.14})$$

Later discussions will heavily refer to these properties.

Combined object of Fermi functions

To simplify notation we introduce another combination of Fermi functions which will regularly appear in later calculations.

$$Q_{12'2} = n^+(s_1) n^+(s_2) - n^+(s_1) n^+(s_2') + n^+(s_2') n^-(s_2) \quad (\text{A.15})$$

For zero temperature this combination of Fermi functions is always positive. This can be easily seen, for instance, by denoting the values of this function in a table spanned by the different energy regimes $\epsilon_{1/2'}/2 \lesseqgtr 0$.

We mention that this combination of Fermi functions re-appears in Fermi liquid theory and point out at [29] where such aspects are discussed.

Appendix B

Pre-diagonalization for an impurity with several spin levels

On this page we show what conditions are necessary to reduce a two-level impurity to an effective one-level impurity for the purpose of applying the pre-diagonalization. The transformation \mathcal{T} described in this context is exemplary for similar approaches (e.g. the treatment of asymmetric hybridization strength).

Decoupling of a channel

The starting point is a general two level system. Two different operators d_1 and d_2 are introduced to describe the impurity orbitals, which might couple differently to the band electrons. The hybridization splits up into V_1 and V_2 , the energy levels of the orbitals are generally non-degenerate $\varepsilon_1 \neq \varepsilon_2$. Under the usual assumptions, the Hamiltonian acquires the following structure:

$$H = \sum_k \varepsilon_k c_k^\dagger c_k + \varepsilon_1 d_1^\dagger d_1 + \varepsilon_2 d_2^\dagger d_2 + \sum_k \left[V_1 \left(c_k^\dagger d_1 + d_1^\dagger c_k \right) + V_2 \left(c_k^\dagger d_2 + d_2^\dagger c_k \right) \right] \quad (\text{B.1})$$

A linear transformation

$$\begin{aligned} \mathcal{T} : (A_1, A_2) &\rightarrow (A_+, A_-) \\ A_+ &= \frac{1}{\sqrt{2}}(A_1 + A_2) \\ A_- &= \frac{1}{\sqrt{2}}(A_1 - A_2) \end{aligned}$$

is applied to the pairs of operators $(d_1^\dagger, d_2^\dagger)$, (d_1, d_2) and the hybridization (V_1, V_2) and produces the transformed Hamiltonian

$$\begin{aligned} H_{transformed} &= \frac{\varepsilon_1 + \varepsilon_2}{2} \left(d_+^\dagger d_+ + d_-^\dagger d_- \right) + \frac{\varepsilon_1 - \varepsilon_2}{2} \left(d_+^\dagger d_- + d_-^\dagger d_+ \right) + \\ &\quad \frac{V_1 + V_2}{\sqrt{2}} \left(c_k^\dagger d_+ + d_+^\dagger c_k \right) + \frac{V_1 - V_2}{\sqrt{2}} \left(c_k^\dagger d_- + d_-^\dagger c_k \right) \end{aligned}$$

It is easily read off that for an energetically degenerate two-level system ($\varepsilon_1 = \varepsilon_2$) with a uniform coupling of both orbitals to the band ($V_1 = V_2$) effectively one channel decouples.

Such models can therefore be treated like one-level impurities with a modified hybridization $V_+ = \sqrt{2}V$ after a transformation T is performed.

This result can be directly applied for degenerate spin levels on the impurity which both couple. Effectively, this only leads to a renormalization of the hybridization strength. We simply write down V as a renormalized constant.

Appendix C

Some commutators and correlators

In this part of the appendix some non-trivial commutators of normal-ordered operator products are presented. For their derivation, some helpful general relations have been used. We refer to (10) where a detailed calculation of the $[:4:, 2]$ -commutator is presented to make the reader familiar with this kind of calculation.

C.1 General relations

Let A, B, C, D, E, F, G, H be arbitrary operators, i.e. elements of a common operator space. Then the following relations hold:

Decomposition of commutators into commutators

$$\begin{aligned}[AB, C] &= A[B, C] + [A, C]B \\ [AB, CD] &= AC[B, D] + A[B, C]D + C[A, D]B + [A, C]DB\end{aligned}$$

Decomposition of commutators into anticommutators

$$\begin{aligned}[AB, C] &= A\{B, C\} - \{A, C\}B \\ [AB, CD] &= -AC\{B, D\} + A\{B, C\}D - C\{A, D\}B + \{A, C\}DB \\ [ABCD, EF] &= ABEC\{D, F\} - ABE\{C, F\}D + \\ &\quad ABC\{D, E\}F - AB\{C, E\}DF + \\ &\quad EA\{B, F\}CD - E\{A, F\}BCD + \\ &\quad A\{B, E\}FCD - \{A, E\}BFCD\end{aligned}$$

$$\begin{aligned}
[ABCD, EFGH] = & ABEFC \{D, G\} H - ABEFG \{C, H\} D + \\
& ABEF \{C, G\} HD - ABEFCG \{D, H\} + \\
& ABC \{D, E\} FGH - ABE \{C, F\} DGH + \\
& AB \{C, E\} FDGH - ABCE \{D, F\} GH + \\
& EFA \{B, G\} HCD - EFG \{A, H\} BCD + \\
& EF \{A, G\} HBCD - EFAG \{B, H\} CD + \\
& A \{B, E\} FGHCD - E \{A, F\} BGHCD + \\
& \{A, E\} FBGHCD - AE \{B, F\} GHCD
\end{aligned}$$

C.2 Commutators and correlators of normal ordered operator products

For a fermionic theory $\{b_i, b_j\} = \delta_i^j$, we evaluate higher commutators of normal ordered operator products. For the calculation we have made use of the Wegner formula (A.9). We only present results¹.

Explicit form of the $[:4:, :4:]$ -commutator

$$\begin{aligned}
& [:b_{s'_1\beta_1}^\dagger b_{s_1\beta_1} b_{s'_2\beta_2}^\dagger b_{s_2\beta_2} : , :b_{s'_5\beta_5}^\dagger b_{s_5\beta_5} b_{s'_6\beta_6}^\dagger b_{s_6\beta_6} :] = \\
& = \left\{ \begin{aligned}
& + :b_{s'_1\beta_1}^\dagger b_{s_1\beta_1} b_{s'_5\beta_5}^\dagger b_{s_5\beta_5} b_{s'_2\beta_2}^\dagger b_{s_2\beta_2} b_{s_6\beta_6} : \delta_{s_2}^{s'_6} \delta_{\beta_2}^{\beta_6} \\
& - :b_{s'_1\beta_1}^\dagger b_{s_1\beta_1} b_{s'_5\beta_5}^\dagger b_{s_5\beta_5} b_{s'_6\beta_6}^\dagger b_{s_6\beta_6} b_{s_2\beta_2} : \delta_{s_6}^{s'_2} \delta_{\beta_2}^{\beta_6} \\
& + :b_{s'_1\beta_1}^\dagger b_{s_1\beta_1} b_{s'_2\beta_2}^\dagger b_{s_2\beta_2} b_{s_5\beta_5} b_{s'_6\beta_6}^\dagger b_{s_6\beta_6} : \delta_{s_2}^{s'_5} \delta_{\beta_2}^{\beta_5} \\
& - :b_{s'_1\beta_1}^\dagger b_{s_1\beta_1} b_{s'_5\beta_5}^\dagger b_{s_5\beta_5} b_{s'_2\beta_2}^\dagger b_{s_2\beta_2} b_{s_6\beta_6} : \delta_{s_5}^{s'_2} \delta_{\beta_2}^{\beta_5} \\
& + :b_{s'_5\beta_5}^\dagger b_{s_5\beta_5} b_{s'_1\beta_1}^\dagger b_{s_1\beta_1} b_{s'_6\beta_6}^\dagger b_{s_6\beta_6} b_{s_2\beta_2} : \delta_{s_1}^{s'_6} \delta_{\beta_1}^{\beta_6} \\
& - :b_{s'_5\beta_5}^\dagger b_{s_5\beta_5} b_{s'_6\beta_6}^\dagger b_{s_6\beta_6} b_{s_1\beta_1} b_{s'_2\beta_2}^\dagger b_{s_2\beta_2} : \delta_{s_6}^{s'_1} \delta_{\beta_1}^{\beta_6} \\
& + :b_{s'_1\beta_1}^\dagger b_{s_1\beta_1} b_{s'_5\beta_5}^\dagger b_{s_5\beta_5} b_{s'_6\beta_6}^\dagger b_{s_6\beta_6} b_{s_2\beta_2} : \delta_{s_1}^{s'_5} \delta_{\beta_1}^{\beta_5} \\
& - :b_{s'_5\beta_5}^\dagger b_{s_5\beta_5} b_{s'_1\beta_1}^\dagger b_{s_1\beta_1} b_{s'_6\beta_6}^\dagger b_{s_6\beta_6} b_{s_2\beta_2} : \delta_{s_5}^{s'_1} \delta_{\beta_1}^{\beta_5}
\end{aligned} \right.
\end{aligned}$$

¹Great care has been taken for the typesetting of these commutators. But due to their complex structure typing errors cannot be fully excluded. If in doubt, the reader should perform some simple consistency checks. For instance, any index s_i appears exactly once in any contraction. (Anti-)symmetries under index permutation are easily seen in the commutators and must hold for the set of contractions as well.

$$\begin{aligned}
& + :b_{s'_1\beta_1}^\dagger b_{s_1\beta_1} b_{s'_5\beta_5}^\dagger b_{s_5\beta_5} : (n^+(s_{2'}) - n^+(s_2)) \delta_{s_6}^{s_{2'}} \delta_{s_2}^{s_{6'}} \delta_{\beta_2}^{\beta_6} \\
& + :b_{s'_1\beta_1}^\dagger b_{s_5\beta_5} b_{s'_2\beta_2}^\dagger b_{s_6\beta_6} : n^-(s_1) \delta_{s_1}^{s_{5'}} \delta_{s_2}^{s_{6'}} \delta_{\beta_1}^{\beta_5} \delta_{\beta_2}^{\beta_6} \\
& - :b_{s'_1\beta_1}^\dagger b_{s_5\beta_5} b_{s'_6\beta_6}^\dagger b_{s_2\beta_2} : n^-(s_1) \delta_{s_1}^{s_{5'}} \delta_{s_6}^{s_{2'}} \delta_{\beta_1}^{\beta_5} \delta_{\beta_2}^{\beta_6} \\
& - :b_{s'_5\beta_5}^\dagger b_{s_1\beta_1} b_{s'_2\beta_2}^\dagger b_{s_6\beta_6} : n^+(s_{1'}) \delta_{s_5}^{s_{1'}} \delta_{s_2}^{s_{6'}} \delta_{\beta_1}^{\beta_5} \delta_{\beta_2}^{\beta_6} \\
& + :b_{s'_5\beta_5}^\dagger b_{s_1\beta_1} b_{s'_6\beta_6}^\dagger b_{s_2\beta_2} : n^+(s_{1'}) \delta_{s_5}^{s_{1'}} \delta_{s_6}^{s_{2'}} \delta_{\beta_1}^{\beta_5} \delta_{\beta_2}^{\beta_6} \\
\\
& + :b_{s'_1\beta_1}^\dagger b_{s_1\beta_1} b_{s'_6\beta_6}^\dagger b_{s_6\beta_6} : (n^+(s_{2'}) - n^+(s_2)) \delta_{s_5}^{s_{2'}} \delta_{s_2}^{s_{6'}} \delta_{\beta_2}^{\beta_5} \\
& + :b_{s'_2\beta_2}^\dagger b_{s_1\beta_1} b_{s'_6\beta_6}^\dagger b_{s_5\beta_5} : n^+(s_{1'}) \delta_{s_6}^{s_{1'}} \delta_{s_2}^{s_{5'}} \delta_{\beta_1}^{\beta_6} \delta_{\beta_2}^{\beta_5} \\
& - :b_{s'_1\beta_1}^\dagger b_{s_5\beta_5} b_{s'_2\beta_2}^\dagger b_{s_6\beta_6} : n^-(s_1) \delta_{s_1}^{s_{6'}} \delta_{s_2}^{s_{5'}} \delta_{\beta_1}^{\beta_6} \delta_{\beta_2}^{\beta_5} \\
& - :b_{s'_5\beta_5}^\dagger b_{s_1\beta_1} b_{s'_6\beta_6}^\dagger b_{s_2\beta_2} : n^+(s_{1'}) \delta_{s_6}^{s_{1'}} \delta_{s_5}^{s_{2'}} \delta_{\beta_1}^{\beta_6} \delta_{\beta_2}^{\beta_5} \\
& + :b_{s'_1\beta_1}^\dagger b_{s_2\beta_2} b_{s'_5\beta_5}^\dagger b_{s_6\beta_6} : n^-(s_1) \delta_{s_1}^{s_{6'}} \delta_{s_5}^{s_{2'}} \delta_{\beta_1}^{\beta_6} \delta_{\beta_2}^{\beta_5} \\
\\
& + :b_{s'_5\beta_5}^\dagger b_{s_5\beta_5} b_{s'_2\beta_2}^\dagger b_{s_2\beta_2} : (n^+(s_{1'}) - n^+(s_1)) \delta_{s_1}^{s_{6'}} \delta_{s_6}^{s_{1'}} \delta_{\beta_1}^{\beta_5} \\
& + :b_{s'_1\beta_1}^\dagger b_{s_5\beta_5} b_{s'_2\beta_2}^\dagger b_{s_6\beta_6} : n^+(s_2) \delta_{s_2}^{s_{5'}} \delta_{s_1}^{s_{6'}} \delta_{\beta_2}^{\beta_5} \delta_{\beta_1}^{\beta_6} \\
& - :b_{s'_5\beta_5}^\dagger b_{s_6\beta_6} b_{s'_1\beta_1}^\dagger b_{s_2\beta_2} : n^-(s_{2'}) \delta_{s_5}^{s_{2'}} \delta_{s_1}^{s_{6'}} \delta_{\beta_2}^{\beta_5} \delta_{\beta_1}^{\beta_6} \\
& - :b_{s'_6\beta_6}^\dagger b_{s_5\beta_5} b_{s'_2\beta_2}^\dagger b_{s_1\beta_1} : n^+(s_2) \delta_{s_2}^{s_{5'}} \delta_{s_6}^{s_{1'}} \delta_{\beta_2}^{\beta_5} \delta_{\beta_1}^{\beta_6} \\
& + :b_{s'_5\beta_5}^\dagger b_{s_1\beta_1} b_{s'_6\beta_6}^\dagger b_{s_2\beta_2} : n^-(s_{2'}) \delta_{s_5}^{s_{2'}} \delta_{s_6}^{s_{1'}} \delta_{\beta_2}^{\beta_5} \delta_{\beta_1}^{\beta_6} \\
\\
& + :b_{s'_6\beta_6}^\dagger b_{s_6\beta_6} b_{s'_2\beta_2}^\dagger b_{s_2\beta_2} : (n^+(s_{1'}) - n^+(s_1)) \delta_{s_1}^{s_{5'}} \delta_{s_5}^{s_{1'}} \delta_{\beta_1}^{\beta_6} \\
& + :b_{s'_1\beta_1}^\dagger b_{s_5\beta_5} b_{s'_6\beta_6}^\dagger b_{s_2\beta_2} : n^-(s_{2'}) \delta_{s_6}^{s_{2'}} \delta_{s_1}^{s_{5'}} \delta_{\beta_1}^{\beta_6} \delta_{\beta_2}^{\beta_5} \\
& - :b_{s'_1\beta_1}^\dagger b_{s_5\beta_5} b_{s'_2\beta_2}^\dagger b_{s_6\beta_6} : n^+(s_2) \delta_{s_1}^{s_{5'}} \delta_{s_2}^{s_{6'}} \delta_{\beta_1}^{\beta_6} \delta_{\beta_2}^{\beta_5} \\
& - :b_{s'_5\beta_5}^\dagger b_{s_1\beta_1} b_{s'_6\beta_6}^\dagger b_{s_2\beta_2} : n^-(s_{2'}) \delta_{s_5}^{s_{1'}} \delta_{s_6}^{s_{2'}} \delta_{\beta_1}^{\beta_5} \delta_{\beta_2}^{\beta_6} \\
& + :b_{s'_5\beta_5}^\dagger b_{s_1\beta_1} b_{s'_2\beta_2}^\dagger b_{s_6\beta_6} : n^+(s_2) \delta_{s_5}^{s_{1'}} \delta_{s_2}^{s_{6'}} \delta_{\beta_1}^{\beta_5} \delta_{\beta_2}^{\beta_6} \\
\\
& + :b_{s'_1\beta_1}^\dagger b_{s_5\beta_5} : n^-(s_1) (n^+(s_{2'}) - n^+(s_2)) \delta_{s_1}^{s_{5'}} \delta_{s_6}^{s_{2'}} \delta_{s_2}^{s_{6'}} \delta_{\beta_1}^{\beta_5} \delta_{\beta_2}^{\beta_6} \\
& - :b_{s'_5\beta_5}^\dagger b_{s_1\beta_1} : n^+(s_{1'}) (n^+(s_{2'}) - n^+(s_2)) \delta_{s_5}^{s_{1'}} \delta_{s_2}^{s_{6'}} \delta_{s_6}^{s_{2'}} \delta_{\beta_1}^{\beta_5} \delta_{\beta_2}^{\beta_6} \\
& + :b_{s'_2\beta_2}^\dagger b_{s_6\beta_6} : n^+(s_{1'}) n^-(s_1) \delta_{s_5}^{s_{1'}} \delta_{s_2}^{s_{6'}} \delta_{s_1}^{s_{5'}} \delta_{\beta_1}^{\beta_5} \delta_{\beta_2}^{\beta_6} \\
& - :b_{s'_6\beta_6}^\dagger b_{s_2\beta_2} : n^+(s_{1'}) n^-(s_1) \delta_{s_5}^{s_{1'}} \delta_{s_6}^{s_{2'}} \delta_{s_1}^{s_{5'}} \delta_{\beta_1}^{\beta_5} \delta_{\beta_2}^{\beta_6}
\end{aligned}$$

$$\begin{aligned}
& - :b_{s'_6\beta_6}^\dagger b_{s_1\beta_1} : n^+(s_{1'}) (n^+(s_{2'}) - n^+(s_2)) \delta_{s_6}^{s_{1'}} \delta_{s_5}^{s_{2'}} \delta_{s_2}^{s_{5'}} \delta_{\beta_1}^{\beta_6} \delta_{\beta_2}^{\beta_5} \\
& + :b_{s'_1\beta_1}^\dagger b_{s_6\beta_6} : n^-(s_{1'}) (n^+(s_{2'}) - n^+(s_2)) \delta_{s_1}^{s_{6'}} \delta_{s_5}^{s_{2'}} \delta_{s_2}^{s_{5'}} \delta_{\beta_1}^{\beta_6} \delta_{\beta_2}^{\beta_5} \\
& + :b_{s'_2\beta_2}^\dagger b_{s_5\beta_5} : n^+(s_{1'}) n^-(s_1) \delta_{s_6}^{s_{1'}} \delta_{s_1}^{s_{6'}} \delta_{s_2}^{s_{5'}} \delta_{\beta_1}^{\beta_6} \delta_{\beta_2}^{\beta_5} \\
& - :b_{s'_5\beta_5}^\dagger b_{s_2\beta_2} : n^+(s_{1'}) n^-(s_1) \delta_{s_6}^{s_{1'}} \delta_{s_1}^{s_{6'}} \delta_{s_5}^{s_{2'}} \delta_{\beta_1}^{\beta_6} \delta_{\beta_2}^{\beta_5} \\
& \\
& - :b_{s'_2\beta_2}^\dagger b_{s_5\beta_5} : n^+(s_2) (n^+(s_{1'}) - n^+(s_1)) \delta_{s_2}^{s_{5'}} \delta_{s_1}^{s_{6'}} \delta_{s_6}^{s_{1'}} \delta_{\beta_2}^{\beta_5} \delta_{\beta_1}^{\beta_6} \\
& + :b_{s'_5\beta_5}^\dagger b_{s_2\beta_2} : n^-(s_{2'}) (n^+(s_{1'}) - n^+(s_1)) \delta_{s_5}^{s_{2'}} \delta_{s_1}^{s_{6'}} \delta_{s_6}^{s_{1'}} \delta_{\beta_2}^{\beta_5} \delta_{\beta_1}^{\beta_6} \\
& + :b_{s'_1\beta_1}^\dagger b_{s_6\beta_6} : n^+(s_2) n^-(s_{2'}) \delta_{s_2}^{s_{5'}} \delta_{s_5}^{s_{2'}} \delta_{s_1}^{s_{6'}} \delta_{\beta_2}^{\beta_5} \delta_{\beta_1}^{\beta_6} \\
& - :b_{s'_6\beta_6}^\dagger b_{s_1\beta_1} : n^+(s_2) n^-(s_{2'}) \delta_{s_2}^{s_{5'}} \delta_{s_5}^{s_{2'}} \delta_{s_6}^{s_{1'}} \delta_{\beta_2}^{\beta_5} \delta_{\beta_1}^{\beta_6} \\
& \\
& + :b_{s'_6\beta_6}^\dagger b_{s_2\beta_2} : n^-(s_{2'}) (n^+(s_{1'}) - n^+(s_1)) \delta_{s_1}^{s_{5'}} \delta_{s_5}^{s_{1'}} \delta_{s_6}^{s_{2'}} \delta_{\beta_1}^{\beta_5} \delta_{\beta_2}^{\beta_6} \\
& - :b_{s'_2\beta_2}^\dagger b_{s_6\beta_6} : n^+(s_2) (n^+(s_{1'}) - n^+(s_1)) \delta_{s_1}^{s_{5'}} \delta_{s_5}^{s_{1'}} \delta_{s_2}^{s_{6'}} \delta_{\beta_1}^{\beta_5} \delta_{\beta_2}^{\beta_6} \\
& + :b_{s'_1\beta_1}^\dagger b_{s_5\beta_5} : n^+(s_2) n^-(s_{2'}) \delta_{s_1}^{s_{5'}} \delta_{s_2}^{s_{6'}} \delta_{s_6}^{s_{2'}} \delta_{\beta_1}^{\beta_5} \delta_{\beta_2}^{\beta_6} \\
& - :b_{s'_5\beta_5}^\dagger b_{s_1\beta_1} : n^+(s_2) n^-(s_{2'}) \delta_{s_5}^{s_{1'}} \delta_{s_2}^{s_{6'}} \delta_{s_6}^{s_{2'}} \delta_{\beta_1}^{\beta_5} \delta_{\beta_2}^{\beta_6} \\
& \\
& + n^+(s_{1'}) n^-(s_1) (n^+(s_{2'}) - n^+(s_2)) \delta_{s_5}^{s_{1'}} \delta_{s_6}^{s_{2'}} \delta_{s_1}^{s_{5'}} \delta_{s_2}^{s_{6'}} \delta_{\beta_1}^{\beta_5} \delta_{\beta_2}^{\beta_6} \\
& + n^+(s_{1'}) n^-(s_1) (n^+(s_{2'}) - n^+(s_2)) \delta_{s_6}^{s_{1'}} \delta_{s_1}^{s_{6'}} \delta_{s_5}^{s_{2'}} \delta_{s_2}^{s_{5'}} \delta_{\beta_1}^{\beta_6} \delta_{\beta_2}^{\beta_5} \\
& + n^+(s_2) n^-(s_{2'}) (n^+(s_{1'}) - n^+(s_1)) \delta_{s_2}^{s_{5'}} \delta_{s_5}^{s_{2'}} \delta_{s_1}^{s_{6'}} \delta_{s_6}^{s_{1'}} \delta_{\beta_2}^{\beta_5} \delta_{\beta_1}^{\beta_6} \\
& + n^+(s_2) n^-(s_{2'}) (n^+(s_{1'}) - n^+(s_1)) \delta_{s_5}^{s_{1'}} \delta_{s_1}^{s_{5'}} \delta_{s_2}^{s_{6'}} \delta_{s_6}^{s_{2'}} \delta_{\beta_1}^{\beta_5} \delta_{\beta_2}^{\beta_6} \quad \left. \vphantom{\begin{aligned} & + n^+(s_{1'}) n^-(s_1) (n^+(s_{2'}) - n^+(s_2)) \delta_{s_5}^{s_{1'}} \delta_{s_6}^{s_{2'}} \delta_{s_1}^{s_{5'}} \delta_{s_2}^{s_{6'}} \delta_{\beta_1}^{\beta_5} \delta_{\beta_2}^{\beta_6} \\ & + n^+(s_{1'}) n^-(s_1) (n^+(s_{2'}) - n^+(s_2)) \delta_{s_6}^{s_{1'}} \delta_{s_1}^{s_{6'}} \delta_{s_5}^{s_{2'}} \delta_{s_2}^{s_{5'}} \delta_{\beta_1}^{\beta_6} \delta_{\beta_2}^{\beta_5} \\ & + n^+(s_2) n^-(s_{2'}) (n^+(s_{1'}) - n^+(s_1)) \delta_{s_2}^{s_{5'}} \delta_{s_5}^{s_{2'}} \delta_{s_1}^{s_{6'}} \delta_{s_6}^{s_{1'}} \delta_{\beta_2}^{\beta_5} \delta_{\beta_1}^{\beta_6} \\ & + n^+(s_2) n^-(s_{2'}) (n^+(s_{1'}) - n^+(s_1)) \delta_{s_5}^{s_{1'}} \delta_{s_1}^{s_{5'}} \delta_{s_2}^{s_{6'}} \delta_{s_6}^{s_{2'}} \delta_{\beta_1}^{\beta_5} \delta_{\beta_2}^{\beta_6} \end{aligned}} \right\}
\end{aligned}$$

Explicit form of the $[:4:, :3:]$ -commutator

$$\begin{aligned}
& [:b_{s_1}^\dagger b_1 b_2^\dagger b_2 :, :b_{s_5}^\dagger b_{s_6}^\dagger b_{s_5} :] = \\
& = \left\{ \begin{aligned}
& - :b_{s_1}^\dagger b_{s_5}^\dagger b_{s_6}^\dagger b_{s_1} b_{s_2} : \delta_{s_5}^{s_2'} + :b_{s_1}^\dagger b_{s_5}^\dagger b_{s_2}^\dagger b_{s_1} b_{s_5} : \delta_{s_2}^{s_6'} \\
& + :b_{s_1}^\dagger b_{s_2}^\dagger b_{s_6}^\dagger b_{s_1} b_{s_5} : \delta_{s_2}^{s_5'} + :b_{s_5}^\dagger b_{s_6}^\dagger b_{s_2}^\dagger b_{s_1} b_{s_2} : \delta_{s_5}^{s_1'} \\
& - :b_{s_5}^\dagger b_{s_1}^\dagger b_{s_2}^\dagger b_{s_5} b_{s_2} : \delta_{s_1}^{s_6'} - :b_{s_1}^\dagger b_{s_6}^\dagger b_{s_2}^\dagger b_{s_5} b_{s_2} : \delta_{s_1}^{s_5'} \\
& - :b_{s_1}^\dagger b_{s_6}^\dagger b_{s_2} : n^-(1) \delta_{s_1}^{s_5'} \delta_{s_5}^{s_2'} + :b_{s_1}^\dagger b_{s_5}^\dagger b_{s_2} : n^-(1) \delta_{s_1}^{s_6'} \delta_{s_5}^{s_2'} \\
& + :b_{s_2}^\dagger b_{s_5}^\dagger b_{s_1} : n^+(1') \delta_{s_5}^{s_1'} \delta_{s_2}^{s_6'} + :b_{s_1}^\dagger b_{s_2}^\dagger b_{s_5} : n^-(1) \delta_{s_1}^{s_5'} \delta_{s_2}^{s_6'} \\
& - :b_{s_2}^\dagger b_{s_6}^\dagger b_{s_1} : n^+(1') \delta_{s_5}^{s_1'} \delta_{s_2}^{s_5'} - :b_{s_1}^\dagger b_{s_2}^\dagger b_{s_5} : n^-(1) \delta_{s_1}^{s_6'} \delta_{s_5}^{s_5'} \\
& + :b_{s_2}^\dagger b_{s_6}^\dagger b_{s_1} : n^+(2) \delta_{s_2}^{s_5'} \delta_{s_5}^{s_1'} - :b_{s_2}^\dagger b_{s_5}^\dagger b_{s_1} : n^+(2) \delta_{s_2}^{s_6'} \delta_{s_5}^{s_1'} \\
& + :b_{s_1}^\dagger b_{s_2}^\dagger b_{s_5} : n^+(2) \delta_{s_2}^{s_5'} \delta_{s_1}^{s_6'} - :b_{s_1}^\dagger b_{s_5}^\dagger b_{s_2} : n^-(2') \delta_{s_5}^{s_2'} \delta_{s_1}^{s_6'} \\
& - :b_{s_1}^\dagger b_{s_2}^\dagger b_{s_5} : n^+(2) \delta_{s_2}^{s_6'} \delta_{s_1}^{s_5'} + :b_{s_1}^\dagger b_{s_6}^\dagger b_{s_2} : n^-(2') \delta_{s_5}^{s_2'} \delta_{s_1}^{s_5'} \\
& + b_{s_1}^\dagger [n^-(1) (n^+(2') - n^+(2)) + n^+(2) n^-(2')] (\delta_{s_1}^{s_5'} \delta_{s_2}^{s_6'} - \delta_{s_2}^{s_5'} \delta_{s_1}^{s_6'}) \delta_{s_5}^{s_2'} \\
& - b_{s_2}^\dagger [n^+(2) (n^+(1') - n^+(1)) + n^-(1) n^+(1')] (\delta_{s_1}^{s_5'} \delta_{s_2}^{s_6'} - \delta_{s_2}^{s_5'} \delta_{s_1}^{s_6'}) \delta_{s_5}^{s_1'} \\
& + b_{s_5}^\dagger [n^+(1') (n^+(2') - n^+(1)) + (n^+(2) n^-(2') - n^+(1') n^-(1))] \delta_{s_2}^{s_1'} \delta_{s_5}^{s_2'} \delta_{s_1}^{s_6'} \\
& + b_{s_5}^\dagger [-n^-(1) (n^+(1') - n^+(2)) + (n^-(1) n^+(1') - n^-(2') n^+(2))] \delta_{s_5}^{s_1'} \delta_{s_1}^{s_2'} \delta_{s_2}^{s_6'} \\
& + b_{s_6}^\dagger [-n^+(1') (n^+(2') - n^+(1)) + (n^-(1) n^+(1') - n^-(2') n^+(2))] \delta_{s_2}^{s_1'} \delta_{s_5}^{s_2'} \delta_{s_1}^{s_5'} \\
& + b_{s_6}^\dagger [n^-(1) (n^+(1') - n^+(2)) + (n^+(2) n^-(2') - n^+(1') n^-(1))] \delta_{s_5}^{s_1'} \delta_{s_1}^{s_2'} \delta_{s_1}^{s_5'} \quad \left. \vphantom{b_{s_6}^\dagger} \right\}
\end{aligned}
\end{aligned}$$

 $\{ :3:, :3^\dagger : \}$ -Correlator

The result for the ground state $\{ :3:, :3^\dagger : \}$ -correlator is simply given by

$$\left\langle \left\{ :b_{s_5}^\dagger b_{s_6} b_{s_5} :, :b_{s_7}^\dagger b_{s_8}^\dagger b_{s_7} : \right\} \right\rangle = Q_{s_5 s_5' s_6} \delta_{s_7}^{s_5'} \delta_{s_5}^{s_7'} \delta_{s_6}^{s_8'} + Q_{s_6 s_5' s_5} \delta_{s_7}^{s_5'} \delta_{s_6}^{s_7'} \delta_{s_5}^{s_8'} \quad (\text{C.1})$$

where we used the combined Fermi function

$$Q_{12'2} = n^+(s_1) n^+(s_2) - n^+(s_1) n^+(s_2') + n^+(s_2') n^-(s_2) \quad (\rightarrow \text{A.15})$$

List of Figures

1.1	Energy level scheme of an impurity model for a quantum dot.	12
2.1	Renormalization of band energies under the pre-diagonalization	28
5.1	Thumbsketch of symmetries in the case of initial flow	69
5.2	Thumbsketch of symmetries in the case of advanced flow	73
8.1	Correction function in equilibrium for different lattice sizes	110
9.1	Equilibrium impurity spectral function	112
9.2	Correction function for different voltage regimes	113
9.3	Impurity spectral density close to equilibrium ($V = 0.3\Delta$)	114
9.4	Impurity spectral density at unit voltage bias	115
9.5	Impurity spectral density for larger but fixed voltage bias	116
9.6	Impurity spectral density for $U = 0.75\Delta$	117
9.7	Impurity spectral density for $U = 2\Delta$	117
9.8	Impurity spectral density for fixed on-site interaction strength in the strong correlation regime ($U = 5\Delta$).	118

Bibliography

- [1] P. W. Anderson, Phys. Rev. **124**, 41 (1961).
- [2] N. Andrei, Phys. Rev. Lett. **45**, 379 (1980).
- [3] J. R. Schrieffer and P. A. Wolff, Phys. Rev. **149**, 491 (1966).
- [4] P. B. Wiegmann, Phys. Lett. A **31**, 163 (1981).
- [5] D. G.-G. et al., Nature **391**, 156 (1998).
- [6] T. H. O. S. M. Cronenwett and L. P. Kouwenhoven, Science **281**, 540 (1998).
- [7] J. H. D. S. Hershfield and J. W. Wilkins, Phys. Rev. Lett. **67**, 26 (1991).
- [8] D. S. S. P. N. Silver, J. E. Gubernatis and M. Jarrell, Phys. Rev. Lett. **65**, 496 (1990).
- [9] T. Fujii and K. Ueda, Phys. Rev. B **68**, 155310 (2003).
- [10] N. S. Wingreen and Y. Meir, Phys. Rev. B **49**, 16 (1994).
- [11] A. Komnik and A. O. Gogolin, Phys. Rev. B **69**, 153102 (2004).
- [12] P. Mehta and N. Andrei, cond-mat **0508026** (2005).
- [13] C. Kittel, *Introduction to solid state physics* (Wiley, 1996).
- [14] H. I. und H. Lüth, *Festkörperphysik* (Springer, 1993).
- [15] A. C. Hewson, *The Kondo Problem to Heavy Fermions* (Cambridge University Press, 1992).
- [16] M. Sindel, PhD thesis, LMU München (2005).
- [17] S. K. Kehrein and A. Mielke, Ann. Phys. (NY) **252**, 1 (1996).
- [18] O. Parcollet and C. Hooley, Phys. Rev. B **66**, 085315 (2002).
- [19] C. Cohen-Tannoudji, B. Diu, and F. Laloë, *Quantenmechanik* (Walter de Gruyter, 1999).
- [20] J. von Delft and H. Schoeller, Annalen der Physik **7**, 225 (1998).
- [21] M. Abramowitz and I. A. Stegun, *Handbook of mathematical functions* (Dover Publications, Inc., 1968).

-
- [22] I. S. Gradshteyn, *Table of Integrals, Series and Products* (Academic Press, 2000).
- [23] S. D. Glazek and K. G. Wilson, Phys. Rev. D **48**, 5863 (1993).
- [24] S. D. Glazek and K. G. Wilson, Phys. Rev. D **49**, 4214 (1994).
- [25] F. J. Wegner, Annalen der Physik (Leipzig) **3**, 77 (1994).
- [26] S. K. S. Kleff and J. von Delft, Physica E **18**, 343 (2003).
- [27] S. Kehrein, Nucl. Phys. B **592**, 512 (2001).
- [28] S. K. Kehrein, cond-mat/0410341 (2004).
- [29] S. Kehrein, *The Flow Equations Approach to Many-Body-Problems* (Springer, 2006).
- [30] P. W. Anderson, J. Phys. C **3**, 2436 (1970).
- [31] F. D. M. Haldane, Phys. Rev. Lett. **40**, 416 (1978).
- [32] P. W. Anderson, *Basic Notions of Condensed Matter Physics* (Addison-Wesley, 1984).
- [33] E. Lebanon and A. Schiller, Phys. Rev. B **65**, 035308 (2002).
- [34] J. D. W. A. L. Fetter, *Quantum Theory of Many-Particle Systems* (McGraw-Hill Book Company, 1971).
- [35] J. M. Luttinger, Phys. Rev. **119**, 1153 (1960).
- [36] J. M. Luttinger, Phys. Rev. **121**, 942 (1961).
- [37] F. Wegner, unpublished (2000).

Selbstständigkeitserklärung

gemäss Paragraph 24, Absatz (8) der Diplomprüfungsordnung für den Studiengang Physik an der Ludwig-Maximilians-Universität München vom 23. August 1994

Hiermit versichere ich, diese Arbeit selbstständig angefertigt und dabei keine anderen als die angegebenen Quellen und Hilfsmittel verwendet zu haben. Ebensovienig habe ich andere als die mir von der Universität München zur Verfügung gestellte Software benutzt.

München, den 26. September 2005